

9-24-1981

Experimental Determination of Post-buckling Performance of Steel Angles

Rupasiri Purasinghe
Portland State University

Follow this and additional works at: https://pdxscholar.library.pdx.edu/open_access_etds



Part of the [Mechanical Engineering Commons](#), and the [Structural Engineering Commons](#)

Let us know how access to this document benefits you.

Recommended Citation

Purasinghe, Rupasiri, "Experimental Determination of Post-buckling Performance of Steel Angles" (1981).
Dissertations and Theses. Paper 3165.
<https://doi.org/10.15760/etd.3156>

This Thesis is brought to you for free and open access. It has been accepted for inclusion in Dissertations and Theses by an authorized administrator of PDXScholar. Please contact us if we can make this document more accessible: pdxscholar@pdx.edu.

AN ABSTRACT OF THE THESIS OF Rupasiri Purasinghe for the Master of Science in Applied Science presented September 24, 1981.

Title: Experimental Determination of Post-Buckling Performance of Steel Angles

APPROVED BY MEMBERS OF THESIS COMMITTEE:

[Redacted Signature]

Wendelin H. Mueller, III, Advisor

[Redacted Signature]

Hacik Erzurumlu

[Redacted Signature]

Arnold Wagner

[Redacted Signature]

Ray Sommerfeldt

An experimental testing program was conducted to determine the compression member performance in post-buckling region. These results are compared with an analytical computer program developed by Portland State University under Bonneville Power Administration Contract 79-80BP 24005. The paper presents the sensitivity of the performance of single angle compression members to various parameters such as length to radius of gyration ratio, eccentricity, end conditions and yield stress. The effect of local buckling on long member performance is also documented.

Data is presented as axial load vs axial displacement. Dial gages were used to measure translation and rotation of the member ends. Computer

programs documented in this paper calculate the axial displacement using these dial readings. Preliminary study of load transfer characteristics of an indeterminate truss is also documented.

These results are needed as a foundation to verify member performance in a Limit State Analysis of transmission towers.

EXPERIMENTAL DETERMINATION OF POST-BUCKLING
PERFORMANCE OF STEEL ANGLES

by

RUPASIRI PURASINGHE

A thesis submitted in partial fulfillment of
the requirements for the degree of

MASTER OF SCIENCE
in
APPLIED SCIENCE

Portland State University
1981

TO THE OFFICE OF GRADUATE STUDIES AND RESEARCH:

The members of the Committee approve the thesis of Rupasiri Purasinghe presented September 24, 1981.

[Redacted Signature]

Wendelin H. Mueller, III, Advisor

[Redacted Signature]

Hacı Erzurumlu

[Redacted Signature]

Arnold Wagner

[Redacted Signature]

Ray Sommerfeldt

APPROVED:

[Redacted Signature]

Franz N. Rad, Head, Civil-Structural Engineering

[Redacted Signature]

Stanley E. Rauch, Dean of Graduate Studies and Research

TO MY LOVING MOTHER

ACKNOWLEDGMENTS

The author is deeply grateful to Dr. Wendelin H. Mueller for his guidance, help, encouragement and patience throughout this investigation. Gratitude is also expressed to Dr. H. Erzurumlu for his advice and comments during my stay at Portland State University. The author is thankful to Mr. Arnold Wagner and Dr. Ray Sommerfeldt for their comments and criticism.

Financial assistance in the form of a research grant from the Bonneville Power Administration is gratefully appreciated.

Appreciation is also due to Mr. Steve Speer for the help in the experimental work and to Mr. Bahman Daniali and Mr. David Reiser for their assistance in drawing the figures. Last but not least to Ms. Donna Mikulic for the fine job she did in typing this thesis.

TABLE OF CONTENTS

	PAGE
ACKNOWLEDGMENTS	iv
LIST OF TABLES	vii
LIST OF FIGURES	viii
CHAPTER	
I INTRODUCTION	1
1.1 Background and Review of Literature	1
1.2 Objective of this Investigation	5
II EXPERIMENTAL PROGRAM FOR SINGLE ANGLE MEMBERS	7
2.1 Overview	9
2.2 Experimental Setup for Single Angle Member Tests	9
2.3 Instrumentation	19
2.4 Test Procedure	23
2.5 Computation of Axial Displacement	24
2.6 Steel Properties and Coupon Tests	24
2.7 Comparison of Experimental and Analytical Results for Single Angle Member Tests	25
III PRELIMINARY EXPERIMENTAL PROGRAM FOR INDETERMINATE TRUSS TESTS	61
3.1 Overview	61
3.2 Experimental Setup	61
3.3 Instrumentation	64

CHAPTER		
3.4	Test Procedure	64
3.5	Steel Properties and Coupon Tests	65
3.6	Discussion of Results	65
IV	CONCLUSIONS AND RECOMMENDATIONS	80
REFERENCES		83
APPENDIX A		84
APPENDIX B		95

LIST OF TABLES

TABLE		PAGE
I	Test Configuration for Single Members	16
II	Results of Coupon Tests for Single Member Tests	27
III	Failure Load Comparison for Single Member Tests	55
IVA	Diagonal Member Configuration in Preliminary Truss Tests	66
IVB	Comparison of Results in Preliminary Truss Tests	67
V	Steel Properties of Indeterminate Truss Tests	68

LIST OF FIGURES

FIGURE	PAGE
1. Bilinear load vs displacement curve	3
2. Indeterminate truss	8
3. Experimental setup for single angle test member	10
4. Details of end connections for single member tests	12
5. Experimental setup for single member tests	13
6. Experimental setup for single member tests	13
7. Loading configuration for single member tests	14
8. Hinged joint	15
9. Bolted member end connection attached to the ball joint	15
10. Bolted connections for single member tests	18
11. Dial gage setup for measuring displacements	20
12. Gage layout to measure rotation about the axis of the member	21
13. Gage layout for single member tests including the rotational gages	22
14. Typical stress strain curve	26
15. Test S2 HH 50-2	29
16. Test S2 HH 36-1	30
17. Test S2 HH 36-2	31
18. Test S1 HH 50-1	32
19. Test S1 HH 36-2	33
20. Test S3 BB 36-1	34

FIGURE	PAGE
21. Test S3 BB 36-2	35
22. Test S1 BB 36-2	36
23. Test S2 BB 36-3	37
24. Test T2 BB 50-1	38
25. Test T2 BB 36-1	39
26. Test T1 BB 36-1	40
27. Test T1 BB 50-1	41
28. Test T3 BB 50-1	42
29. Test T3 BB 36-1	43
30. Test S3 BB 50-1	44
31. Test S \emptyset BB 50-1	45
32. Test T2 BF 50-1	46
33. Test T2 BF 36-1	47
34. Test SR3 BB 36-1	48
35. Test TR3 BB 50-1 (1)	49
36. Test TR3 BB 50-1	50
37. Test TR2 BB 50-1	51
38. Test TR1 36-1	52
39. Test T4 BB 36-1	53
40. Test T4 BB 36-2	54
41. Setup of truss without diagonal bracing	62
42. Indeterminate truss with diagonal bracing	62
43. Indeterminate truss	63
44. Test Fx1	69
45. Test Fx2	70

FIGURE	PAGE
46. Test Fx3 and Fx 3A	71
47. Test Fx4 and Fx4A	72
48. Test Fx5, Fx5A and Fx5B	73
49. Test Fx6	74
50. Test Fx7, Fx7A and Fx7B	75
51. Test Fx8 and Fx8A	76
52. Test Fx9 and Fx9A	77
53. The end plate and gage layout at one end of the test member	85
54. Translation of the end plate and rotation about the y axis for the hinged-hinged configuration	87
55. Gage layout for single member tests including the rotational gages	89
56. Translation of the end plate with rotation about the x axis	97
57. Rotation of the end plate about the z axis	97
58. Rotation of the end plate about the x axis	100
59. Rotation of the end plate about the y axis	100

CHAPTER I

INTRODUCTION

1.1 BACKGROUND AND REVIEW OF LITERATURE

In the analysis and design of indeterminate structures, two different concepts are used. One is the elastic strength concept which leads to working stress design. In this concept yielding of a member is the failure criteria. A factor of safety is applied to the yield stress to obtain the allowable stress. Members of the structure are then sized to withstand the allowable stress. This gives rise to the allowable load of a member which is lower than the actual load the member can sustain. This results in a conservative structural configuration where few points of the structure are stressed to the allowable stress but the rest of the structure is understressed. The second approach is the Limit State Analysis. Conceptually this approach is similar to plastic analysis and design developed by Beedle (1). It calculates the collapse load of the structure and then applies a factor of safety to this value to calculate the allowable load. This approach allows the redistribution of moments as individual parts of the structure reach the ultimate moments or form plastic hinges. Failure will not occur until enough plastic hinges form to cause the collapse mechanism in the structural system.

Trusses are structures made up of members that sustain axial thrust but not bending. This axial thrust is either a compression or a tensile force depending on the configuration of the truss and loading conditions. Application of a Limit State Approach to indeterminate

trusses allows the redistribution of loads to other members as individual members reach their ultimate load. Tensile members cause no concern in this type of analysis, since once they reach yield or the ultimate load they are able to sustain it through large deflections. Compression members on the other hand because of their susceptibility to buckling are a concern in this type of analysis. Once they reach failure or buckling can they sustain an internal force large enough to allow redistribution of load throughout the structure?

Transmission Towers are highly indeterminate structures and should therefore benefit from a Limit State Analysis. As members reach their ultimate loads and sustain them through larger deflections, the structure is able to redistribute it and resist higher structural loads. In developing a Limit State Analysis for indeterminate trusses like Transmission Towers a thorough knowledge of compression member performance is required. Only when this is accomplished can a Limit State Analysis technique be developed with confidence, utilizing the reserve strength of indeterminate trusses.

There are classical computer analysis techniques to determine internal forces of members in an indeterminate truss. The technique developed by Wang (2) is one of these. These internal forces are obtained by first calculating the joint displacements of the truss. One idealized approach to a Limit State Analysis is to assume a bilinear load-deflection curve for member performance. In this type of analysis it is assumed that when the member reaches its ultimate load capacity, it will provide a constant resisting force for increased member elongation (Fig. 1). Wang (2), Lee (3), Smith and Epstein (4) have assumed the above load-deflection behavior in their analysis techniques. Compression tests

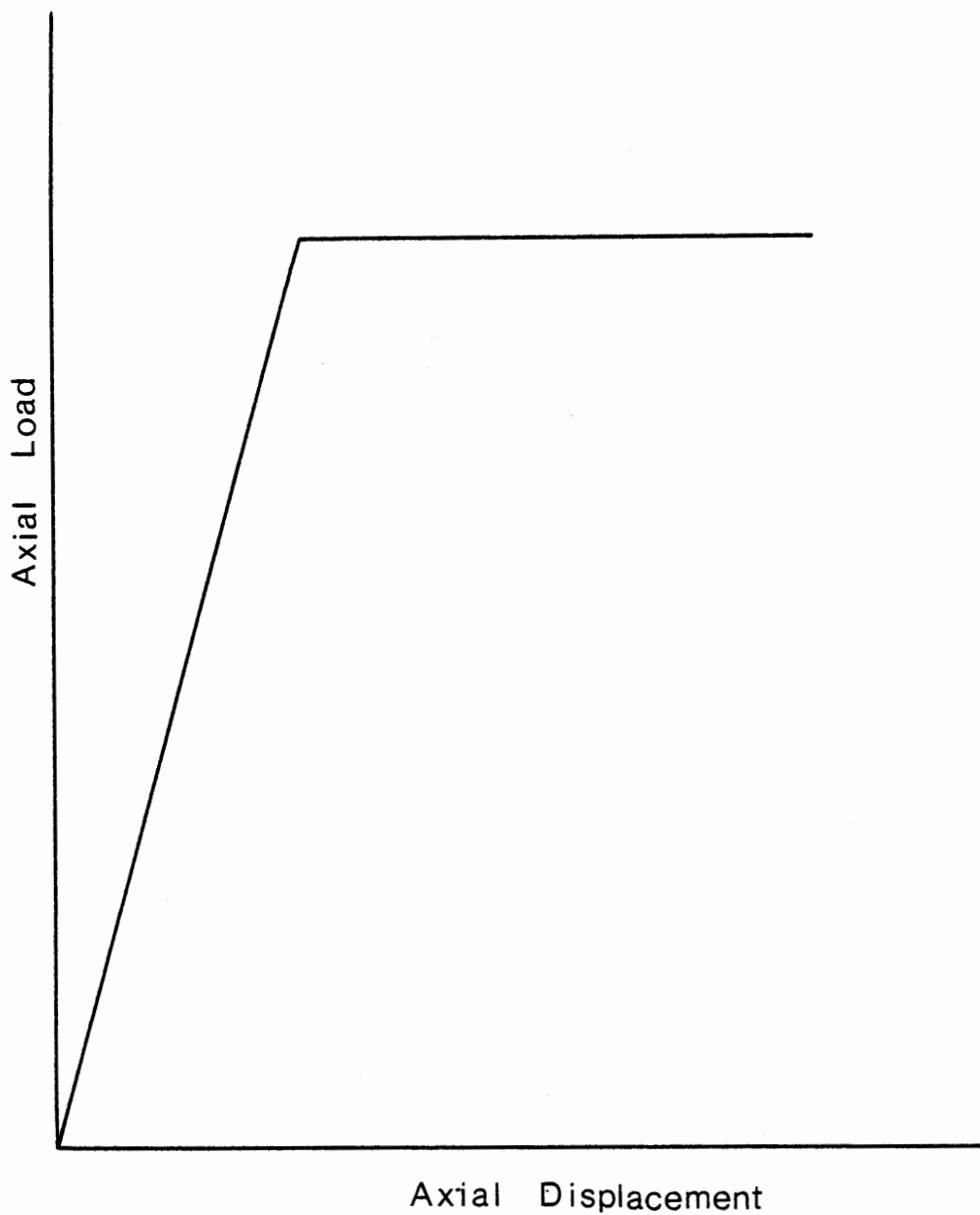


Figure 1 Bilinear load vs displacement curve

reported in 'Force Limiting Devices in Space Trusses' by Schmidt and Hanaor (5) and 'Inelastic Cycles of Axially Loaded Steel Members' by Kahn and Hanson (6) document that this bilinear assumption may be unconservative. The load resistance that was shown in this type of member dropped off after the maximum load was reached. This unloading could affect the manner in which redistribution of load throughout the structure was accomplished if

- a) the unloading was immediate after the ultimate load was reached
- b) the elongation of the member was such as to put the member performance in the unloading phase.

The application of Limit State Analysis of trusses using the bilinear load-deflection curve is valid only if the actual load-deflection curve that depicts the member performance has a large enough plastic plateau to hold a constant force allowing the redistribution of load to other members. Otherwise a refinement to this constant force assumption is warranted. This refinement must account for any unloading which may exist after the plastic plateau is passed. Compression member performance can be categorized into three phases. They are

- a) Elastic
- b) Inelastic
- c) Post buckling

Once the behavior of compression members in these phases are known a decision can be made as to whether a refinement is needed to the constant force approach of Limit State Analysis. If some members are unable to sustain a constant load over a large enough axial displacement then a refinement to the constant force approach will be necessary.

This refinement should allow the individual members to sustain

lower loads than their ultimate load capacity when excessive elongations are attained.

1.2 OBJECTIVE OF THIS INVESTIGATION

As stated in Section 1.1 a thorough knowledge of compression member performance is needed before embarking on a Limit State Analysis of Indeterminate Trusses. This investigation is aimed at investigating compression member performance by conducting an experimental testing program and comparing it with the analytical computer program developed in Bonneville Power Administration contract 79-80BP24005 (7). A series of single member tests with varying lengths, eccentricities and yield strength were performed to investigate the overall member performance and to determine if the results were sensitive to particular parameters. Steel angles are the members used in construction of the majority of transmission towers. Hence a single angle steel member was chosen for this study. The size selected was 3 x 3 x $\frac{1}{4}$ angle because the existing equipment was capable of loading this member to failure in various length configurations and support conditions that are of concern in this investigation.

The lengths selected were such that the length to radius of gyration (L/r) ratio was as close as practical to 60, 120 and 200. The reason for this choice is that these are the L/r ratios of members that are of interest in a Limit State Analysis of a Transmission Tower. Both Grade 50 and A-36 steel were used since these are the two common types of steel used in construction.

The eccentricity of the load from the center of gravity of the test member is the third parameter chosen as relevant to effect

member performance. Eccentricity about the weak axis (e_x) with zero eccentricity about the strong axis and eccentricities about both axes (e_x and e_y not equal to zero) were studied.

Different end connections were studied to obtain information on their effect on member performance. A Hinge-Hinge Connection which allows end rotation about only one axis, a Ball-Ball Connection which allows end rotation in all directions, a Bolted Connection to simulate a typical tower joint and a Fixed end connection, fixed against joint rotations were used. Test members with Hinge or Ball Connections were welded to a plate and then directly connected to the Hinge or Ball as the case may be. Members with Bolted Connection were bolted to a stub angle extending from the ball joint allowing freedom to rotate in all directions.

The effect of local buckling in long member performance is of concern in this investigation. Local buckling causes a sudden decrease in the load resistance capacity of the member, thus if a local buckle formed in a long member which would be expected to have a large plastic plateau, might it not perform more like a short member with no plastic plateau? Hence two $5 \times 3 \times \frac{1}{4}$ non compact single angle steel members were tested using the ball-ball configuration. This angle member had a width-to-thickness ratio of 20 which exceeds the limitation in AISC Manual of Steel Construction (8) for compact members. This limit guards against local buckling.

A two dimensional indeterminate truss was selected to do a preliminary study of load transfer characteristics of diagonal bracing. The test setup was arranged such that the diagonal members control the

limiting load of the structure. Figure 2 is a sketch of this truss. The objectives of these tests were accomplished by constructing the square test frame with large members relative to the diagonal bracing so that the test frame has little influence on the limiting load of the frame. Load is applied at a joint of the truss as shown in Fig. 2. The maximum experimental load capacity of the test frame was determined and compared with the theoretical maximum capacity as determined by statics which was calculated using a zero load in the compression member after failure and assuming yield force in the tension diagonal. This comparison makes it possible to obtain data as to how the buckled compression diagonal aids in the load carrying capacity of the frame by redistributing the loads to the tension member.

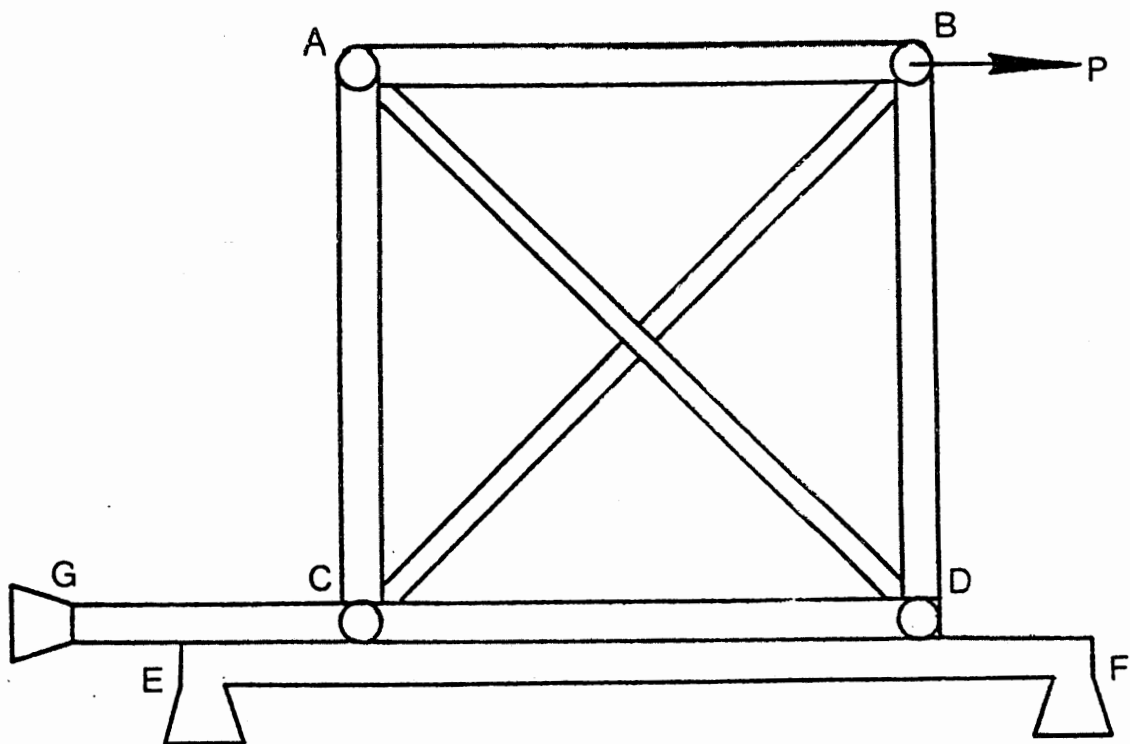


Figure 2 Indeterminate truss

CHAPTER II

EXPERIMENTAL PROGRAM FOR SINGLE ANGLE MEMBERS

2.1 OVERVIEW

This chapter documents the testing program of single angle beam-columns. Attention is given to the experimental setup, instrumentation and test procedure. Steel properties and coupon test results for these angles are included. Experimental results are compared with the load-displacement history predicted by the analytical computer model of Ref. 7.

2.2 EXPERIMENTAL SETUP FOR SINGLE ANGLE MEMBER TESTS

An MTS series 810 Electro-hydraulic Material Testing System was used to test the members. The load was applied using a hydraulic actuator which has a maximum capacity of 110,000 pounds. The system is able to control stroke of the actuator, load and strain.

A horizontal load frame was designed and constructed as part of this research. The load frame consists of two 40 foot long W 10 x 21 wide flanges spaced $47\frac{1}{4}$ inches apart and supported 12 $\frac{9}{16}$ inches from the floor. Lateral stability of this frame is provided by having 4 x 4 x $\frac{1}{4}$ steel angles as cross members across the top flanges of the two W 10 x 21's. The hydraulic actuator is reacted by a W 21 x 44 attached to the inside of the W 10 x 21's. Horizontal stability at the front of the actuator is provided by physical connection to each of the W 10 x 21's. To complete the framework at the other end, a W 21 x 44 reaction block is provided. The test member is then positioned between the front of the actuator and this reaction block. Figure 3 details this configuration.

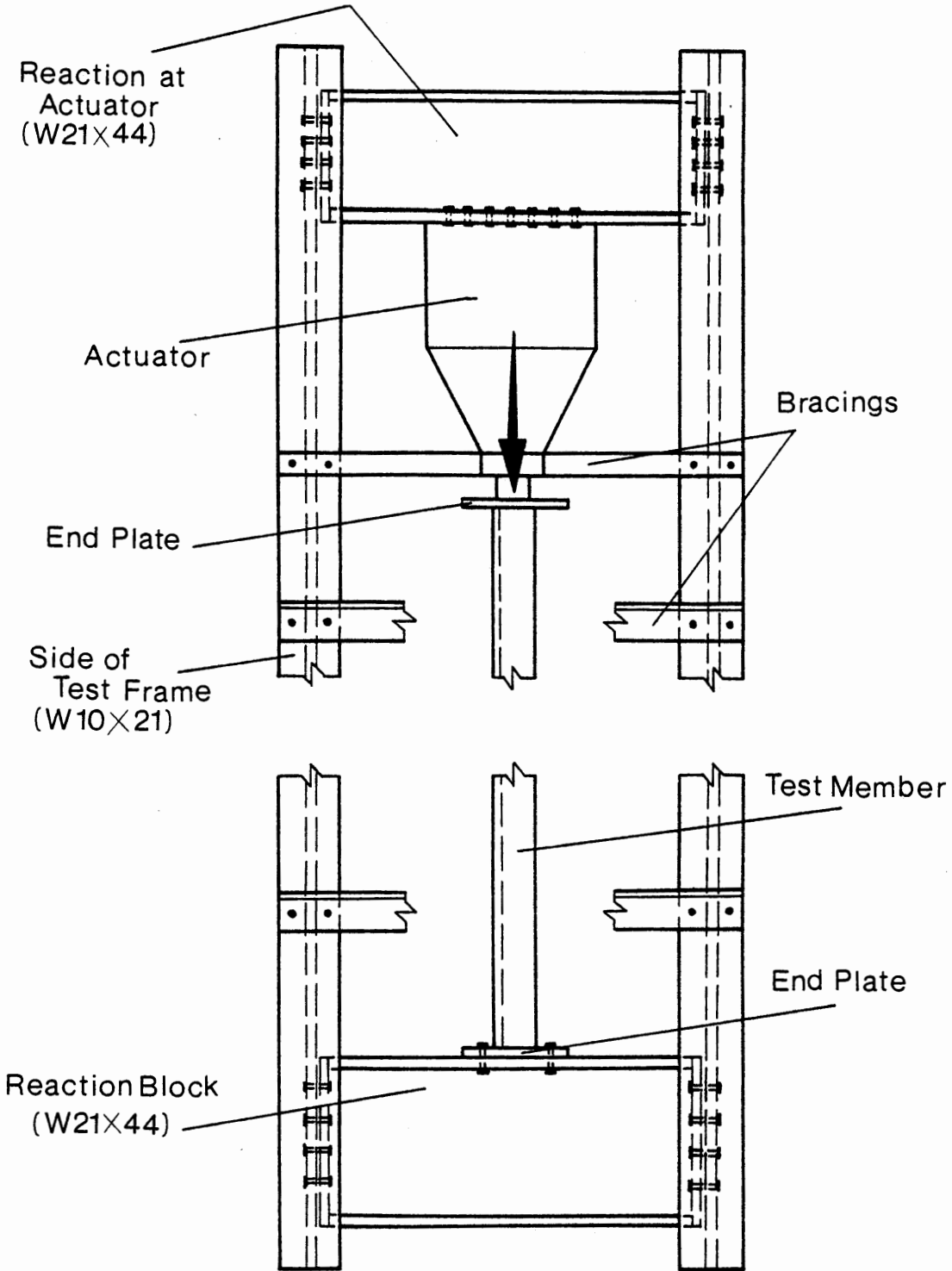


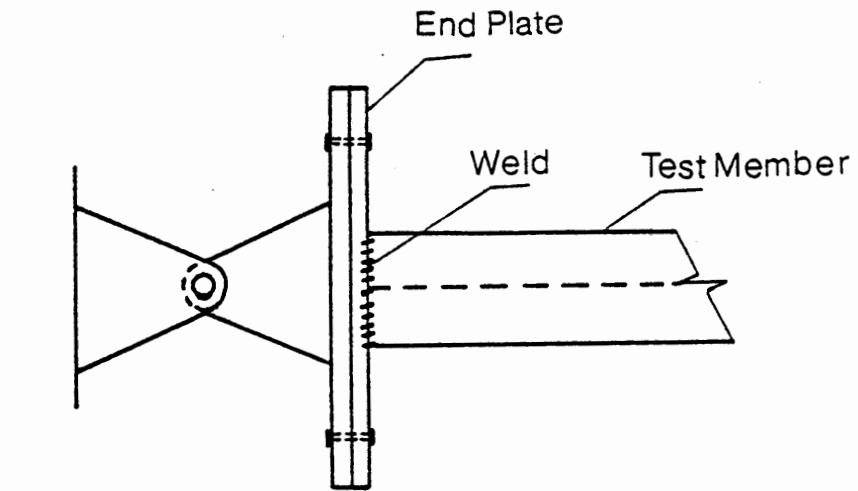
Figure 3 Experimental set up for single angle test member

Two 12" x 10" x $\frac{1}{2}$ " plates are used as end plates at each end of the test member to provide connection to the actuator and the reaction block.

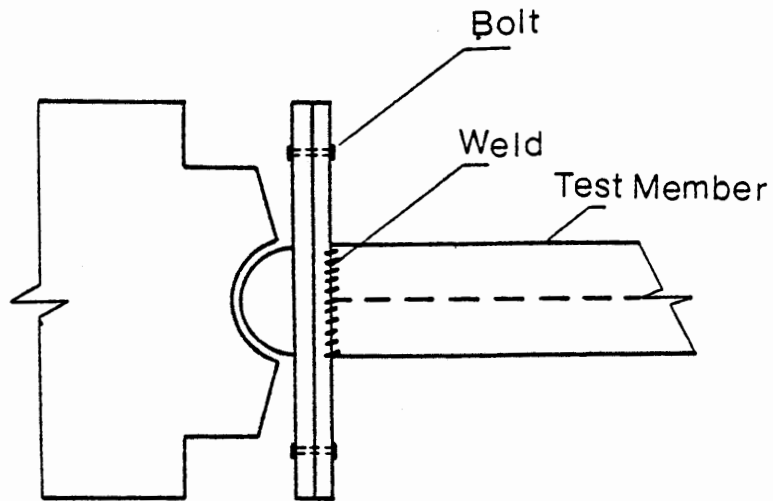
Details of connections of end plates are given in Fig. 4.

Figures 5 and 6 are two views of the experimental setup for single angle member tests. This configuration may be idealized as shown in Fig. 7. Figures 8 and 9 are photographs of the hinge end and the ball joint respectively. The set up for Fig. 9 has a bolted member end connection attached to the ball joint. The eccentricity of the axial load was obtained by connecting the end plates to the test member with the desired offset. A list of the members tested is given in Table 1.

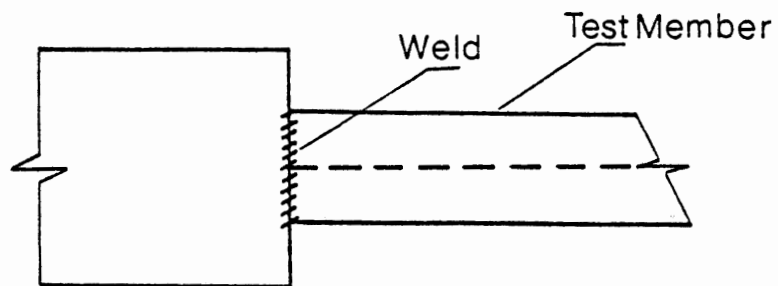
The end conditions consist of a hinge, a ball joint, a fixed end or a bolted connection. The hinged end condition was achieved by fabricating a rocker from a 1.25 inch diameter high strength rod which allowed rotation only about one axis. The ball joint end condition was a 4 inch diameter ball and socket machined to mate and lapped to obtain a contact fit. This ball joint was capable of rotating in all directions. High pressure grease was used to reduce friction in the ball joint. In a hinge or a ball joint the member was welded to the end plate and this plate was directly attached to the joint. A fixed end was achieved by welding the end of the test angle directly to a plate which was bolted to the reaction block of the test frame. Figure 4 details each of these attachments. A bolted joint consists of a bolt pattern as shown in Fig. 10 connecting the angle to be tested to a stub angle. This stub angle is then connected to a ball joint as its final attachment to the test frame. Bolts with $\frac{5}{8}$ inch diameter were used in this connection. The bolts were connected as tight as possible using a standard $\frac{15}{16}$ inch combination wrench. This bolted configuration was chosen to provide



(a) PINNED JOINT



(b) BALL JOINT



(c) FIXED JOINT

Figure 4 Details of end connections for single member tests

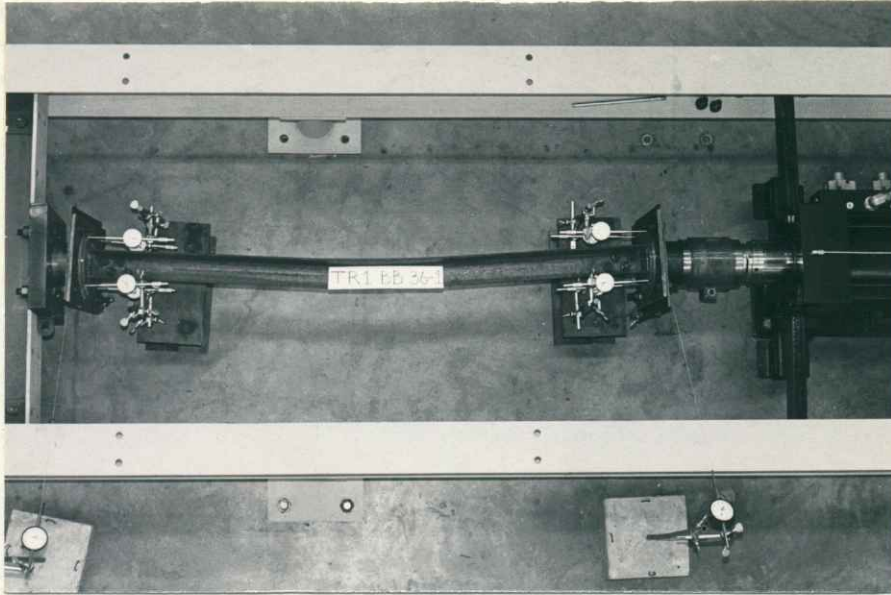


Figure 5. Experimental setup for single member tests

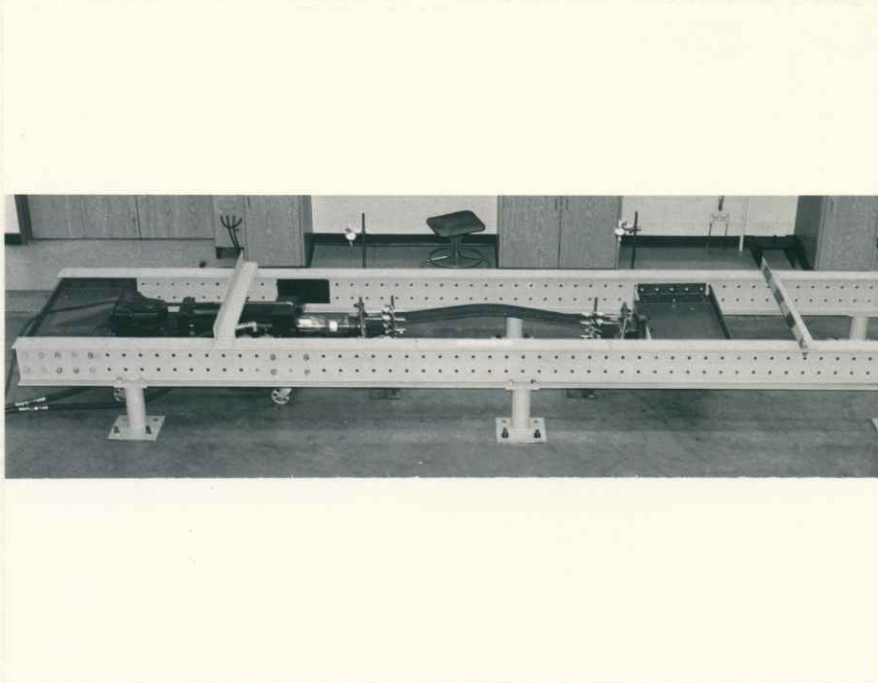


Figure 6. Experimental setup for single member tests

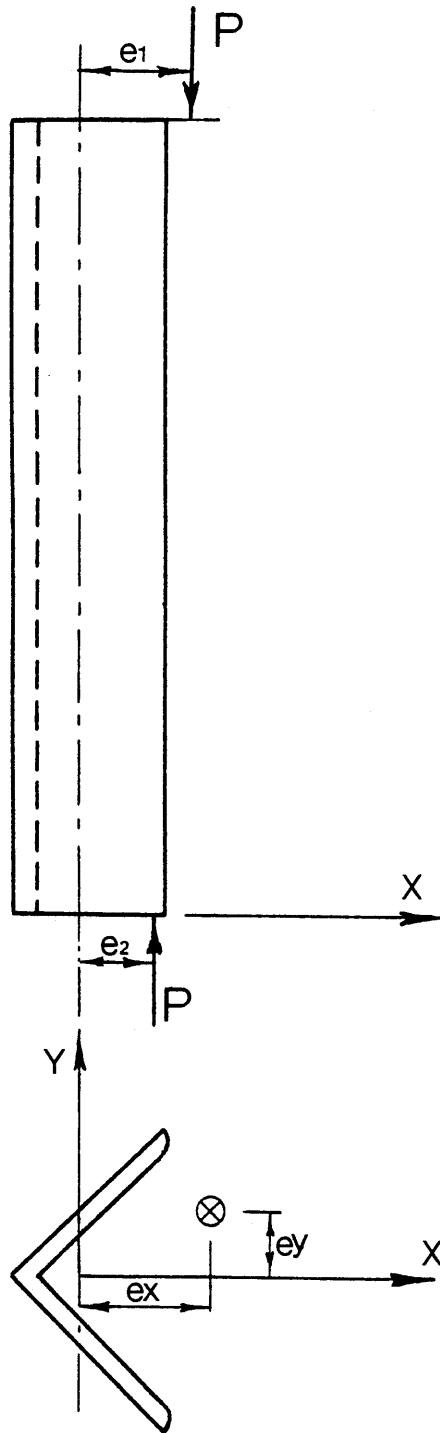


Figure 7 Loading configuration for single member tests



Figure 8. Hinged joint

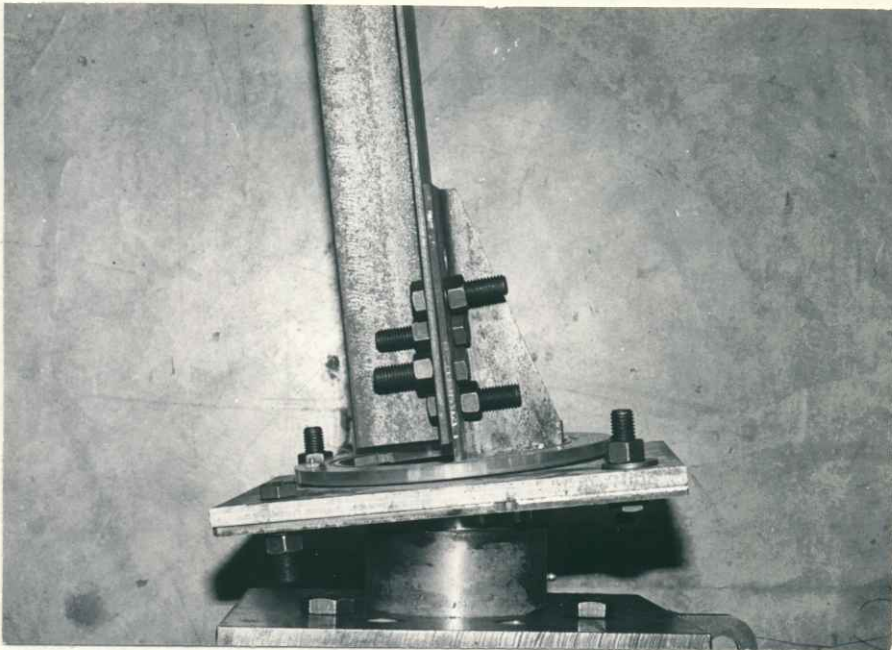


Figure 9. Bolted member end connection attached to the ball joint

TABLE I
TEST CONFIGURATION FOR SINGLE MEMBERS

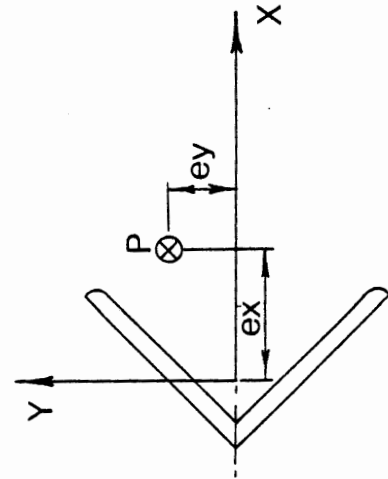
TEST	MEMBER SIZE	LENGTH (in.)	L/r	F _y (ksi)	ECCENTRICITIES (in.)				END CONDITIONS	
					TOP		BOTTOM		TOP	BOTTOM
					X	Y	X	Y		
S2 HH 50-2	3x3x $\frac{1}{4}$	117.625	198.7	56.4	-0.150	0	-0.250	0	H	H
S2 HH 36-1	3x3x $\frac{1}{4}$	117.625	198.7	54.8	0	0	-0.100	0	H	H
S2 HH 36-2	3x3x $\frac{1}{4}$	117.625	198.7	54.8	0	0	0	0	H	H
S1 HH 50-1	3x3x $\frac{1}{4}$	69.625	117.6	56.4	0	0	0	0	H	H
S1 HH 36-2	3x3x $\frac{1}{4}$	69.625	117.6	54.8	0	0	0	0	H	H
S3 BB 36-1	3x3x $\frac{1}{4}$	36.000	60.8	54.8	-0.200	0	-0.200	0	BJ	BJ
S3 BB 36-2	3x3x $\frac{1}{4}$	36.000	60.8	54.8	+0.200	0	+0.200	0	BJ	BJ
S1 BB 36-2	3x3x $\frac{1}{4}$	66.000	111.5	54.8	+0.200	0	+0.200	0	BJ	BJ
S2 BB 36-3	3x3x $\frac{1}{4}$	114.000	192.6	50.6	+0.200	0	+0.200	0	BJ	BJ
T2 BB 50-1	3x3x $\frac{1}{4}$	114.000	192.6	53.8	-0.086	-1.105	-0.086	-1.105	B	B
T2 BB 36-1	3x3x $\frac{1}{4}$	114.000	192.6	54.8	-0.086	-1.105	-0.086	-1.105	B	B
T1 BB 36-1	3x3x $\frac{1}{4}$	66.000	111.5	54.8	-0.086	-1.105	-0.086	-1.105	B	B
T1 BB 50-1	3x3x $\frac{1}{4}$	66.000	111.5	53.8	-0.086	-1.105	-0.086	-1.105	B	B
T3 BB 50-1	3x3x $\frac{1}{4}$	36.000	60.8	53.8	-0.086	-1.105	-0.086	-1.105	B	B
T3 BB 36-1	3x3x $\frac{1}{4}$	36.000	60.8	54.8	-0.086	-1.105	-0.086	-1.105	B	B
S3 BB 50-1	3x3x $\frac{1}{4}$	36.000	60.8	56.4	+0.200	+1.390	+0.200	+1.390	B	B
S0 BB 50-1	3x3x $\frac{1}{4}$	90.000	152.0	56.4	0	0	0	0	B	B
T2 BF 50-1	3x3x $\frac{1}{4}$	114.000	192.6	53.8	-0.086	-1.105	-0.086	-1.105	B	F
T2 BF 36-1	3x3x $\frac{1}{4}$	114.250	193.0	54.8	-0.086	-1.105	-0.086	-1.105	B	F

continued on the next page

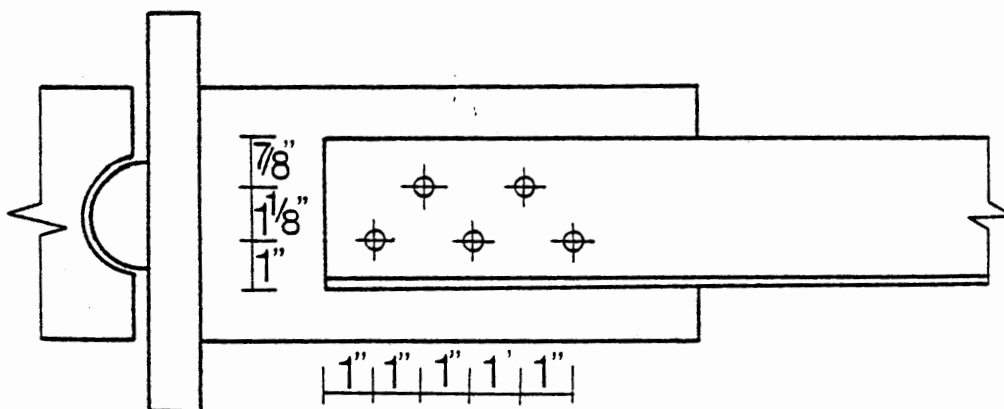
TABLE I (continued)

TEST CONFIGURATION FOR SINGLE MEMBERS

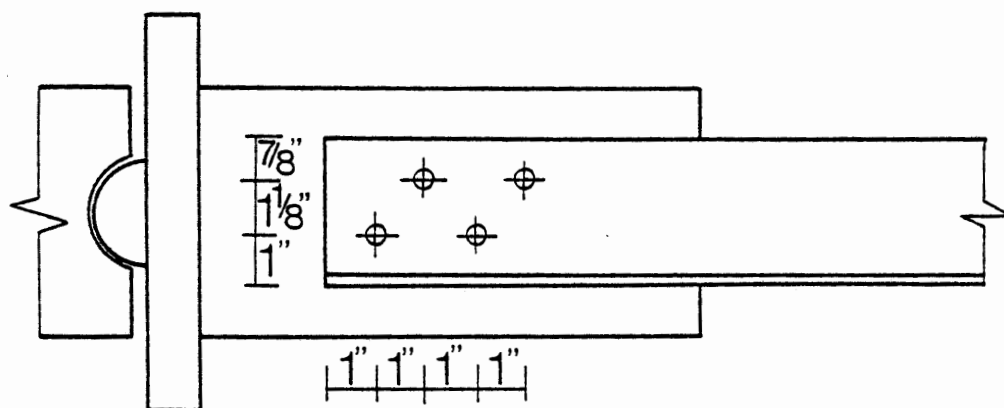
TEST	MEMBER SIZE	LENGTH (in.)	L/r	FY (ksi)	ECCENTRICITIES (in.)				END CONDITIONS	
					TOP		BOTTOM		TOP	BOTTOM
					X	Y	X	Y		
SR3 BB 36-1	3x3x $\frac{1}{4}$	36.000	60.8	54.8	-0.200	0	-0.200	0	BJ	BJ
TR3 BB 50-1 (1)	3x3x $\frac{1}{4}$	36.000	60.8	61.3	-0.086	-1.105	-0.086	-1.105	B	B
TR3 BB 50-1	3x3x $\frac{1}{4}$	36.000	60.8	61.3	-0.086	-1.105	-0.086	-1.105	B	B
TR2 BB 50-1	3x3x $\frac{1}{4}$	113.750	192.6	51.0	-0.086	-1.105	-0.086	-1.105	B	B
TR1 BB 36-1	3x3x $\frac{1}{4}$	113.750	111.5	61.3	-0.086	-1.105	-0.086	-1.105	B	B
T4 BB 36-1	5x3x $\frac{1}{4}$	132.625	200.0	48.1	0.200	0	0.200	0	B	B
T4 BB 36-2	5x3x $\frac{1}{4}$	132.625	200.0	48.1	0.200	0	0.200	0	B	B



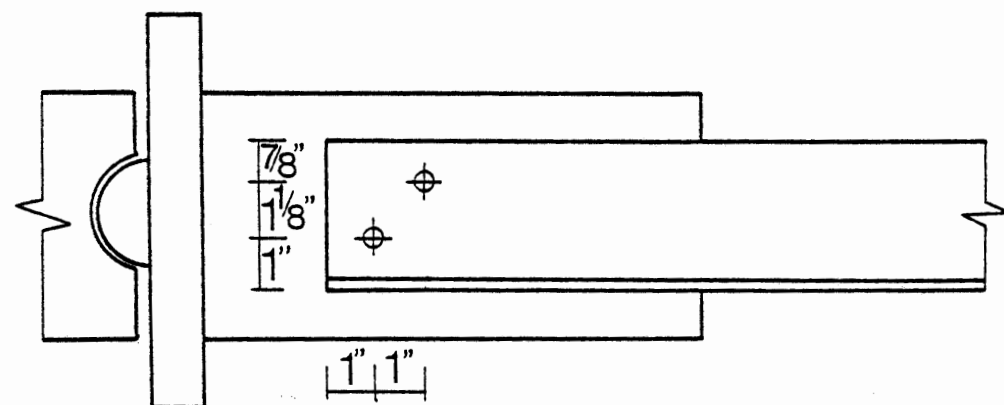
H - HINGED JOINT
 F - FIXED JOINT
 B - BOLTED JOINT
 BJ - BALL JOINT



36 in. Members



66 in. Members



114 in. Members

Figure 10 Bolted connections for single member tests

eccentricities similar to those found in transmission towers.

2.3 INSTRUMENTATION

The instrumentation was similar for each of the angles tested. The MTS was used to load the specimen. As stated earlier in this chapter, this system has the capability to control actuator stroke. Since these tests were beyond the point of stability, safety dictated the use of stroke control. The stroke rate was set at 10^{-4} inch per second which resulted in a stress rate of 0.08 ksi per second for the shortest member tests. ASTM (9) specification for static tests is a stress rate of less than 1.66 ksi per second. The load value was read directly from the MTS control panel.

Four dial gages at each end were used to measure the axial deflection and end rotation. They were placed an equal distance from the center of the endplate to form a square. Figure 11 is a photograph of this configuration. Taking measurements at each end allowed the elimination of the effect of test frame slippage on the displacement readings.

In the case of a Ball or a Bolted Joint where a Ball-Ball connection is used, the rotation of the joint about the axis of the test member is possible. This rotation at the ends of the test member was measured by a dial gage located perpendicular to the beam column at each end and connected by a circular offset to the center of gravity of the member. This circular offset allowed unwinding of the connecting cable and hence kept the offset constant. Figure 12 is a sketch of this setup. Rotation is given by the gage reading (linear displacement of the circumference of the circle) divided by the radius of the circle. Figure 13 is a sketch of gage layout for the test member including the gages used for

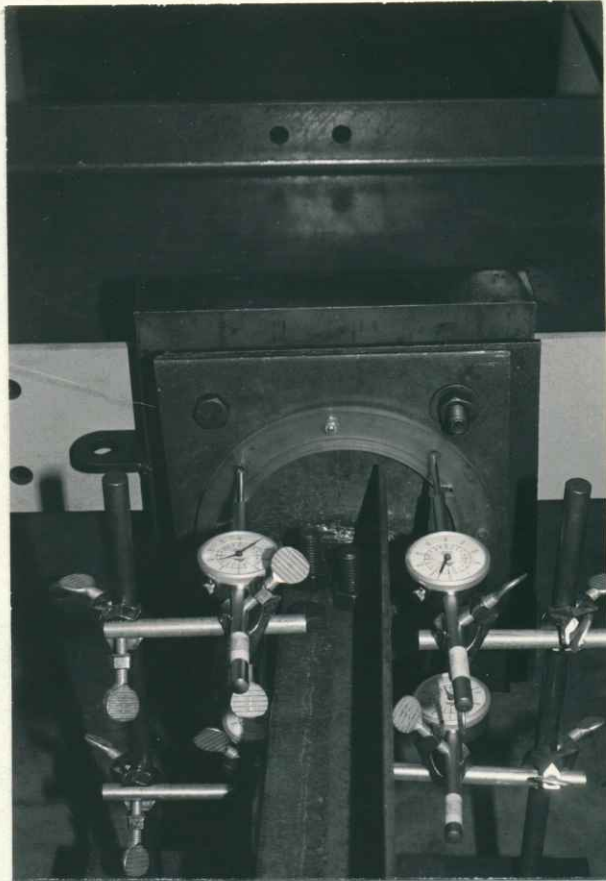


Figure 11. Dial gage setup for measuring displacements

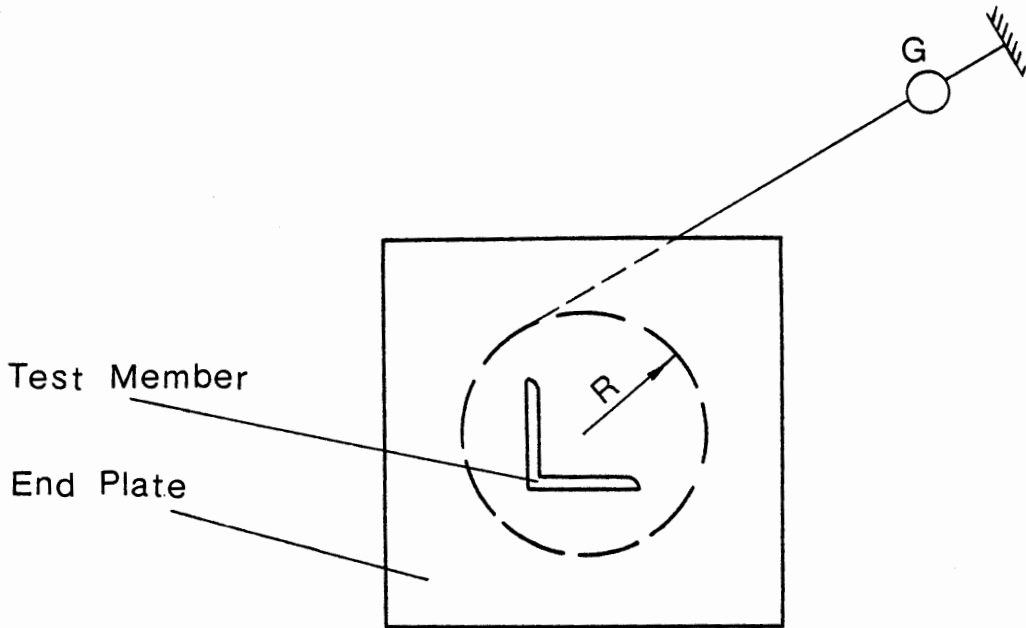


Figure 12 Gage layout to measure rotation about the axis of the member

measuring rotations about the axis of the test member.

2.4 TEST PROCEDURE

The purpose of the chosen test procedure is to ensure that valid load vs. axial deflection data is obtained. To determine load resistance of the member, readings of load and axial deflection were taken at pre-determined intervals chosen to be approximately 20% of the expected failure load. A loading rate was chosen to ensure that the static load resistance of the member could be determined.

The test procedure was as follows.

- a) Load the member to 15% of the expected ultimate failure of the member, (this load was estimated using Euler buckling criteria) and take initial readings of the dial gages.
- b) Readings of dial gages are taken for each load where the increment of load was 20% of the failure load.
- c) Continue to deform the member beyond its ultimate load in decrements of 15% of the ultimate load. Readings of dial gages are taken at these intervals.
- d) Resetting of gages was done just before any of the dial gages reached their maximum range. The reading of such a gage in its current position is noted and then moved to a new position either towards or away from the plate to facilitate further readings with the same set of gages. Reading at this new position is again noted, and the difference in reading due to resetting is accounted for when calculating the axial displacements.
- e) Terminate the test when the load was reduced to 20% of the

ultimate load.

2.5 COMPUTATION OF AXIAL DISPLACEMENT

The single angle member tests were configured using two types of end connections which connects the endplates to the actuator or the reaction block. They are the Hinged-Hinged and the Ball-Ball configurations. The Hinge in the Hinged-Hinged configuration was 1.75 inches from the end plate. The ball of the Ball-Ball configuration was fabricated such that the center of the ball coincides with the center of the end plate.

Derivation of axial displacement and the computer program to calculate this axial displacement for the Hinged-Hinged configuration is documented in Appendix A. Derivation of axial displacement and the computer program to calculate this axial displacement documented in Appendix B is for the Ball-Ball configuration. Derivation for this configuration takes into account the eccentricity of the test member.

2.6 STEEL PROPERTIES AND COUPON TESTS

To obtain data on the material properties of the steel angles tested, coupon tests were performed using the MTS system. Tests were done for each batch of steel angles and for each grade of steel A-36 and Grade 50. Two coupons for the same material were cut in the longitudinal direction from a section of angle member. These were tested using load control with a load rate of 110 lb/sec which corresponds to a stress rate of 450 psi/sec.

One of the test results obtained in the form of a stress-strain

curve is illustrated in Fig. 14. All other coupon test curves followed the same shape as this curve, with a well defined yield point and large plastic deformation which are typical of mild steel materials. Table II details the Yield stress, Ultimate stress, Modulus of Elasticity and Percent Elongation for each test. Percent elongation is a measure of ductility of the material.

2.7 COMPARISON OF EXPERIMENTAL AND ANALYTICAL RESULTS FOR SINGLE ANGLE MEMBER TESTS

The derivation of axial displacements using the data obtained in the single member tests, and the computer programs to perform these calculations are documented in Appendix A and B. Appendix A is for the members with the hinged end condition. Appendix B documents these calculations for the members where the end plates are connected through a ball joint. Axial load vs. Axial displacement (P vs δ) curves are plotted for each of these tests. Displacement at preload was taken as datum for measurements.

The P vs δ curves plotted includes the experimental test curve as well as the prediction of the member behavior of the analytical computer program of Ref. 7. The analytical computer model of Ref. 7 is a non-linear computer code which includes the analysis in the post-buckling region. The buckling modes considered includes flexural, torsional and combined flexural-torsional. The "secant stiffness" approach was selected in this to consider the yielding of cross sections both prior to the ultimate load and in the post-buckling range. In two dimension analysis the "secant stiffness" at a particular point in the moment-curvature diagram is the gradient of the line joining the origin and that particular point.

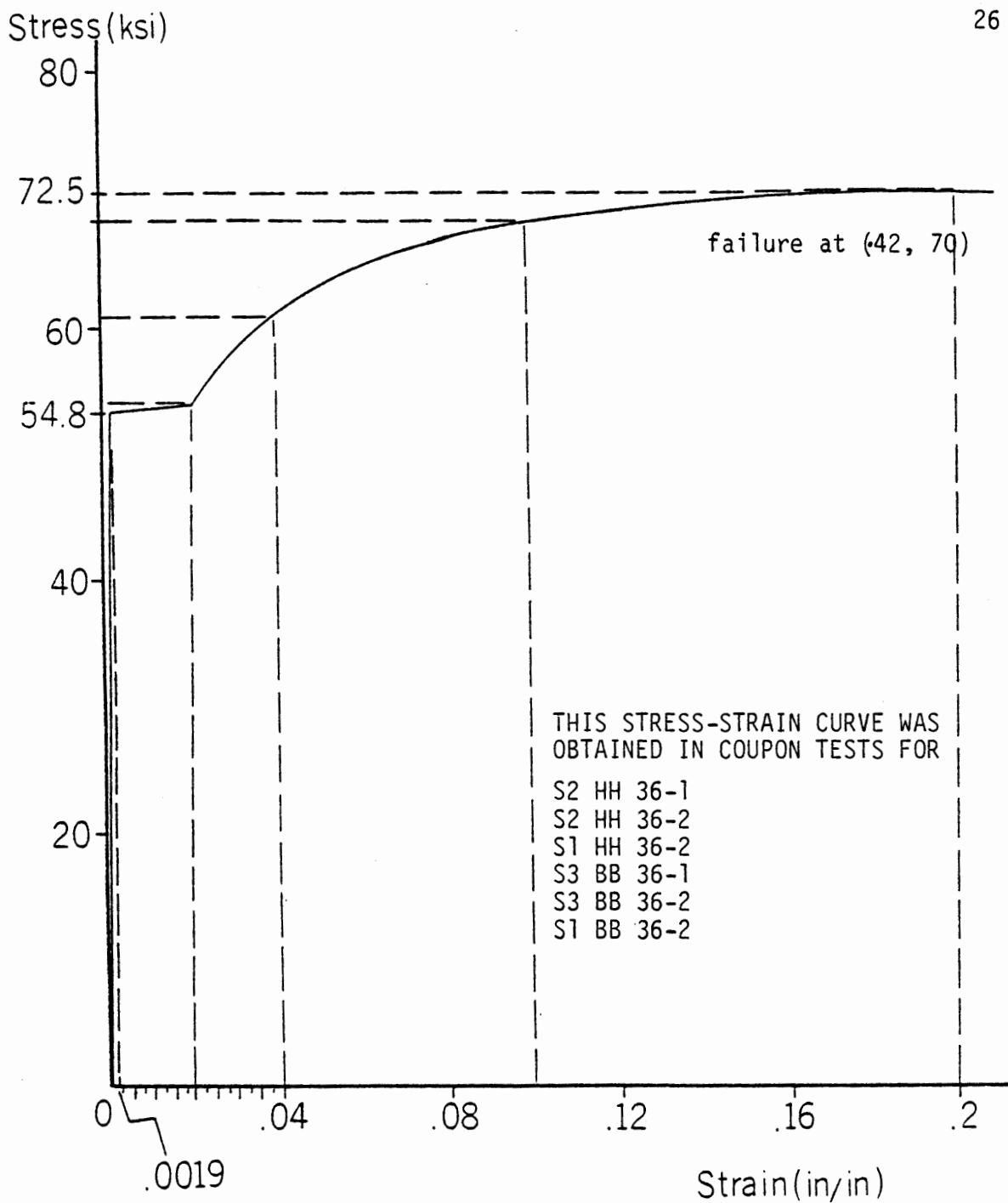


Figure 14 Typical stress strain curve

TABLE II
RESULTS OF COUPON TESTS FOR SINGLE MEMBER TESTS

TEST	YIELD STRESS (KSI)	ULTIMATE STRESS (KSI)	MODULUS OF ELASTICITY (KSI)	PERCENTAGE ELONGATION (%)
S2 HH 50-2	56.4	73.5	29100.0	42.0
S2 HH 36-1	54.8	72.5	30700.0	41.5
S2 HH 36-2	54.8	72.5	30700.0	41.5
S1 HH 50-1	56.4	73.5	29100.0	42.0
S1 HH 36-2	54.8	72.5	30700.0	41.5
S3 BB 36-1	54.8	72.5	30700.0	41.5
S3 BB 36-2	54.8	72.5	30700.0	41.5
S1 BB 36-2	54.8	72.5	30700.0	41.5
S2 BB 36-3	50.6	68.4	30325.0	38.0
T2 BB 50-1	53.8	76.3	29100.0	40.0
T2 BB 36-1	54.8	71.2	29100.0	38.0
T1 BB 36-1	54.8	71.2	29100.0	38.0
T1 BB 50-1	53.8	76.3	29100.0	40.0
T3 BB 50-1	53.8	76.3	29100.0	40.0
T3 BB 36-1	54.8	71.2	29100.0	38.0
S3 BB 50-1	56.4	73.5	29100.0	42.0
S0 BB 50-1	56.4	73.5	29100.0	42.0
T2 BF 50-1	53.8	76.3	29100.0	40.0
T2 BF 36-1	54.8	71.2	29100.0	38.0
SR3 BB 36-1	54.8	71.2	29100.0	38.0
TR3 BB 50-1 (1)	61.3	78.5	29400.0	32.0
TR3 BB 50-1	61.3	78.5	29400.0	32.0
TR2 BB 50-1	51.0	67.8	29200.0	34.0
TR1 BB 36-1	61.3	79.0	29300.0	32.0
T4 BB 36-1	48.1	63.0	29000.0	37.0
T4 BB 36-2	48.1	63.0	29000.0	37.0

The stiffness of the member is adjusted using this method in the inelastic and post-buckling region to predict the load-deflection curve.

The P vs δ curves given in Figs. 15 to 40 detail the comparison of experimental and analytical results for all the single member tests performed.

Tests performed can be placed in the following five categories:

- (1) Equal angle test members with hinged-hinged end configuration
- (2) Equal angle test members with ball-ball end configuration with 0.2 in. eccentricity in the X-direction only (Fig. 13)
- (3) Equal angle test members with bolted connection having eccentricity in the X and Y directions (Fig. 13)
- (4) Equal angle test members with bolted configuration at one end and fixed at the other end.
- (5) Unequal angle test members with ball-ball configurations.

These five categories were sufficient to study the effect of various parameters that are of concern in member performance of single angle members. In the first category basically the effect of length to radius of gyration (L/r) ratio and the yield stress were the parameters used. In the second category the effect of L/r ratio, yield stress and the eccentricity of loading on the stronger axis were used to study the effect of these on the member behavior. The eccentricity of loading on the weaker axis and the effect of bolted connection were the new parameters used in the third category. As the effect of local buckling in member behavior of non compact long members are of concern, the last category includes these members.

Table III compares the experimental and analytical values of ultimate

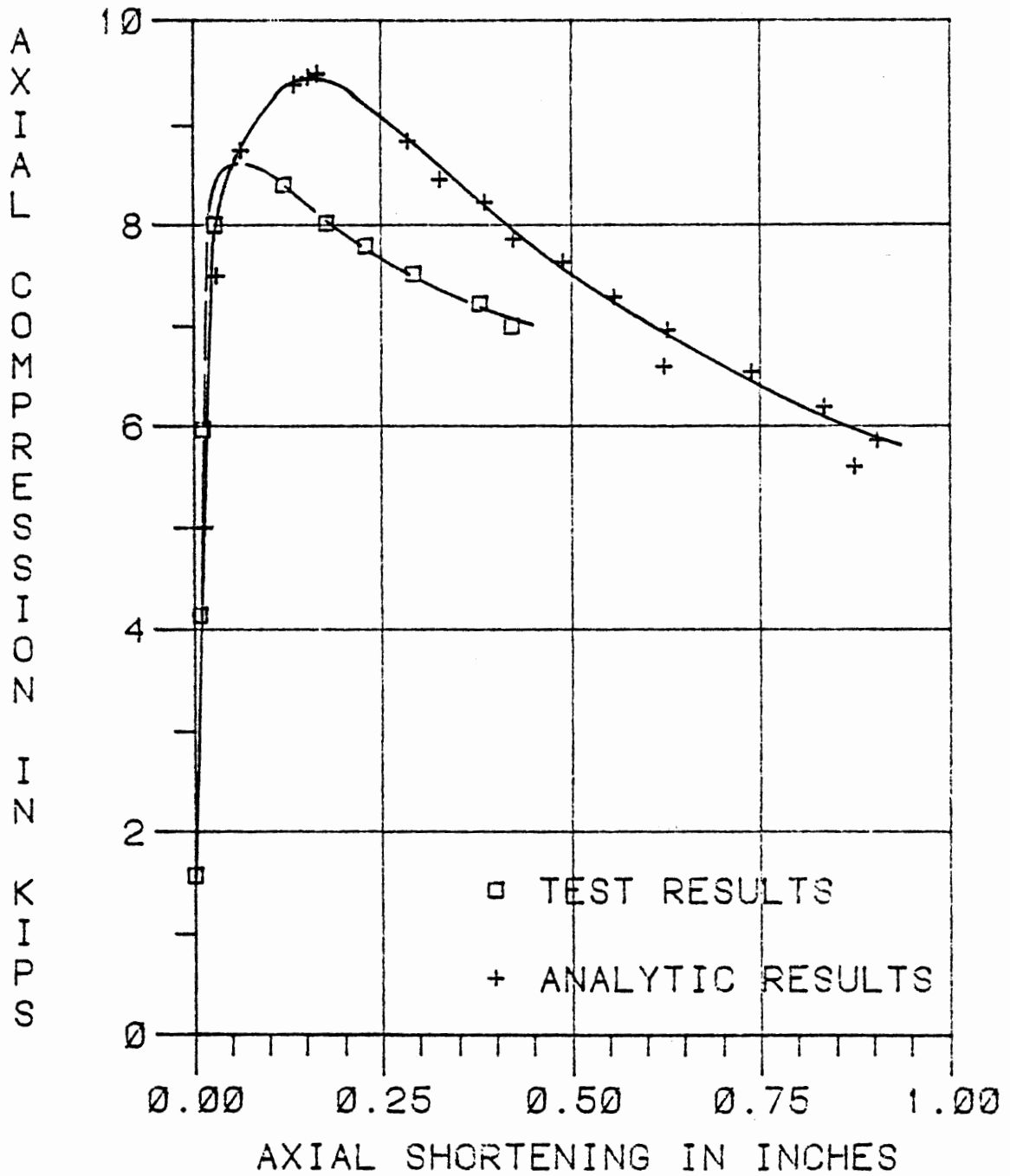
TEST S2 HH 50-2 $L/r=198.7$ 

Figure 15. Test S2 HH 50-2

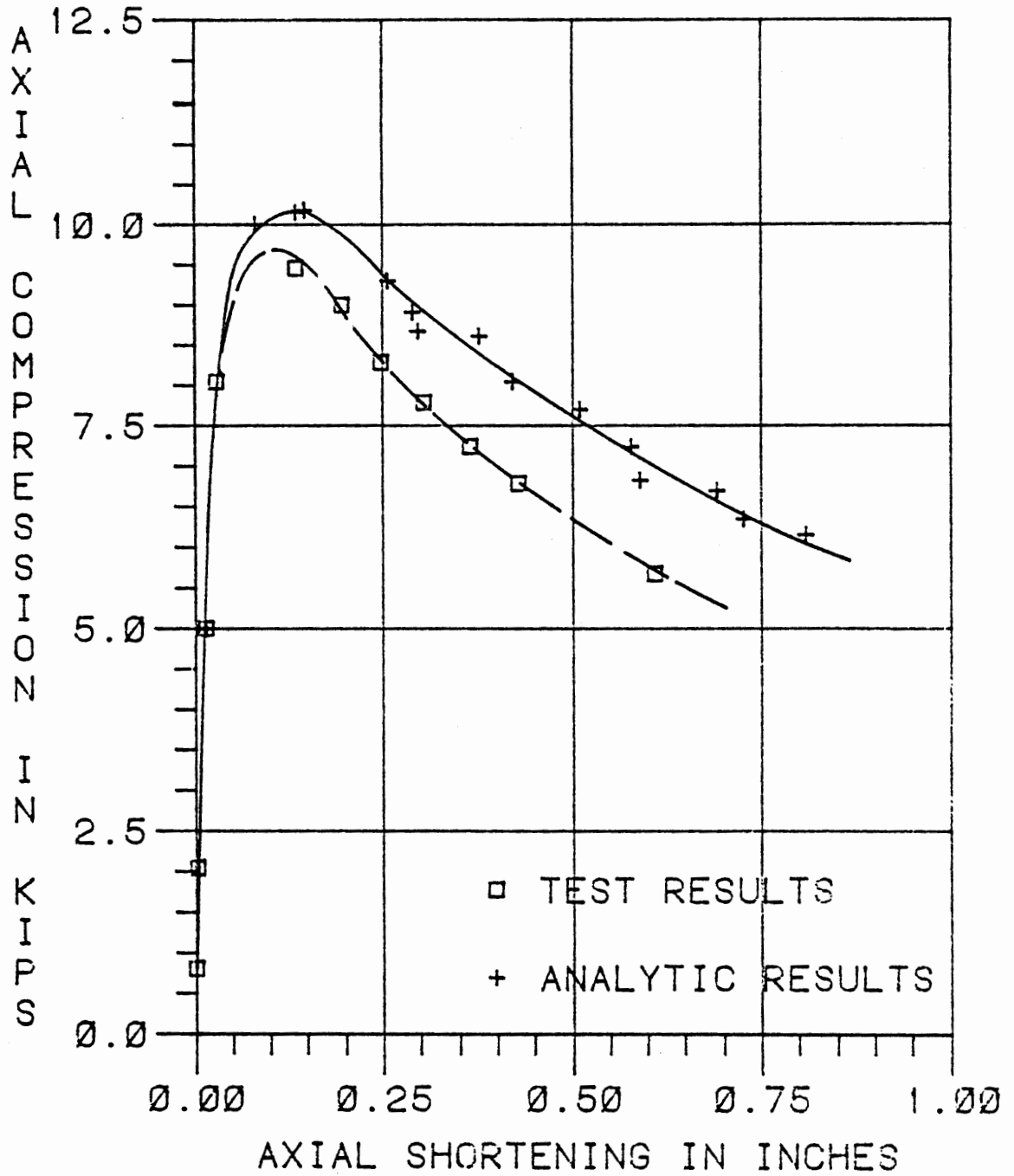
TEST S2 HH 36-1 $L/r=198.7$ 

Figure 16. Test S2 HH 36-1

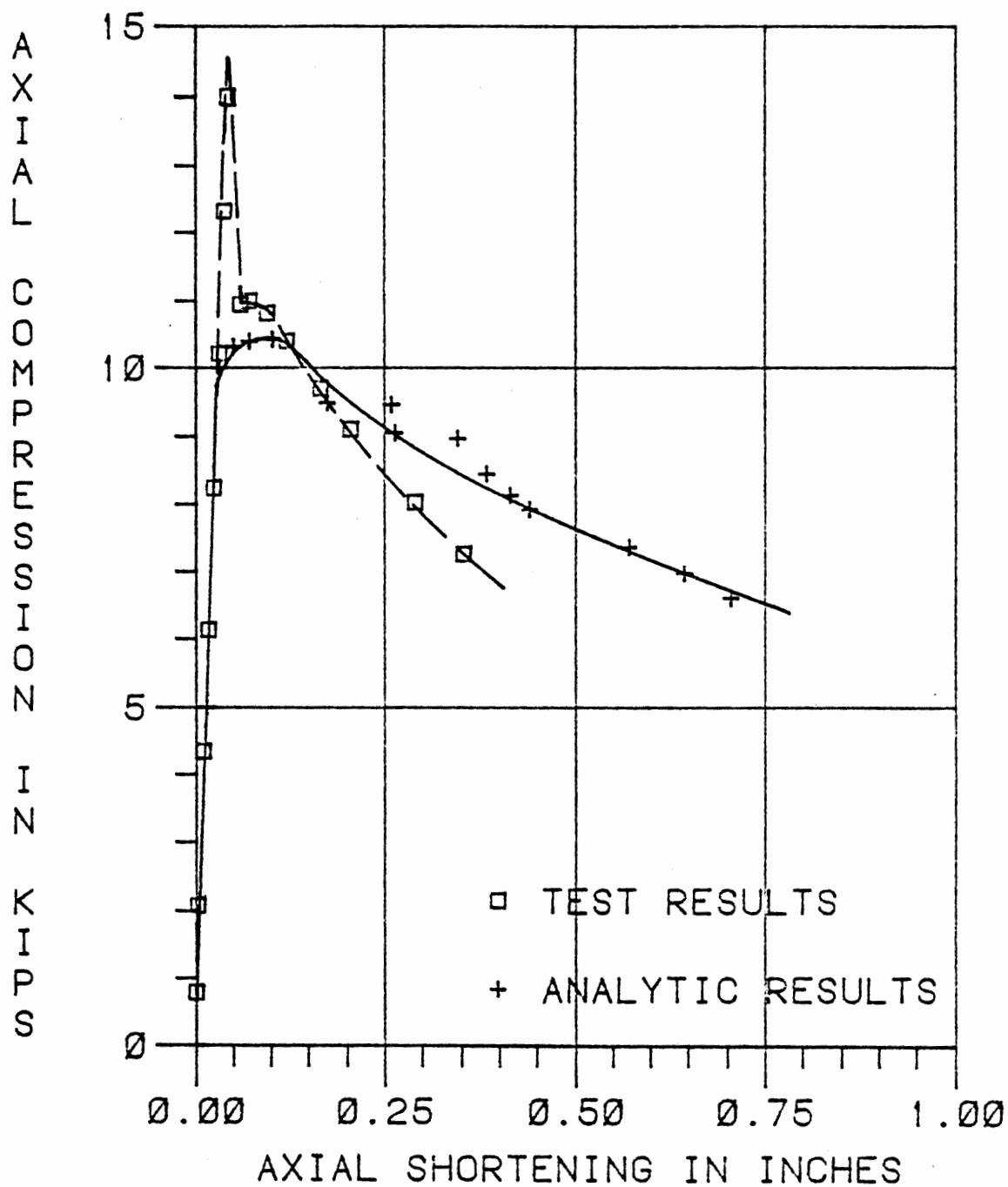
TEST S2 HH 36-2 $L/r=198.7$ 

Figure 17. Test S2 HH 36-2

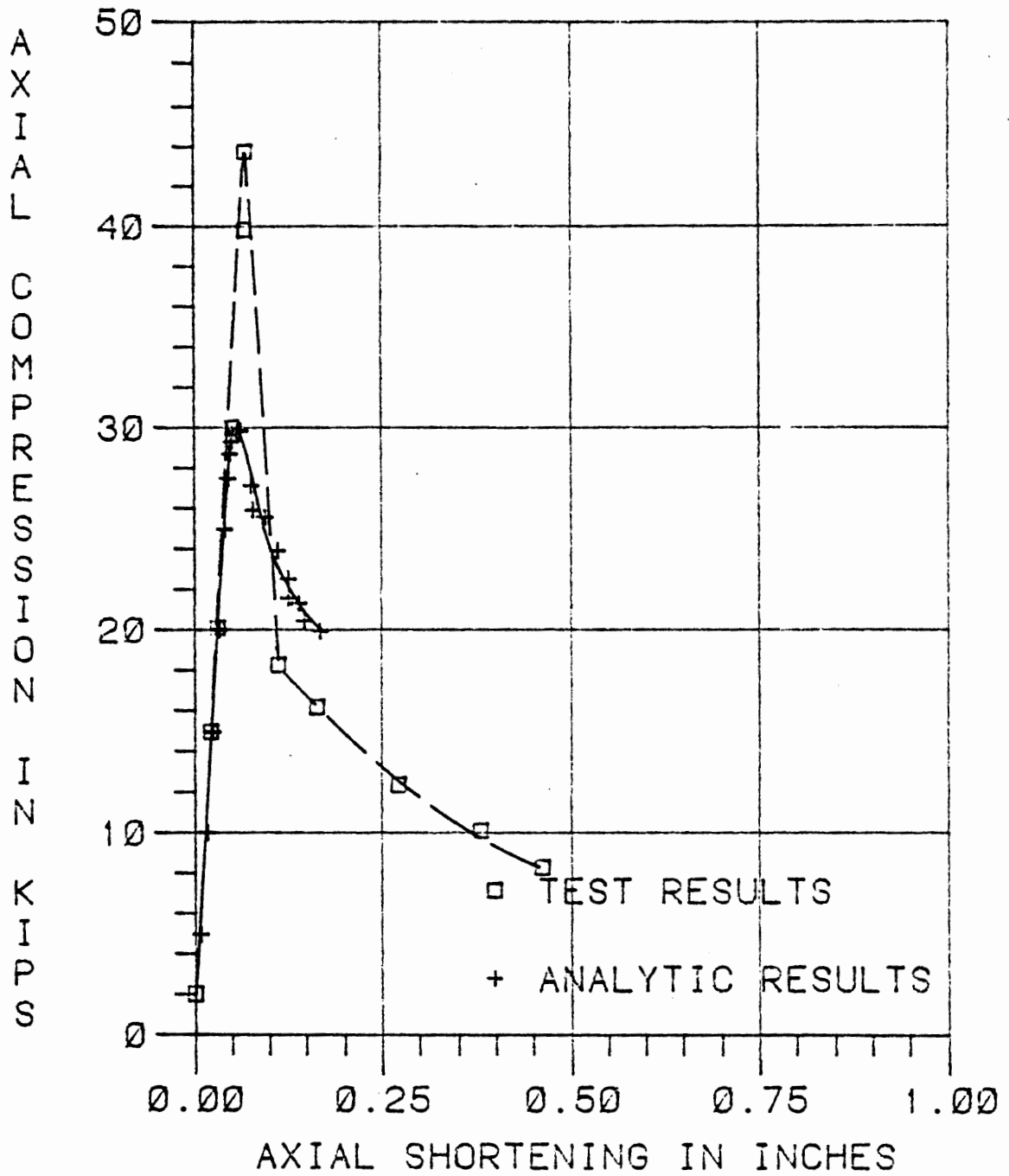
TEST S1 HH 50-1 $L/r=117.6$ 

Figure 18. Test S1 HH 50-1

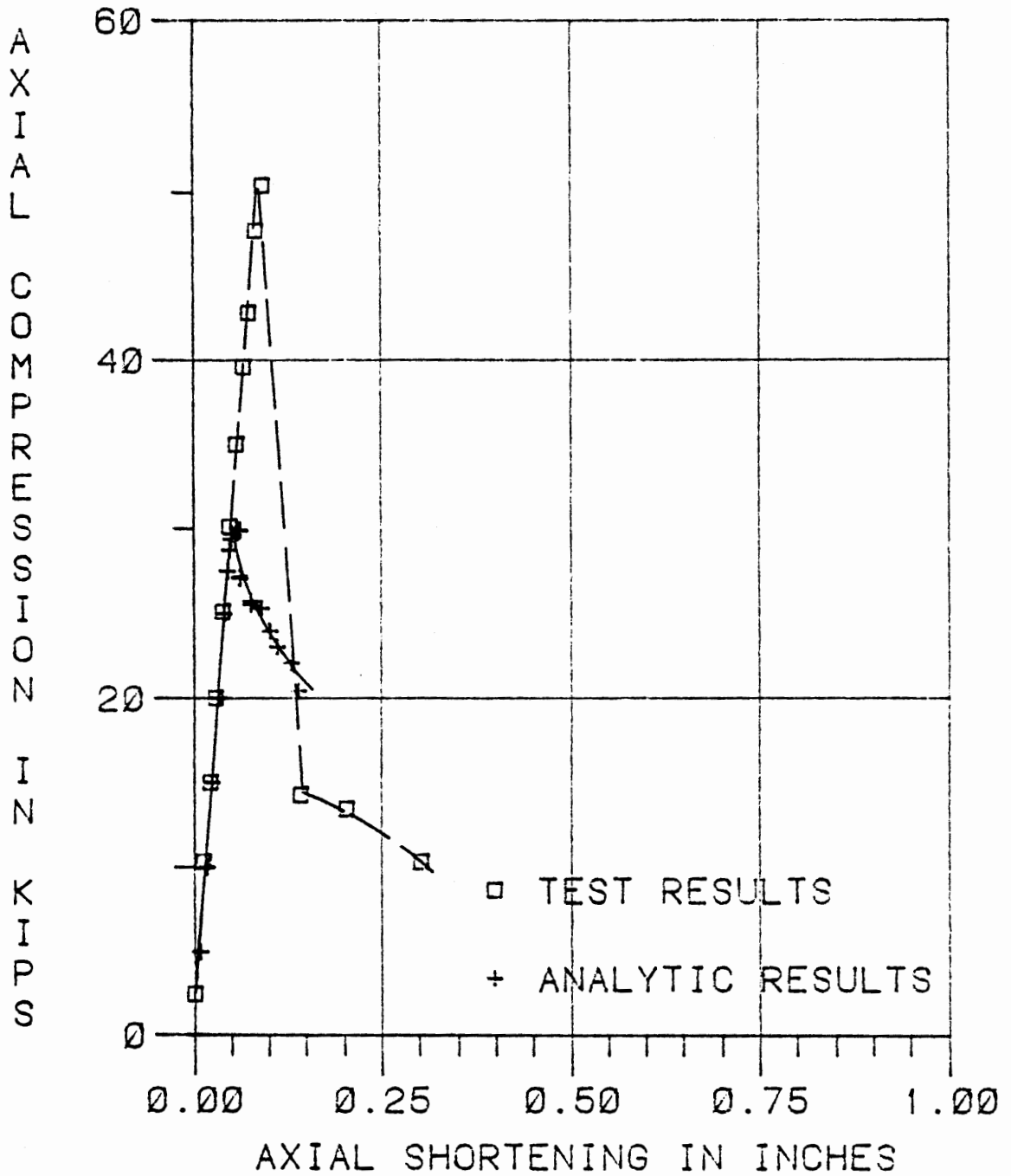
TEST S1 HH 36-2 $L/r=117.6$ 

Figure 19. Test S1 HH 36-2

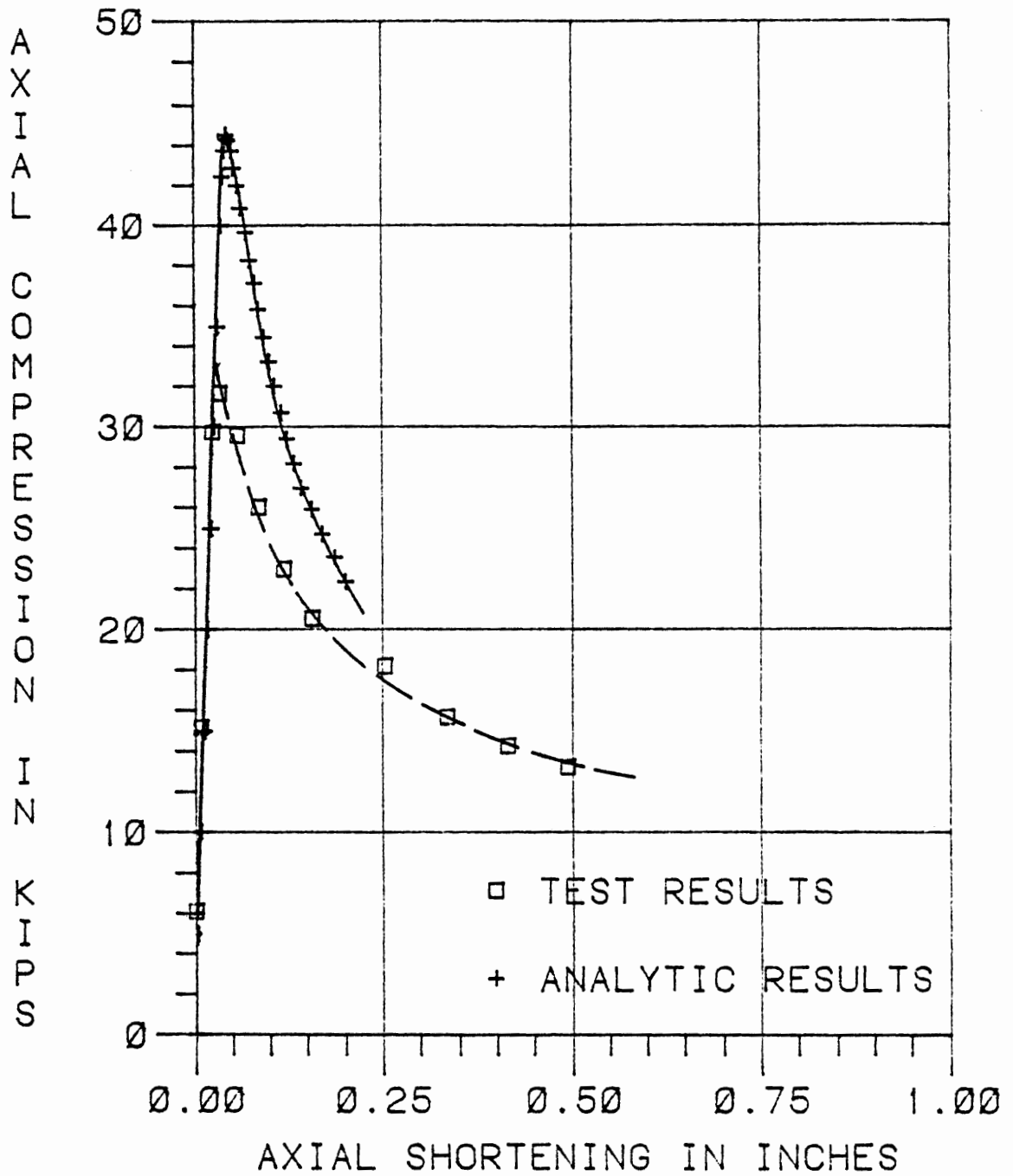
TEST S3 BB 36-1 $L/r=60.8$ 

Figure 20. Test S3 BB 36-1

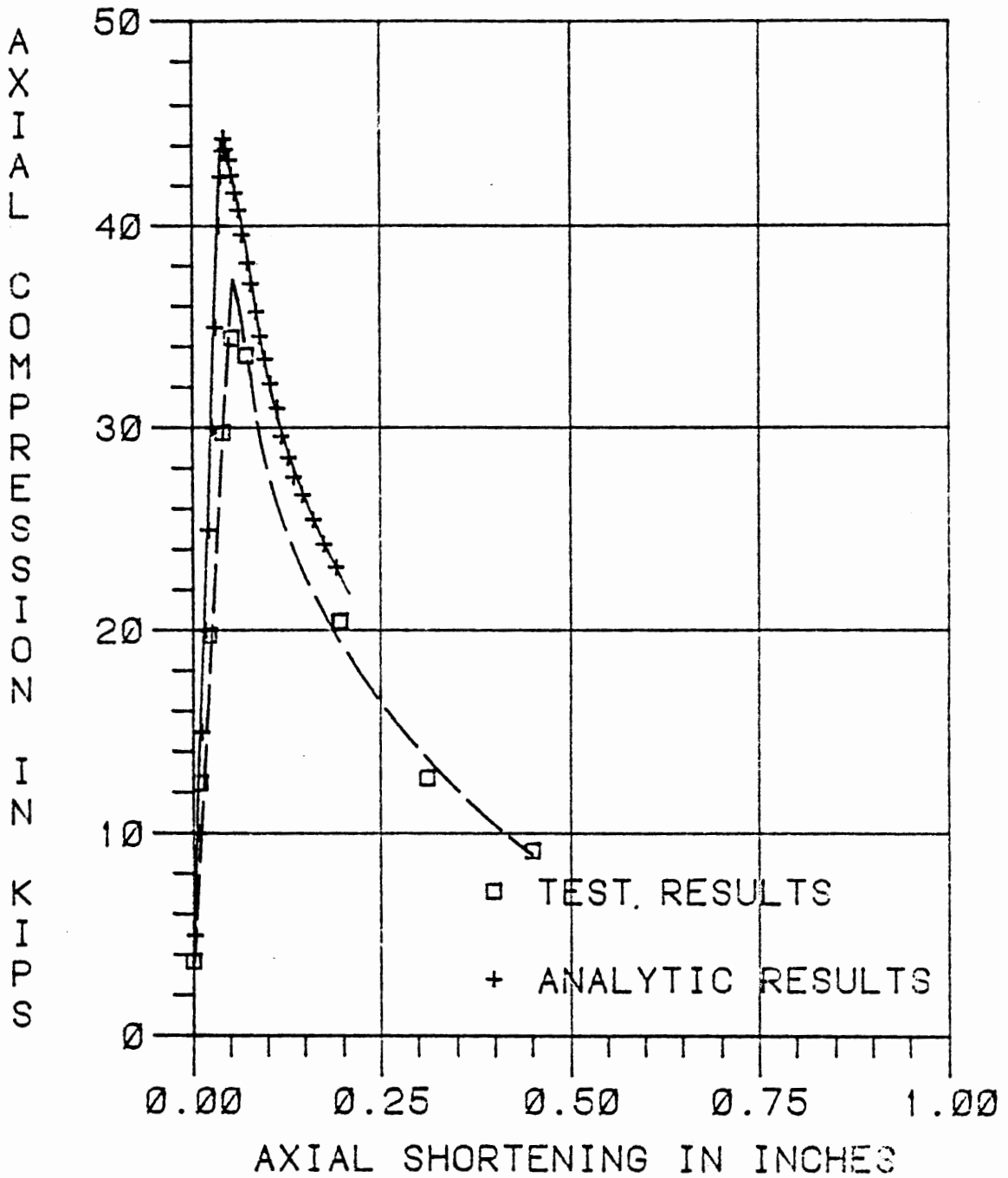
TEST S3 BB 36-2 $L/r=60.8$ 

Figure 21. Test S3 BB 36-2

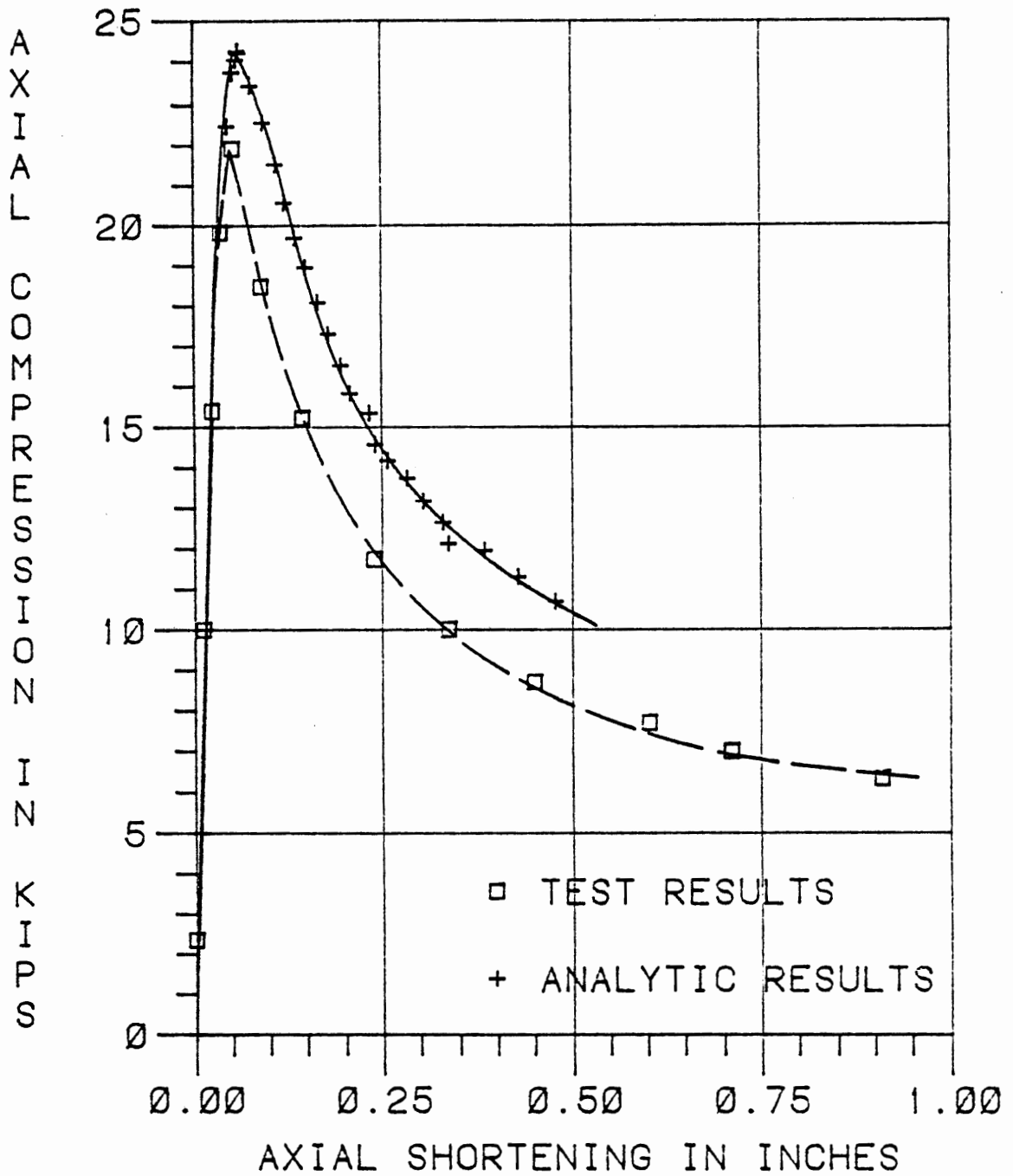
TEST S1 BB 36-2 $L/r=111.5$ 

Figure 22. Test S1 BB 36-2

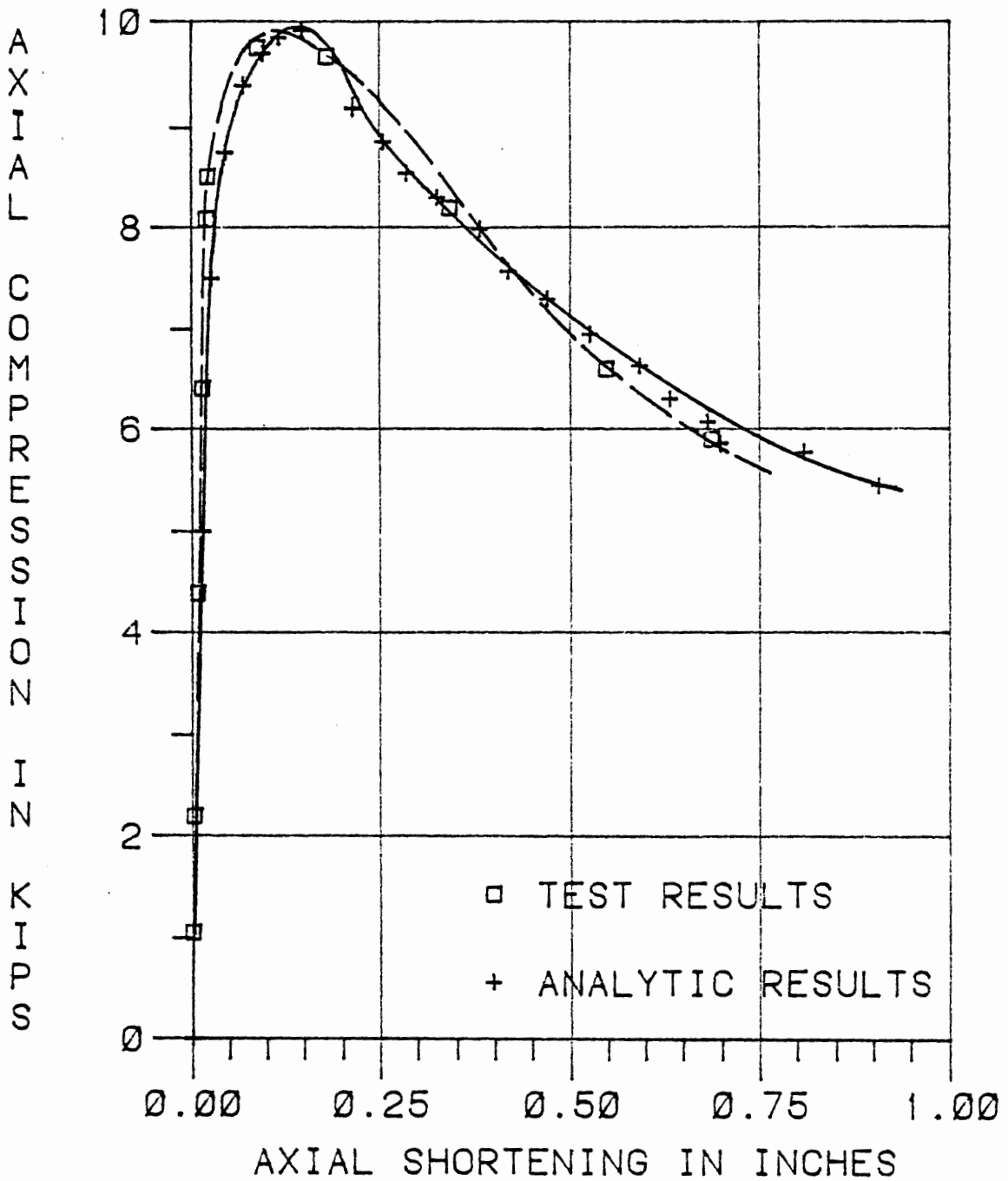
TEST S2 BB 36-3 $L/r=192.6$ 

Figure 23. Test S2 BB 36-3

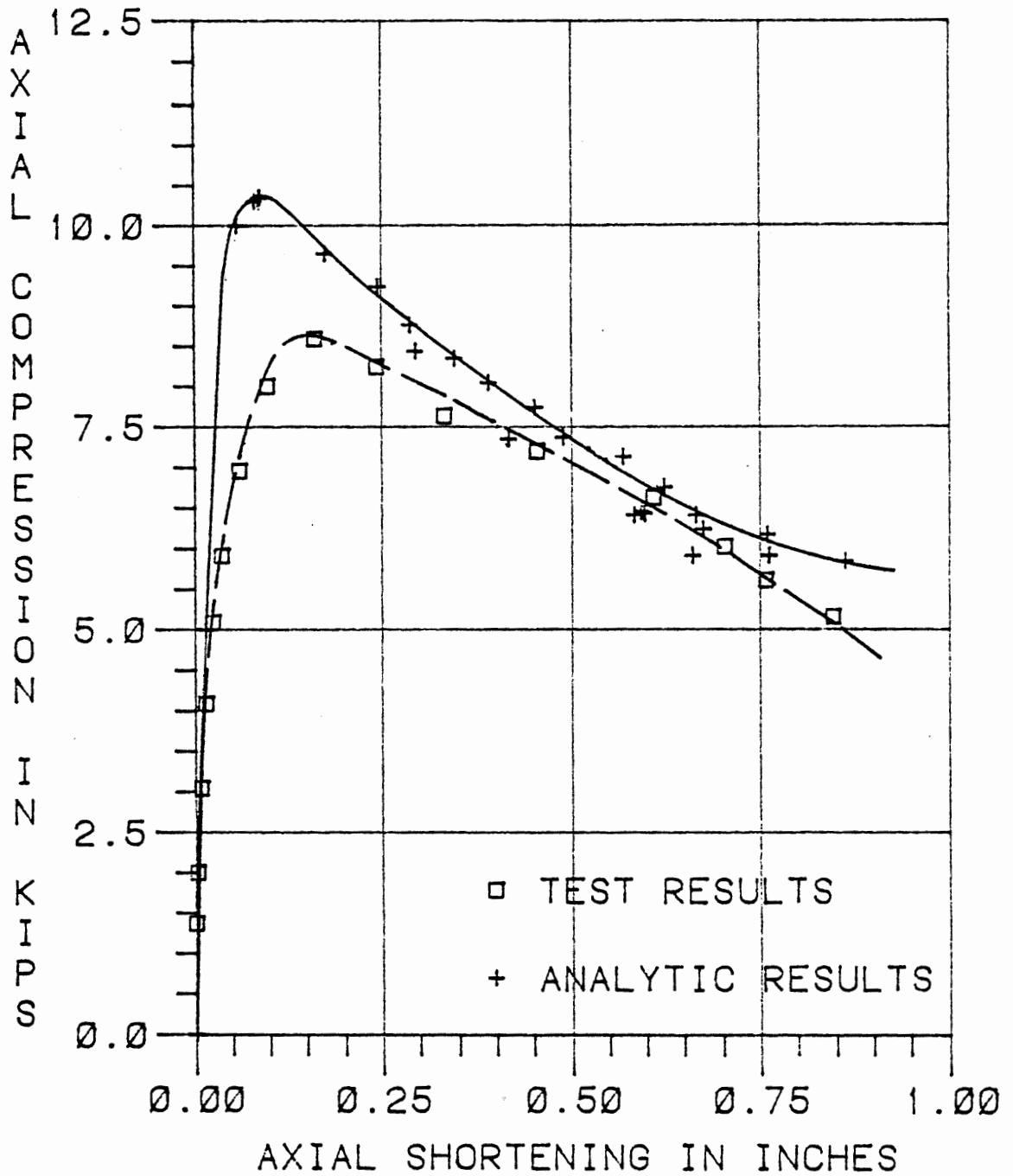
TEST T2 BB 50-1 $L/r=192.6$ 

Figure 24. Test T2 BB 50-1

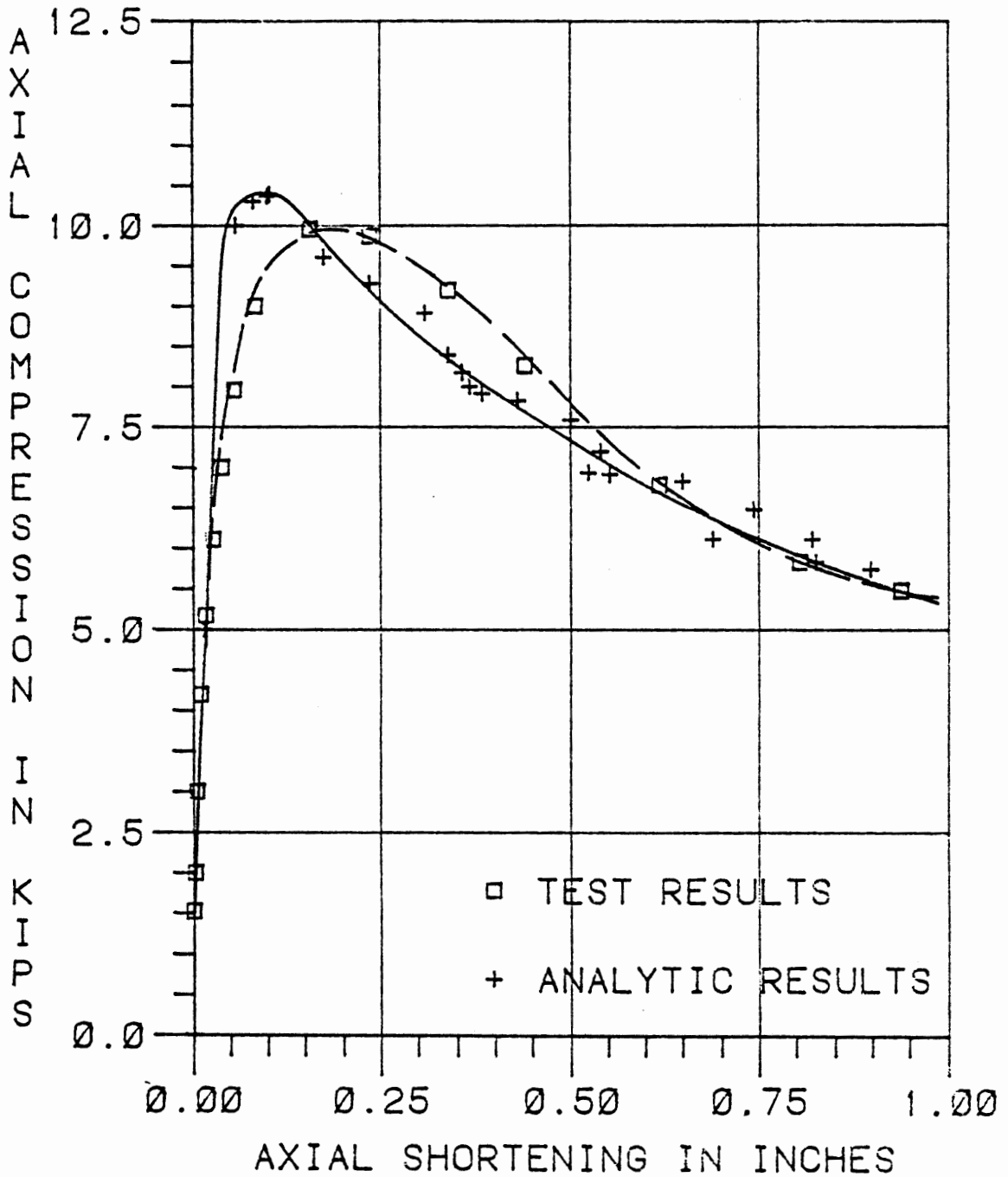
TEST T2 BB 36-1 $L/r=192.6$ 

Figure 25. Test T2 BB 36-1

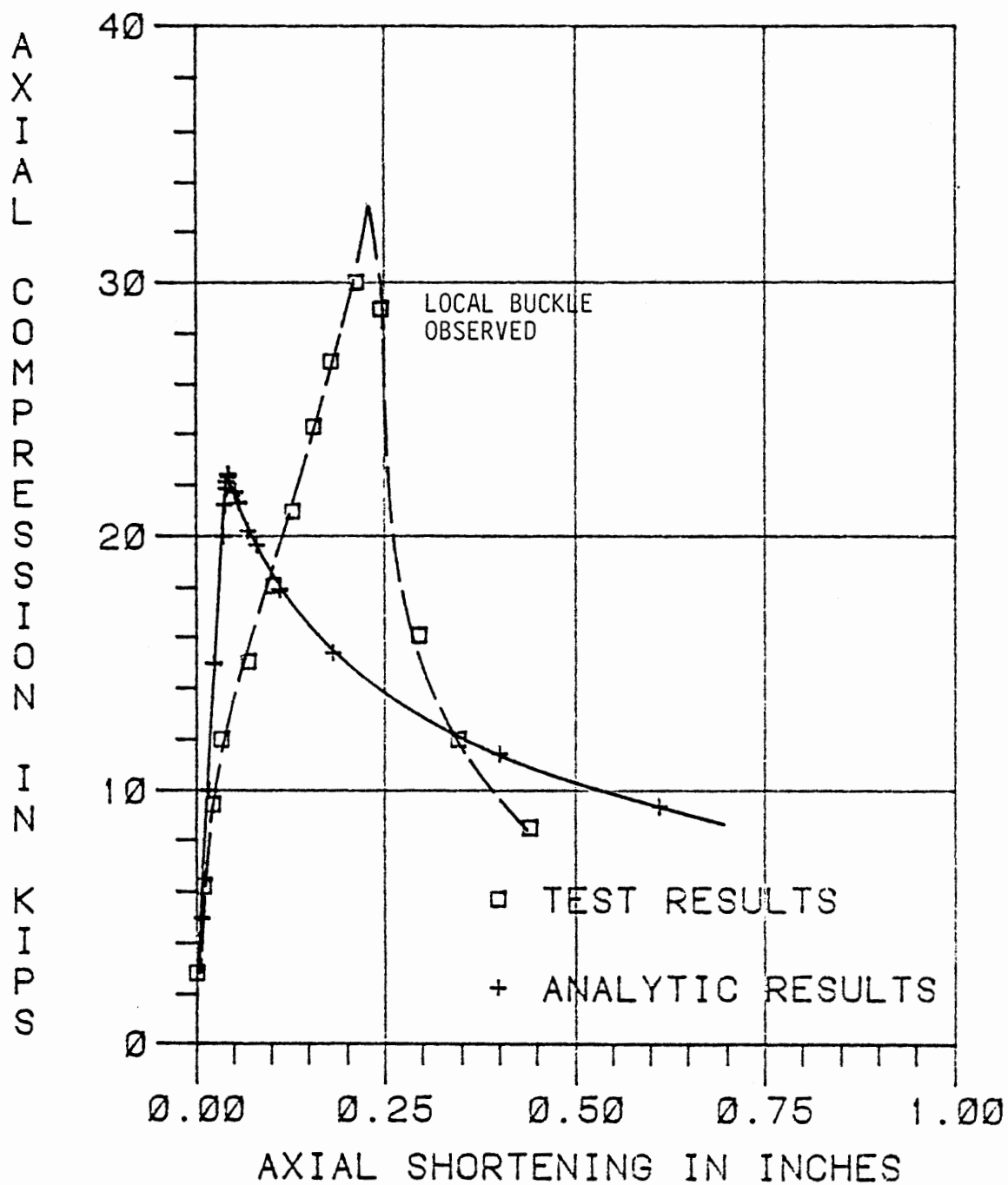
TEST T1 BB 36-1 $L/r=111.5$ 

Figure 26 Test T1 BB 36-1

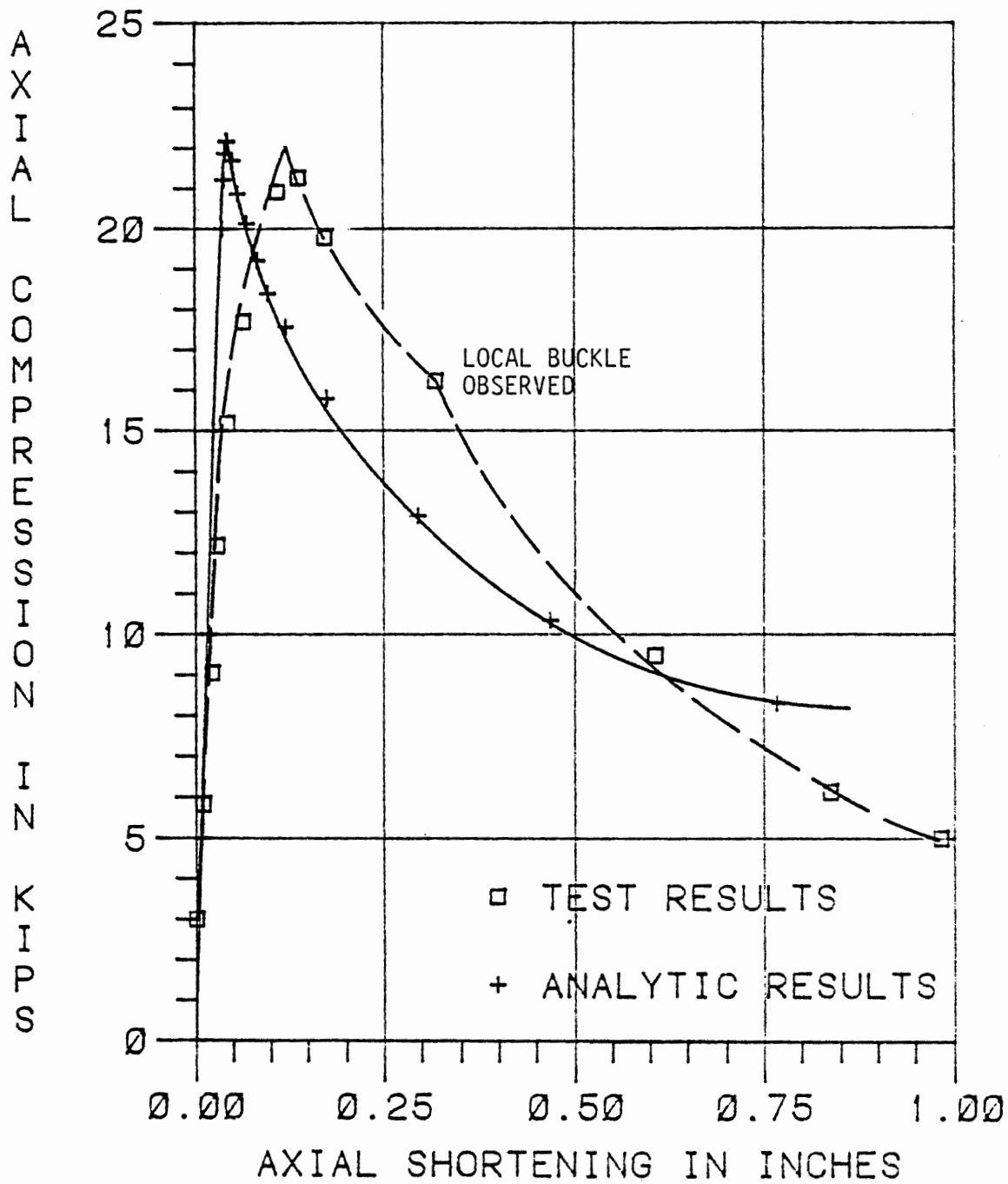
TEST T1 BB 50-1 $L/r=111.5$ 

Figure 27 Test T1 BB 50-1

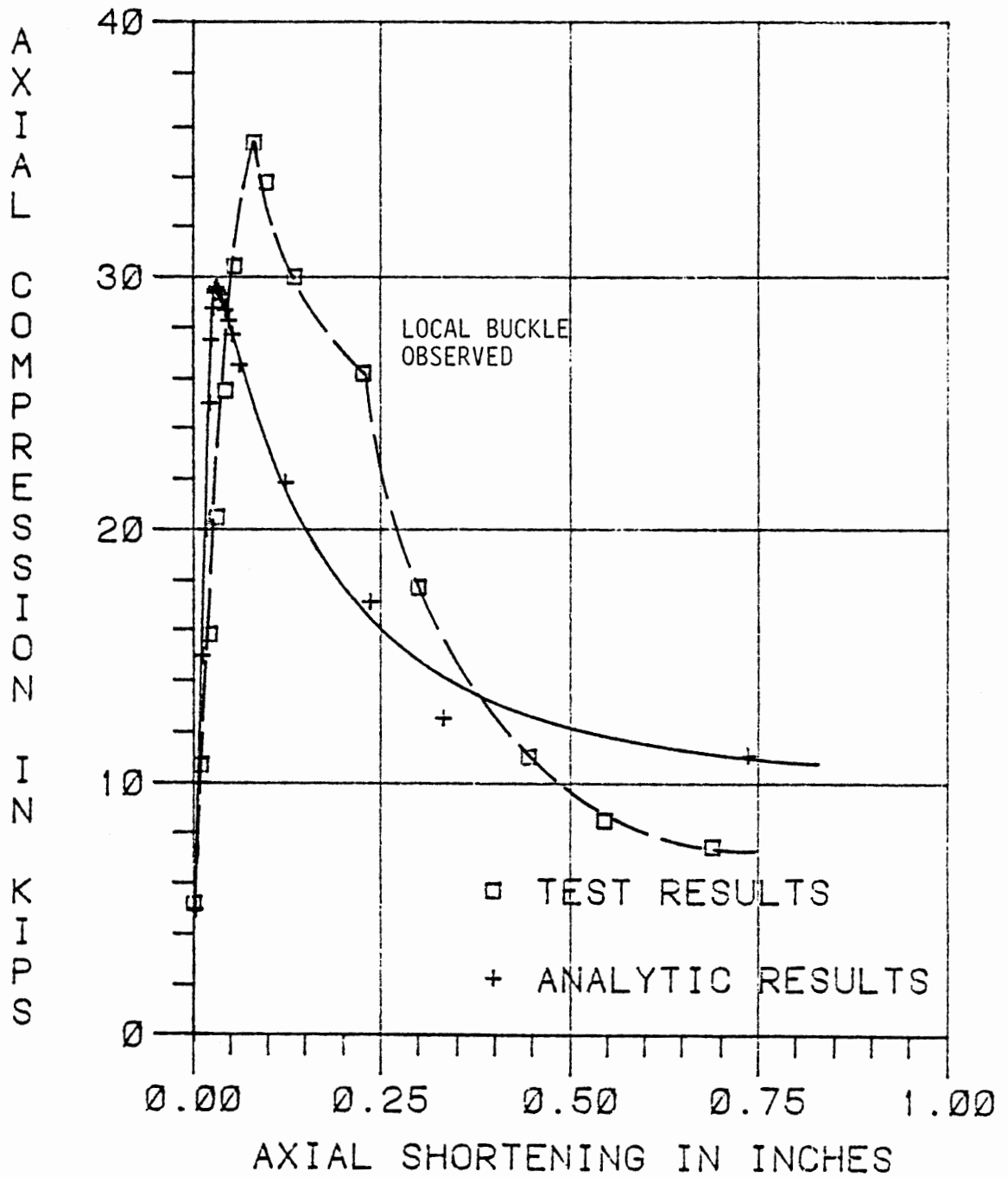
TEST T3 BB 50-1 $L/r=60.8$ 

Figure 28 Test T3 BB 50-1

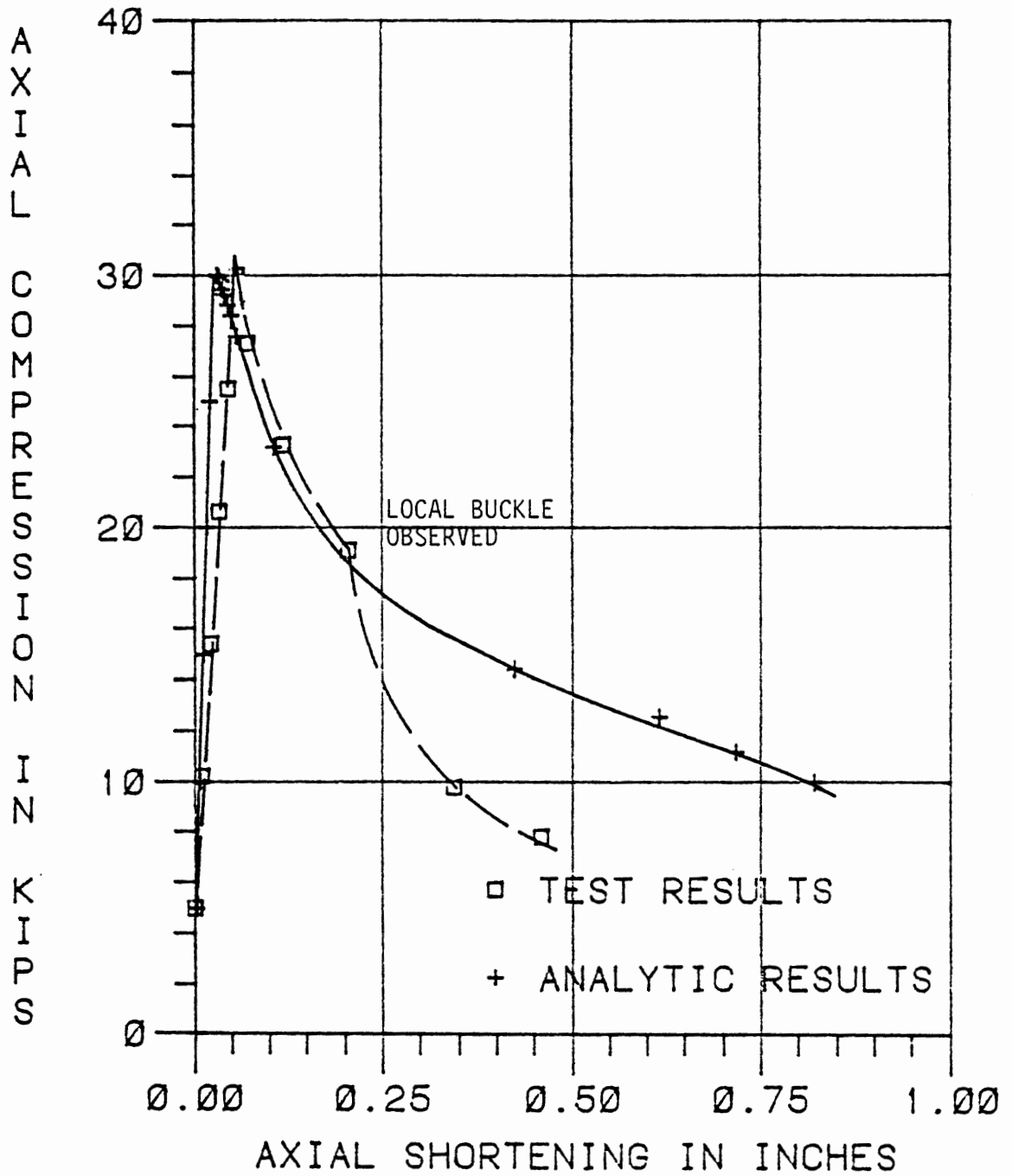
TEST T3 BB 36-1 $L/r=60.8$ 

Figure 29 Test T3 BB 36-1

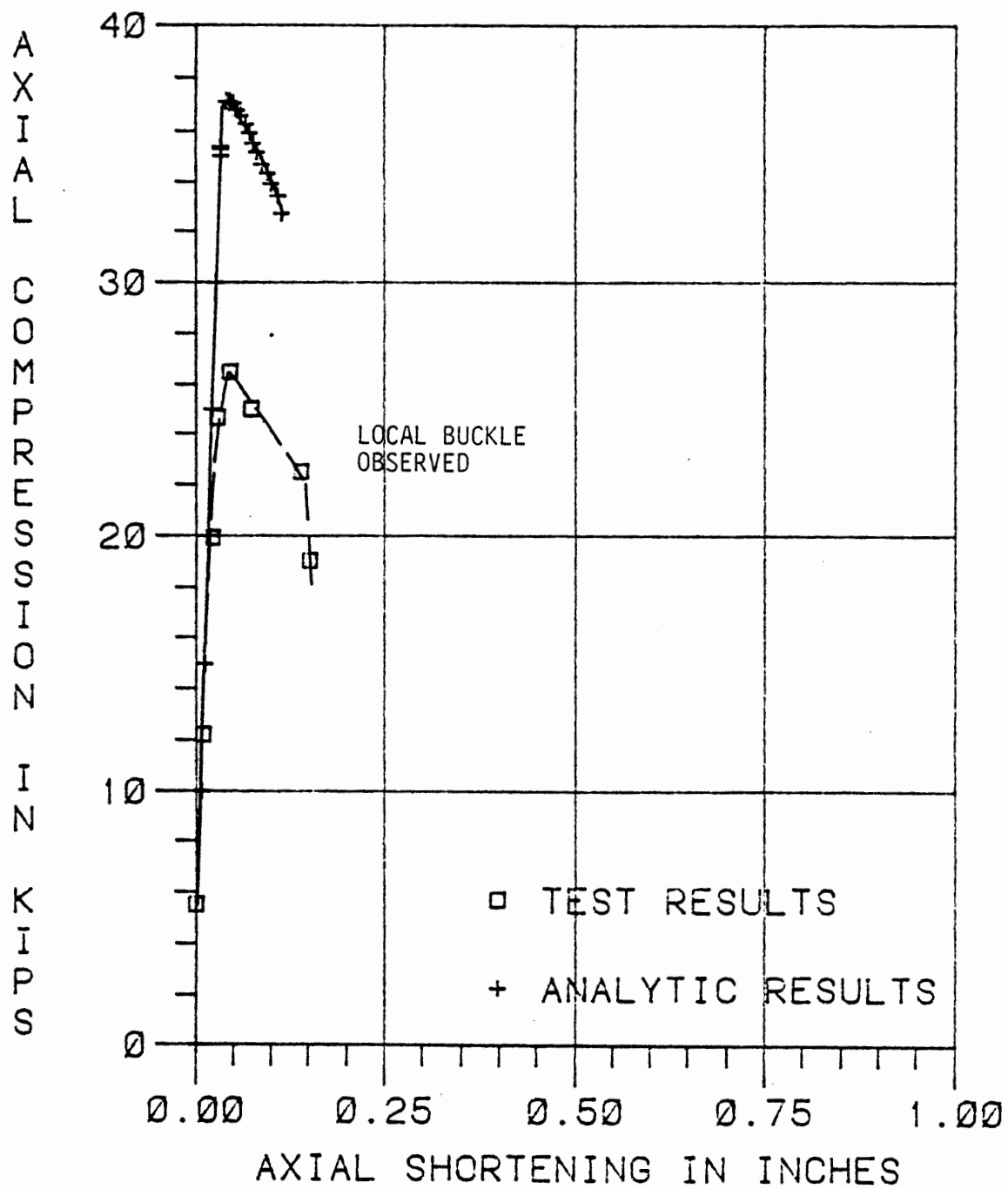
TEST S3 BB 50-1 $L/r=60.8$ 

Figure 30 Test S3 BB 50-1

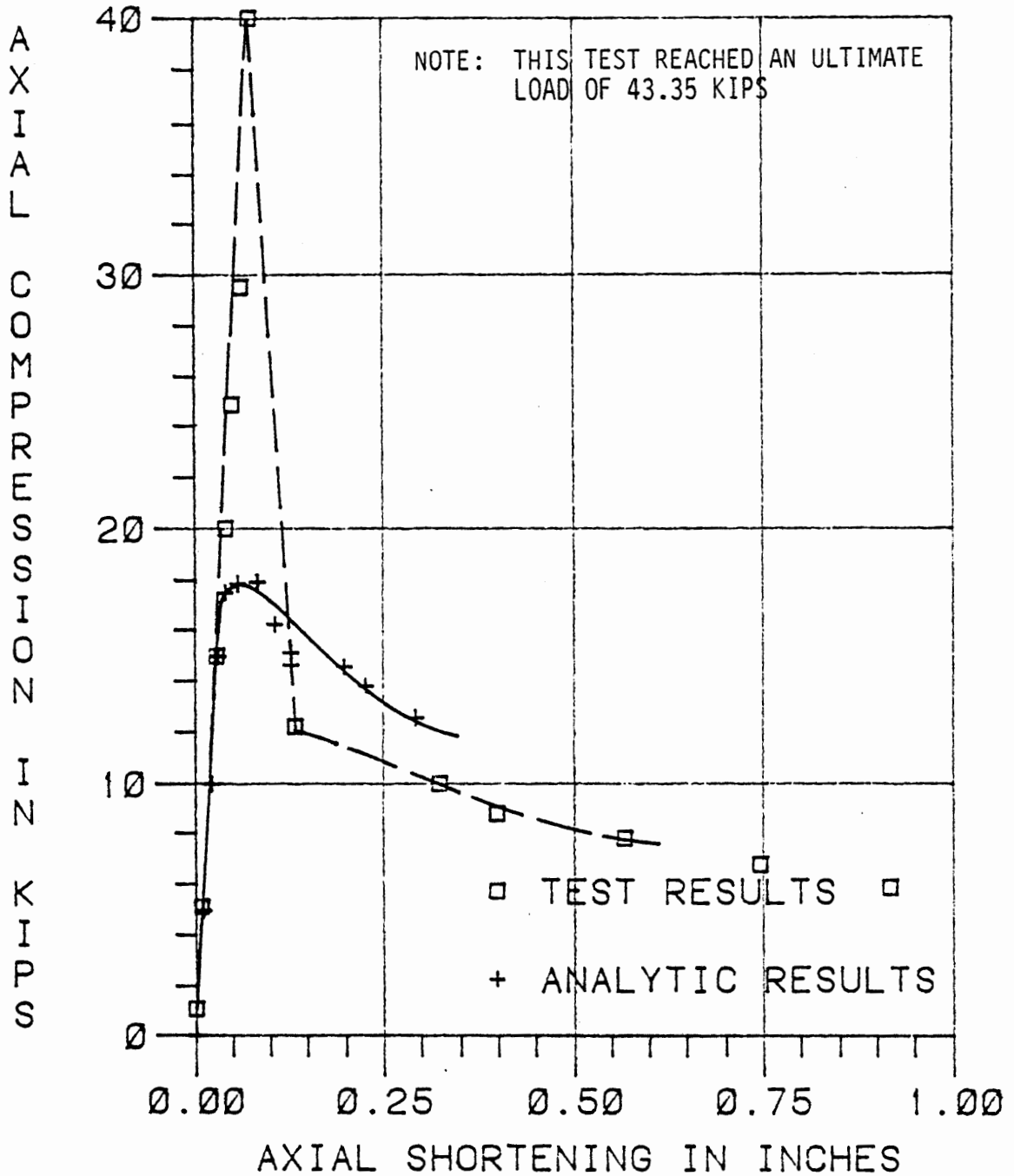
TEST SØ BB 50-1 $L/r=152.0$ 

Figure 31 Test SØ BB 50-1

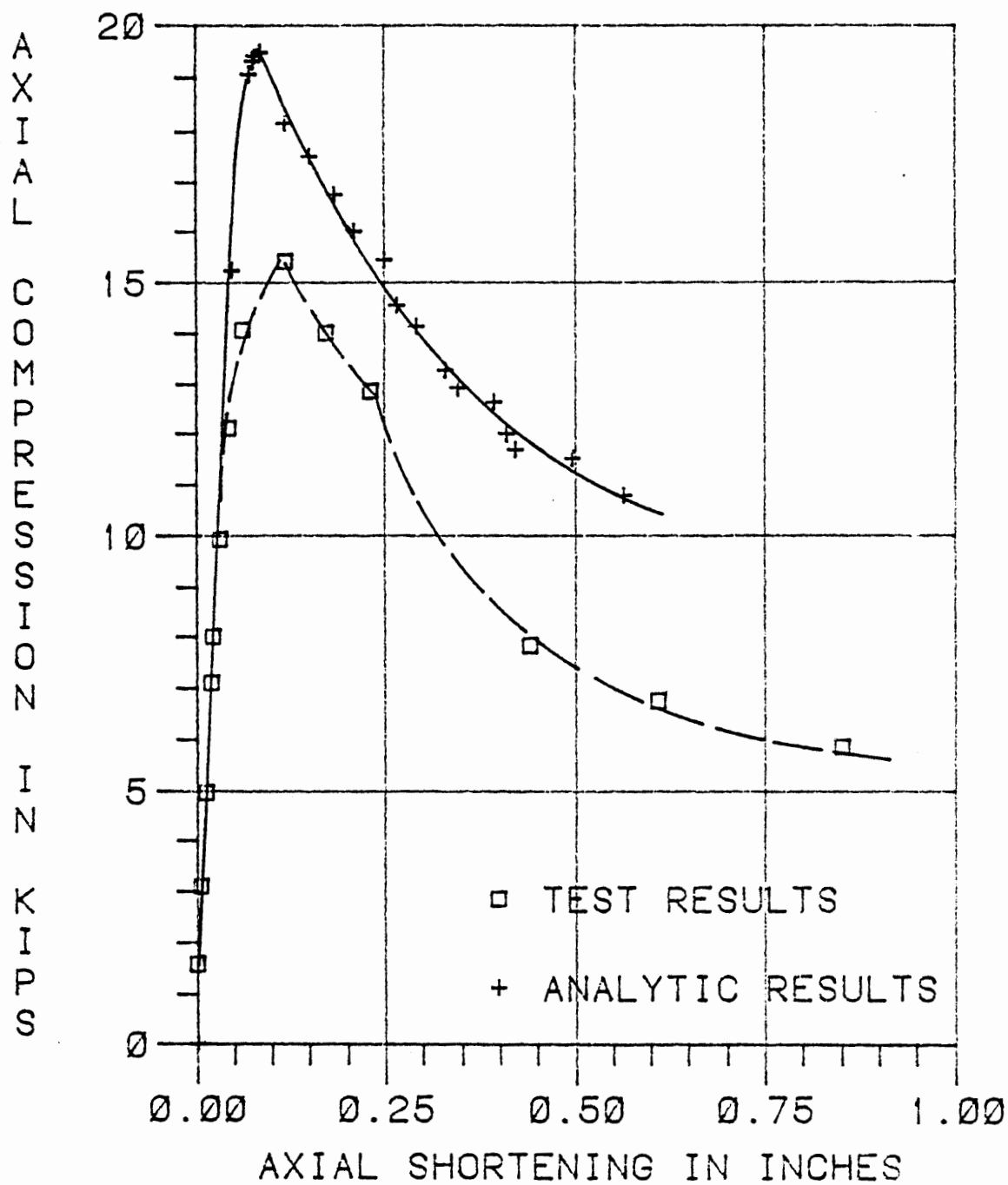
TEST T2 BF 50-1 $L/r=192.6$ 

Figure 32 Test T2 BF 50-1

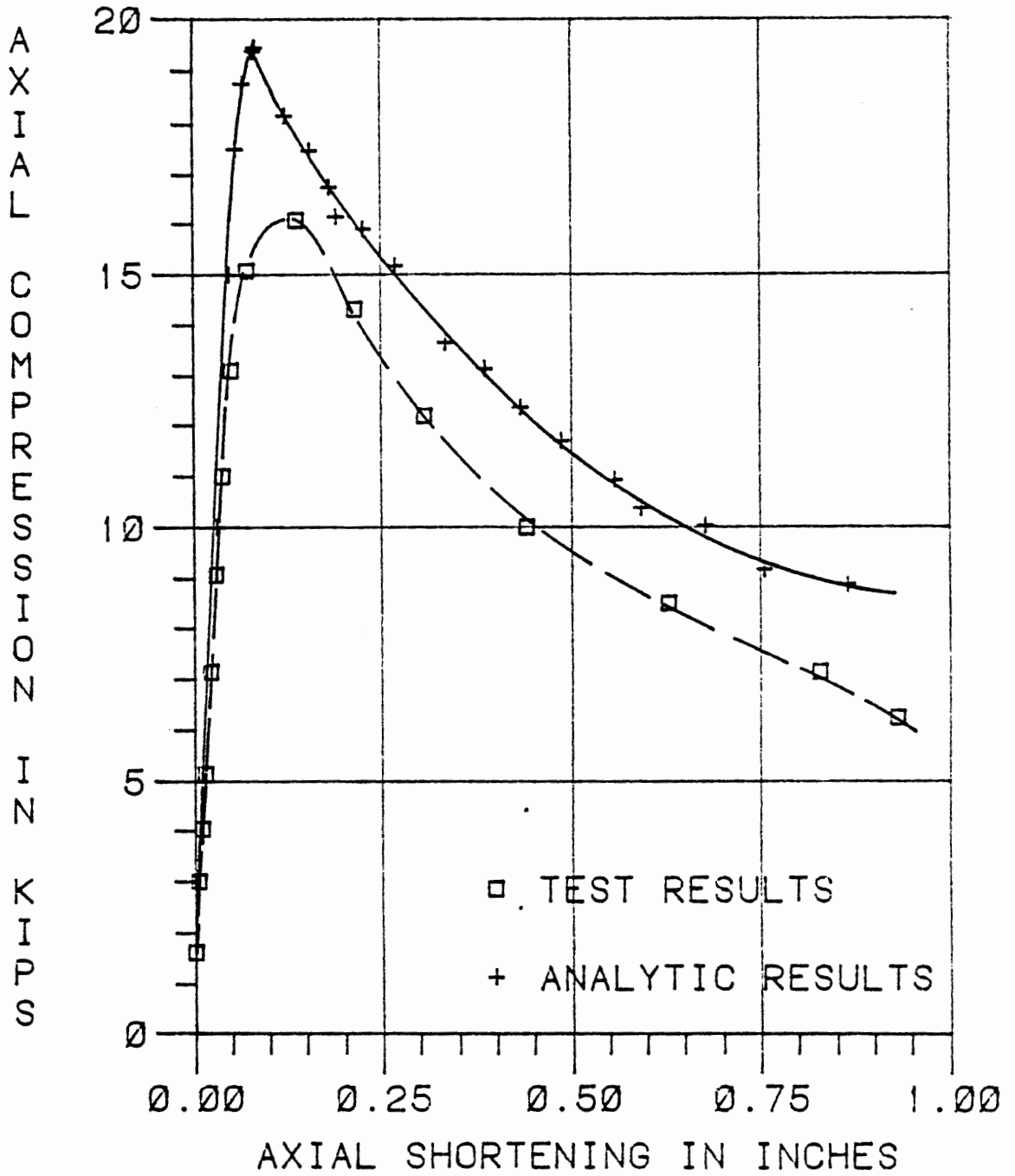
TEST T2 BF 36-1 $L/r=193.0$ 

Figure 33. Test T2 BF 36-1

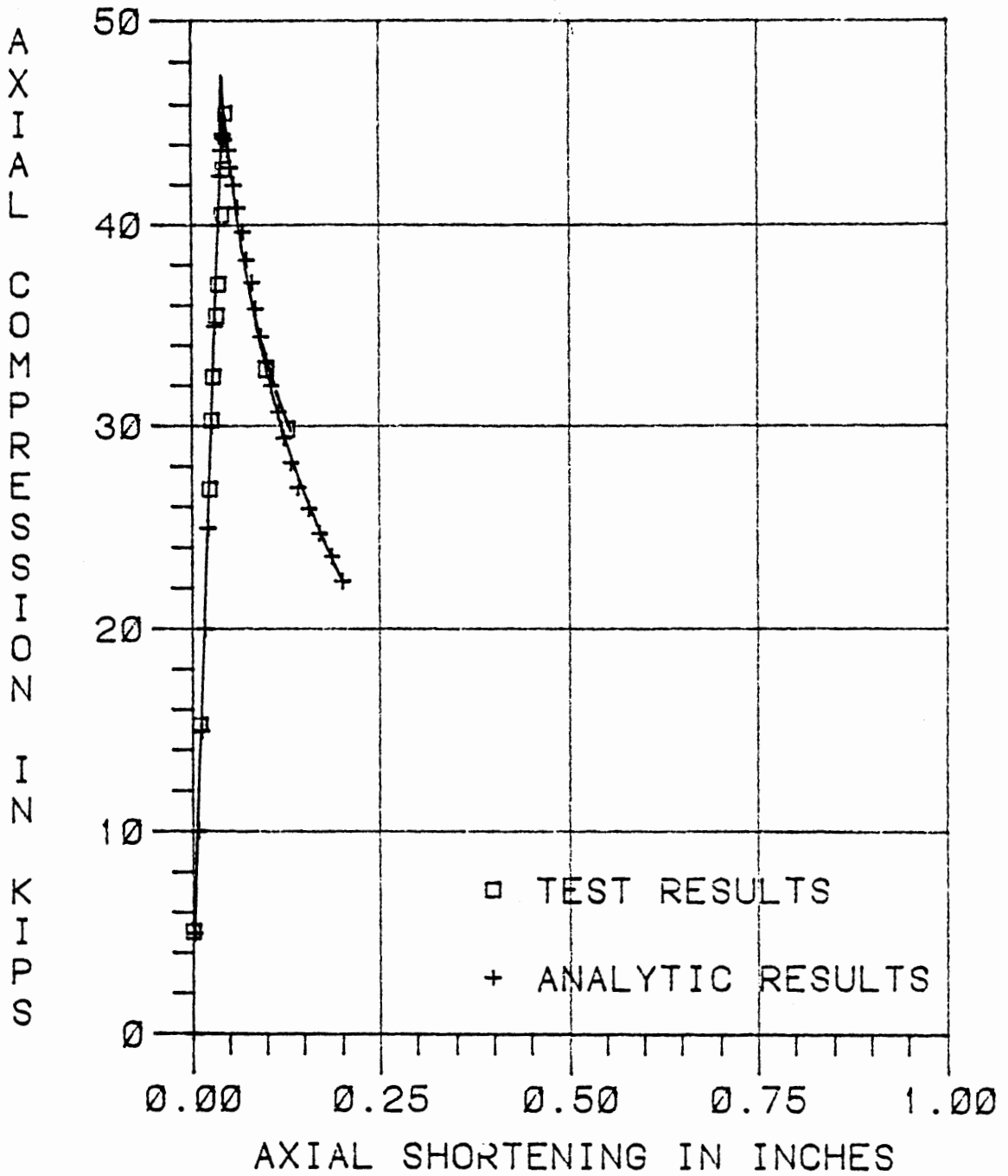
TEST SR3 BB 36-1 $L/r=60.8$ 

Figure 34 Test SR3 BB 36-1

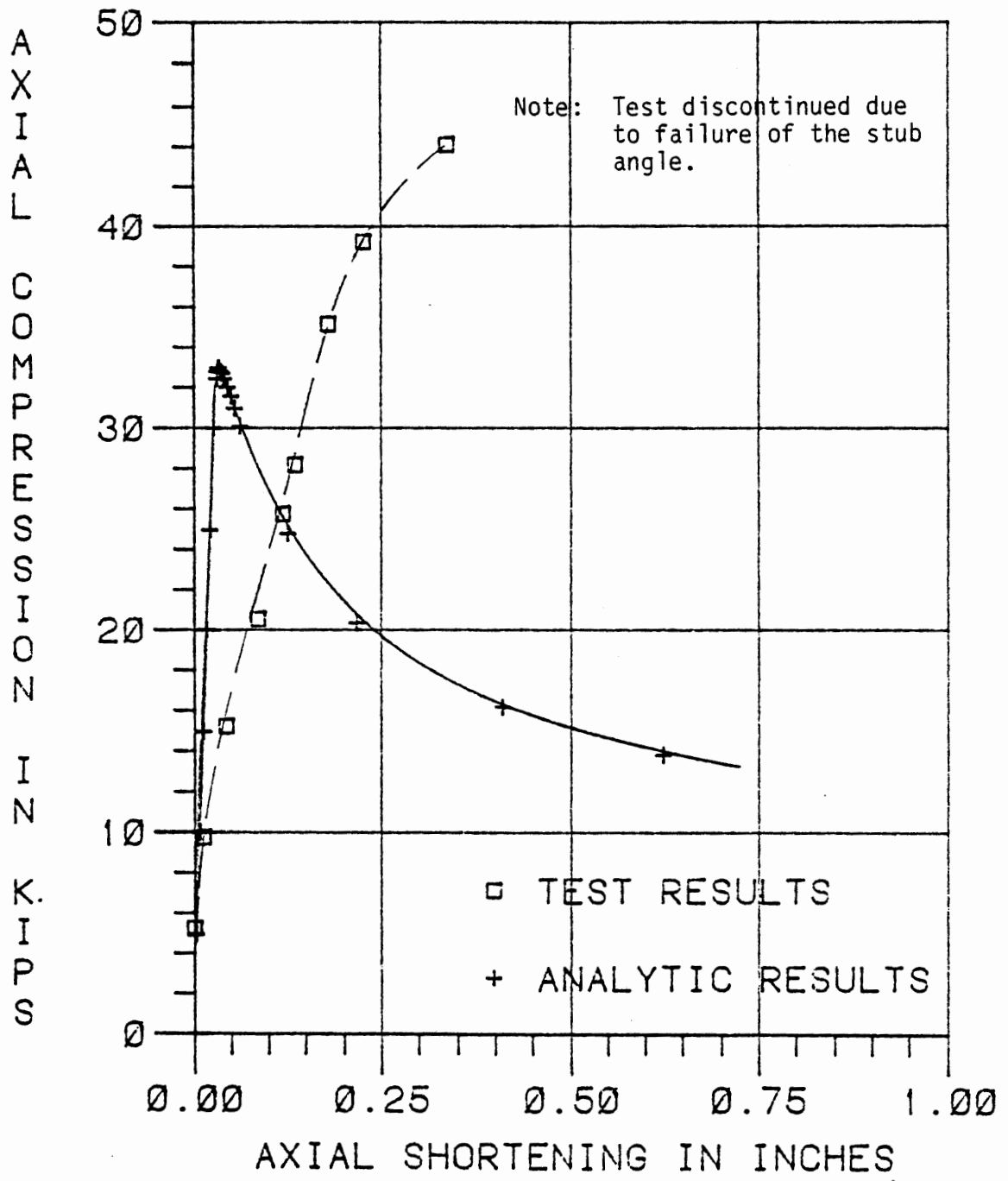
TEST TR3 BB 50-1(1) $L/r=60.8$ 

Figure 35 Test TR3 BB 50-1 (1)

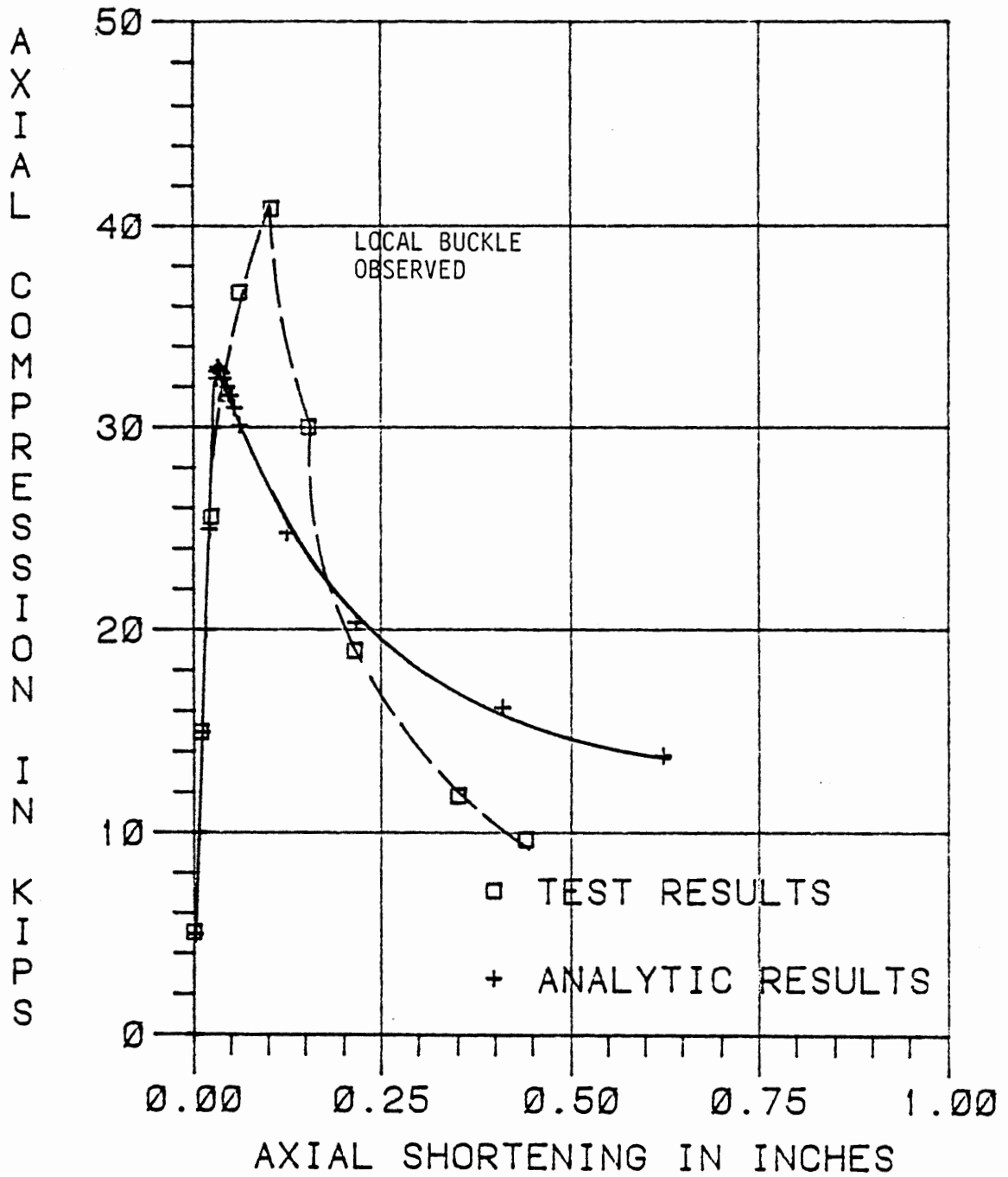
TEST TR3 BB 50-1 $L/r=60.8$ 

Figure 36 Test TR3 BB 50-1

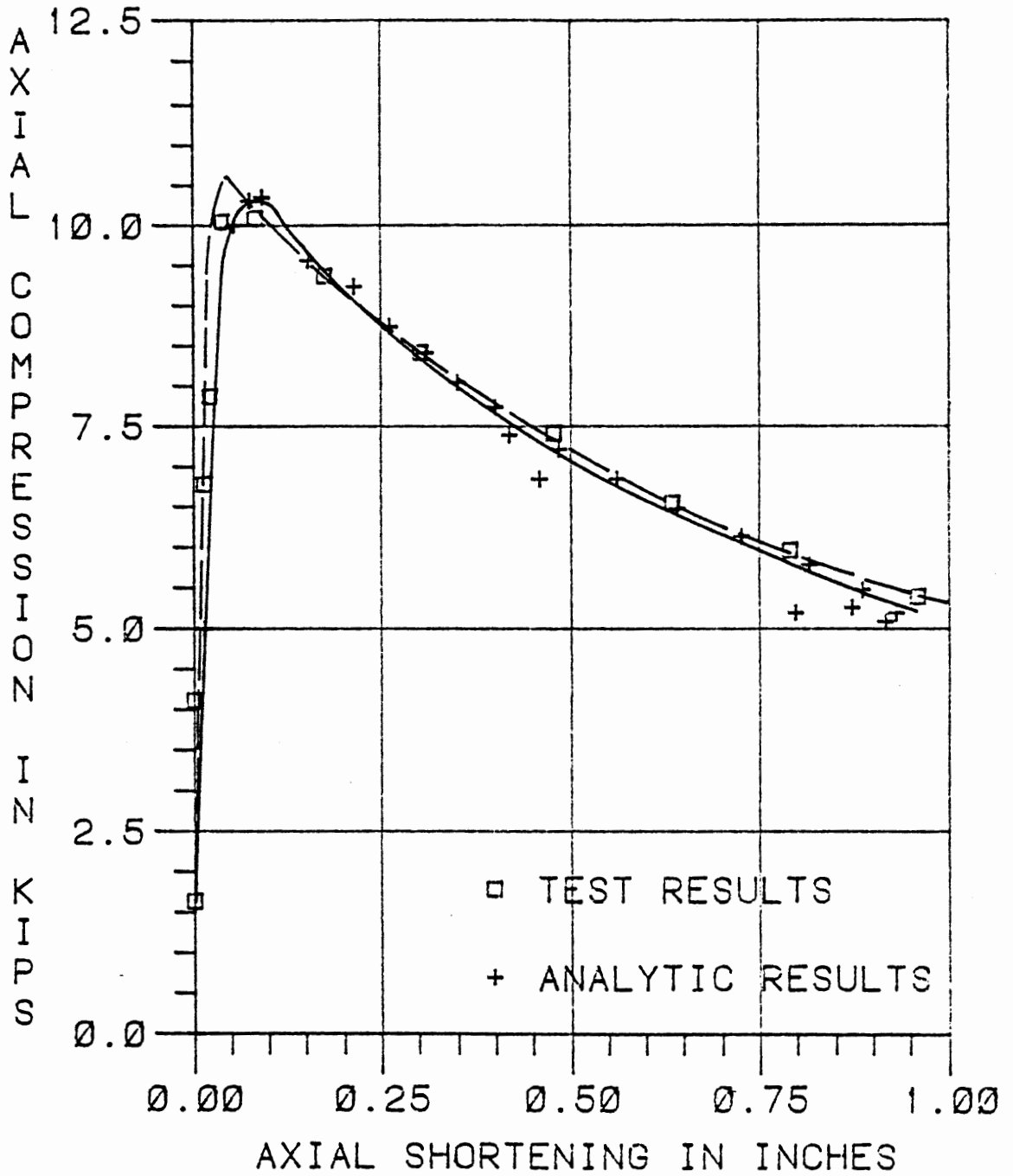
TEST TR2 BB 50-1 $L/r=192.6$ 

Figure 37 Test TR2 BB 50-1

TEST TR1 BB 36-1 L/R=111.5

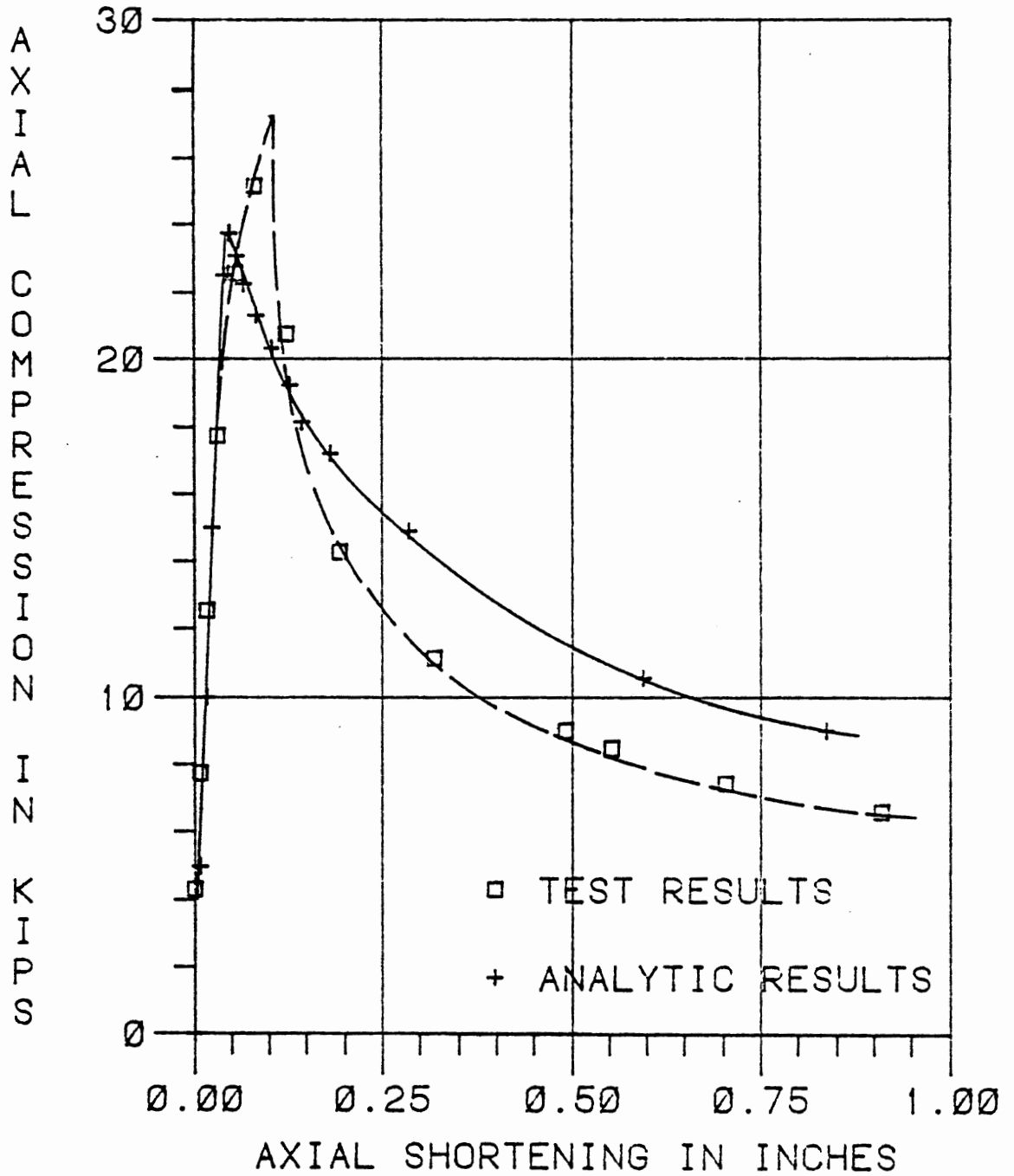


Figure 38 Test TR1 BB 36-1

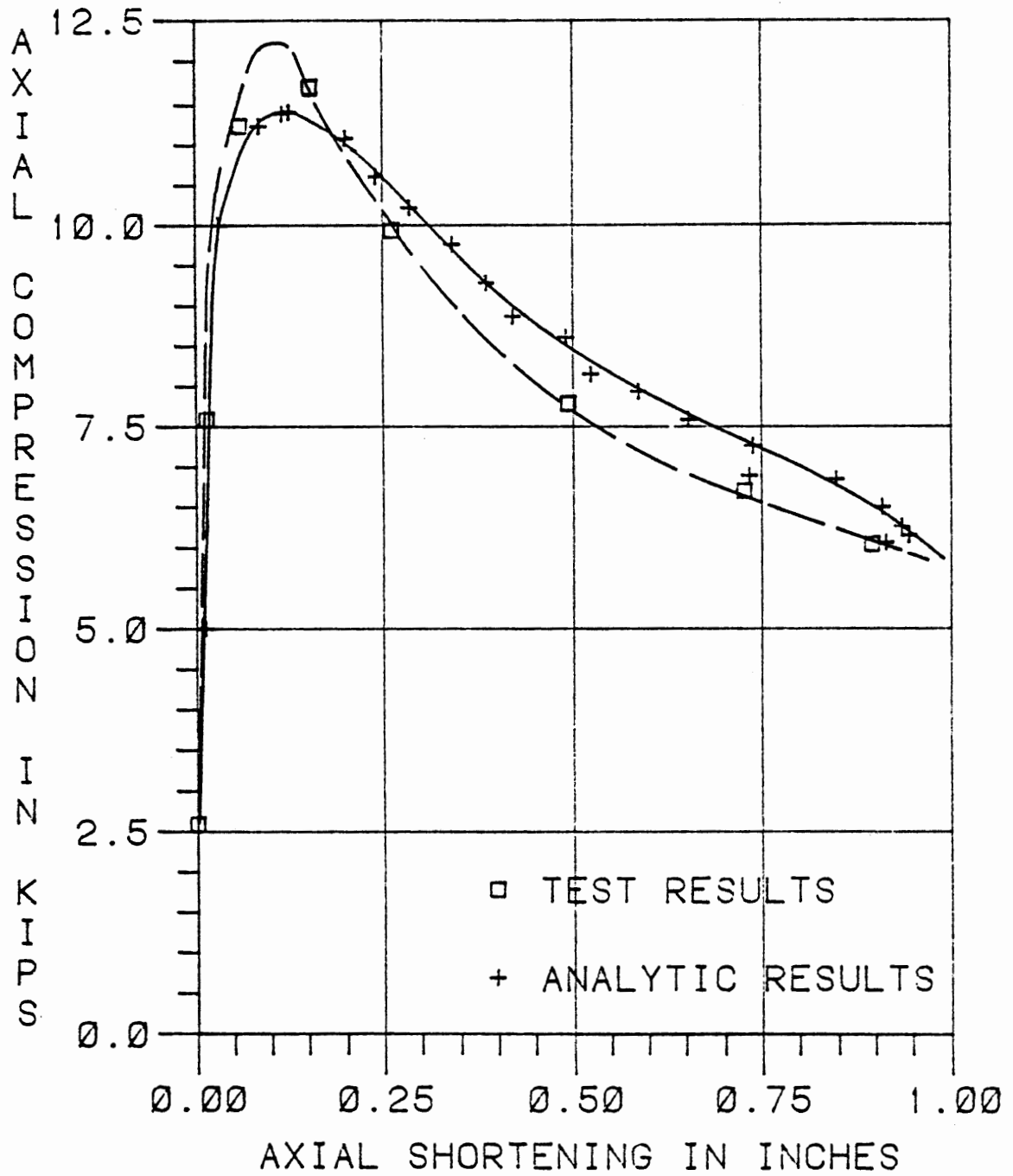
TEST T4 BB 36-1 $L/r=200.0$ 

Figure 39 Test T4 BB 36-1

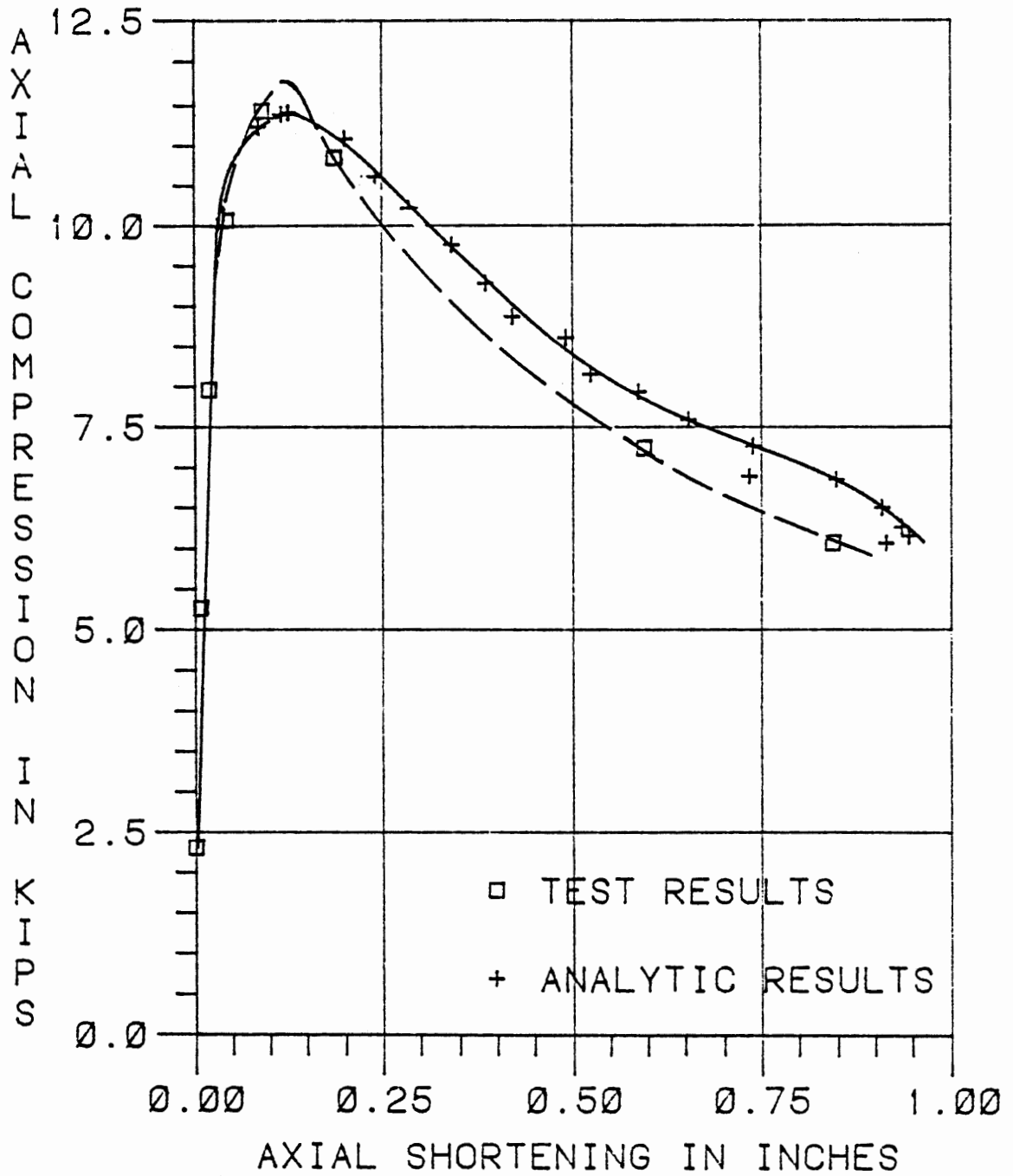
TEST T4 BB 36-2 $L/r=200.0$ 

Figure 40 Test T4 BB 36-2

TABLE III
FAILURE LOAD COMPARISON FOR SINGLE MEMBER TESTS

TEST	ULTIMATE LOAD (KIPS)		
	CALCULATED	EXPERIMENTAL	% DIFF.
S2 HH 50-2	9.5	8.7	8.4
S2 HH 36-1	10.2	9.7	4.9
S2 HH 36-2	10.4	14.7	41.3*
S1 HH 50-1	29.9	43.8	46.5*
S1 HH 36-2	29.9	50.4	68.6*
S3 BB 36-1	44.5	33.0	25.8
S3 BB 36-2	44.4	37.4	15.9
S1 BB 36-2	24.3	21.9	9.9
S2 BB 36-3	9.9	9.8	1.0
T2 BB 50-1	10.4	8.7	16.3
T2 BB 36-1	10.4	10.0	3.8
T1 BB 36-1	22.4	31.3	39.7
T1 BB 50-1	22.2	21.9	1.4
T3 BB 50-1	29.6	35.9	21.3
T3 BB 36-1	30.0	30.4	1.3
S3 BB 50-1	37.2	26.5	28.8
S0 BB 50-1	17.9	43.4	142.4*
T2 BF 50-1	19.5	15.4	21.0
T2 BF 36-1	19.5	16.2	16.9
SR3 BB 36-1	44.5	47.8	7.4
TR3 BB 50-1 (1)	33.0	44.0	33.3
TR3 BB 50-1	33.0	41.2	24.8
TR2 BB 50-1	10.4	10.7	2.9
TR1 BB 36-1	23.8	27.2	14.3
T4 BB 36-1	11.4	12.2	9.9
T4 BB 36-2	11.4	11.8	3.5

$$\% \text{ DIFF.} = \frac{\text{CALC.} - \text{EXP.}}{\text{CALC.}} \times 100$$

*ECCENTRICITY = 0 (BOTH ENDS)

loads. Computer results are somewhat higher than the test values. This may be due to the fact that the computer model assumes a perfect column which is not possible to achieve in tests.

In the tests where the axial load was applied at the center of gravity of the member, large differences in peak load values did occur. In tests S2 HH 36-2 (Fig. 17), S1 HH 50-1 (Fig. 18), S1 HH 36-2 (Fig. 19) and SØ BB 50-1 (Fig. 31) where the eccentricities of the applied load was zero, the load reached a considerably higher value than that predicted by the computer program (Ref. 7) and dropped suddenly. This rise and abrupt drop of load is known as the 'spike.' It is believed to be caused by the internal friction of the end joints. The holding force in the end joints causes the member to function as a fixed ended column rather than the assumed case of a pin-ended column, thus explaining the higher ultimate loads observed in these tests. When other imperfections overcome this holding force the load drops rapidly because the member changes instantly to a pinned-pinned case from a fixed-fixed case. The comparison of test S2 HH 36-1 (Fig. 16) and S2 HH 36-2 (Fig. 17) gives supporting evidence to this phenomena. It should be noted that all parameters were the same for these two tests except for the small eccentricity at one end of the test S2 HH 36-1. This small eccentricity was instrumental in displacing the member without causing a temporary fixed-fixed condition.

Tests S2 HH 50-2 and S2 HH 36-1 are those with hinged-hinged connections which had loading eccentricities. They followed a gradual curve in the inelastic and post buckling region without a spike. The post buckling strength of the tests were about 10-15% less than that predicted by the analytical model. This may be due to the fact that the analytical model assumes a perfect column which is not possible to achieve in tests.

Tests S3 BB 36-1, S3 BB 36-2, S1 BB 36-2 and S2 BB 36-3 used the ball-ball configuration with eccentricity on the x-axis only. Favorable comparison of these tests with the computer model of Ref. 7 were obtained (Fig. 20 to Fig. 23), except for tests S3 BB 36-1 and S3 BB 36-2. In these two tests the ultimate load values were lower than that predicted by the computer program of Ref. 7 by 25.8% and 15.9% respectively. These two tests are the same except that the value of eccentricities are in opposite directions from the center of gravity of the angle. Test S3 BB 36-1 was repeated as given in SR 3 BB 36-1 (Fig. 34) and a good correlation was obtained with the computer model of Ref. 7.

The next six tests are those with bolted joints with eccentricities about both axes which simulate a typical tower joint. In this series, tests T3 BB 50-1, T2 BB 50-1 and T1 BB 36-1 were repeated in an attempt to obtain better data. They are documented in TR 3 BB 50-1 (1), TR 3 BB 50-1, TR 2 BB 50-1 and TR 1 BB 36-1 (Fig. 35 to Fig. 38). Test TR 3 BB 50-1 (1) was discontinued after the failure of the stub angle. All tests in this series exhibit a "softer" load vs axial displacement (P vs δ) curve in the elastic range. This can be attributed to the slippage of the bolted joints when the load is being applied. Another factor causing this wider P vs δ curve is the eccentricity of the load from the center of gravity of the member. The fact that the bolt slippage is the predominant factor contributing to this softer load vs axial displacement (P vs δ) curve is supported by comparing test results for S3 BB 50-1 (Fig. 30) and T3 BB 50-1 (Fig. 28). Both of these tests are loaded with eccentricity of load in both directions from the center of gravity. In spite of the fact that test S3 BB 50-1 had higher eccentricity than test T3 BB 50-1, the test T3 BB 50-1 exhibited a softer curve in the

elastic range.

The tests T2 BF 50-1 (Fig. 32) and T2 BF 36-1 (Fig. 33) are the tests with one end fixed and the other with a ball joint. The computer model of Ref. 7 is not capable of handling fixed joints. Hence a fixed joint was simulated by two hinged joints at close proximity at one end. The difference in experimental and theoretical curves may be due to this assumption or to the difficulty in fabricating a truly fixed end in the experimental set up.

Tests T4 BB 36-1 and T4 BB 36-2 were performed to ascertain the effect of local buckling in long compression members. These angle members had a width-to-thickness ratio (w/t) of 20 which exceeds the limitation in the AISC Manual of Steel Construction (8) for compact members. These tests did not show the formation of a local buckle before the yielding of the member as they failed in an elastic buckling mode and thus the stress level remained low.

The formation of a local buckle if any, is indicated on the curves presented in Figs. 15 to 40. It is noted that all the local buckling observed has occurred after attaining the full ultimate strength of the member. The formation of a local buckle was predominantly seen in shorter members, because members with smaller L/r ratios sustained high stresses.

In general the test results show that a long member has greater ability to sustain load after the critical buckling load than the shorter members. However, in all cases some resistance to axial load was evident in the post buckling region. Hence members with larger L/r ratios exhibit larger load plateaus before a gradual drop-off of load occurs. This is because the members with larger L/r ratios require large axial displacements to cause yielding due to the bowing of the member. On the other-

hand members with smaller L/r ratios displayed a brittle type failure with steep drop-off of load capacity after reaching the ultimate strength.

By comparing the P vs δ curves for various tests it is evident that the effect of the eccentricity of applied load from the center of gravity of the member is to make the P vs δ curve softer. A typical example is the comparison of tests S2 HH 50-2 and S2 HH 36-2. The test S2 HH 50-2 (Fig. 15) being loaded eccentrically from the center of gravity of the angle has a softer curve than the curve for the test S2 HH 36-2. Eccentrically loaded members have a more ductile type of failure with a wider plateau but attain a lower ultimate load.

It is evident that the effect of a fixed end condition is to attain higher ultimate strength of the member than in ball or hinge connections. This is expected as fixed ends give greater resistance to applied loads. However tests with bolted connections demonstrated their susceptibility to bolt slippage, which resulted in wider P vs δ curves.

The study of the effect of the yield strength on the member performance was handicapped to a certain extent by the non-availability of the steel stock with wide range of yield strengths. It is shown in Table I that the yield strengths of members tested do not exhibit a considerable difference in value between A-36 steel and Grade 50 steel. However it is observed that members with higher yield strength with other parameters being constant give rise to higher ultimate strengths as expected.

It should be emphasized that the above observations pertaining to the effect of various parameters in the member performance are done in general terms. The limited number of tests performed and the test data

scatter was a problem when extrapolating the results. However, it is evident that the tests performed were sufficient to verify the analytical computer program of Ref. 7.

CHAPTER III

PRELIMINARY EXPERIMENTAL PROGRAM FOR INDETERMINATE TRUSS TESTS

3.1 OVERVIEW

This chapter documents the Preliminary Experimental Program carried out to investigate the load transfer characteristics of diagonal bracing in an indeterminate truss. Attention is given to the Experimental set up, Instrumentation and the Test Procedure. The Steel Properties and Coupon test results are included. The experimental load capacity of the test frame for various diagonal members tested were compared with the theoretical capacity determined by statics.

3.2 EXPERIMENTAL SET UP

Experimental set up for the indeterminate truss is shown in Figures 41 and 42. Figure 41 is a picture of the indeterminate truss without diagonal bracing. Diagonal bracing is shown in Fig. 42. The idealized configuration is shown in Fig. 43. A 48 inch square frame was constructed using 8 x 8 x 7/8 double angles as a model to do preliminary study of load transfer characteristics in an indeterminate truss. The double angles between CD (Fig. 43) are welded to a W 24 x 68 which is restrained at E and F. From the geometry the reactions at E and F are equal and opposite and the magnitude is less than the pulling force in the actuator. The reaction at G is equal to the pulling force in the actuator (assuming supports E and F do not contribute reactions in the CD direction). Supports were provided at E, F and G to resist the above reactions

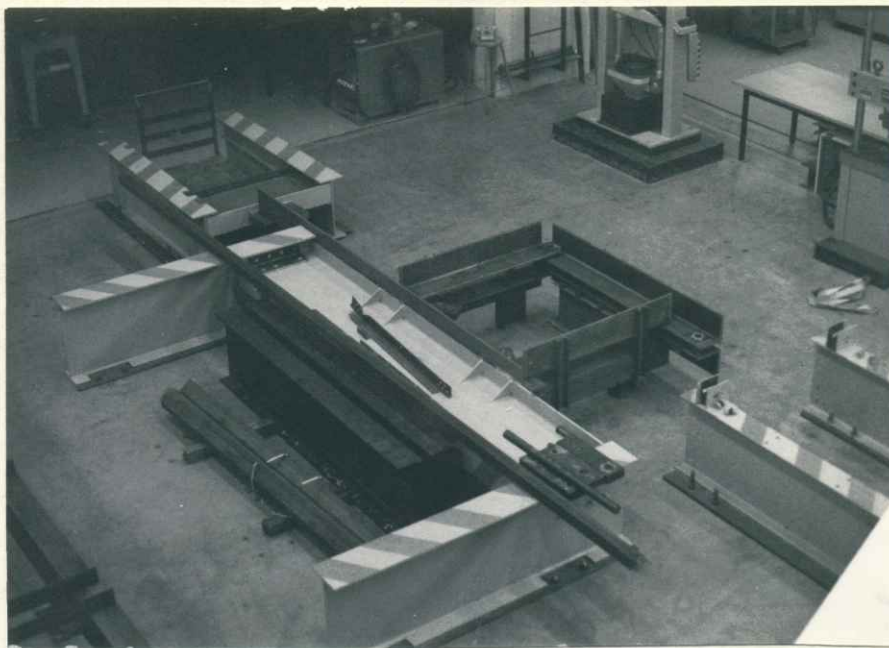


Figure 41. Setup of truss without diagonal bracing



Figure 42. Indeterminate truss with diagonal bracing.

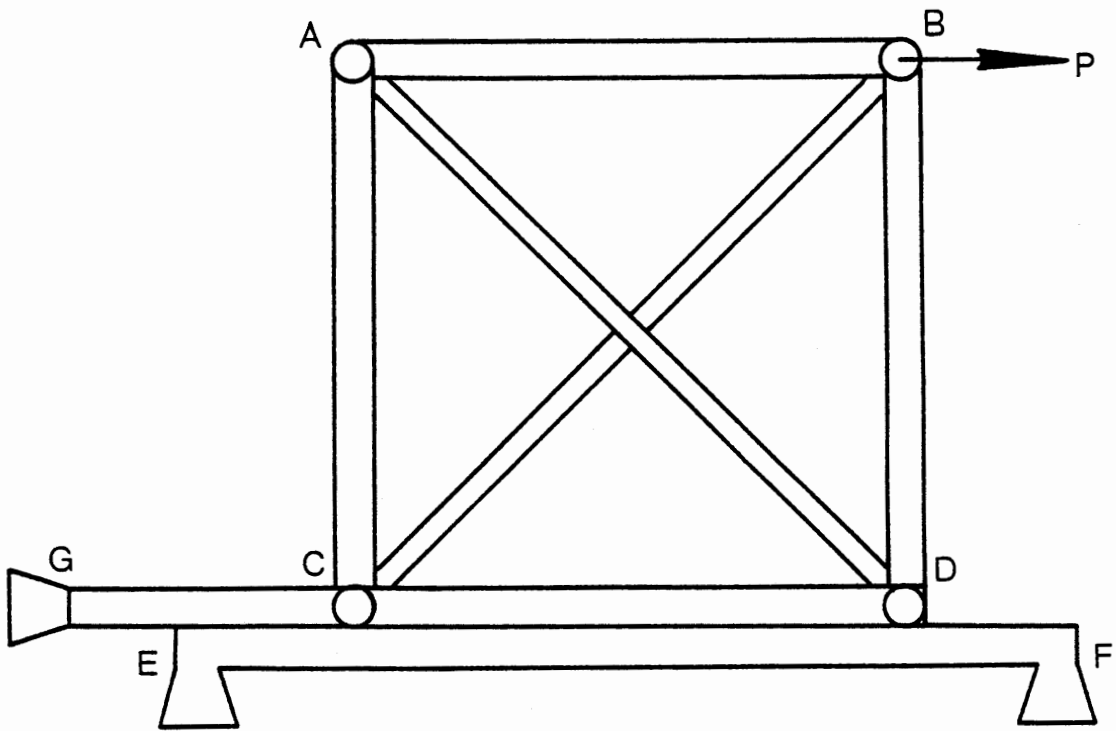


Figure 43 Indeterminate truss

(Fig. 43). The 8 x 8 x 7/8 angles were separated by 2 inches to facilitate connection of the diagonal test member to the frame. The diagonal test angles are bolted to a 13" x 5" x 2" connecting plate with 5/8 inch bolts at each end. These plates are then pin connected to the frame to simulate a frame as shown in Fig. 43. Members of the test frame were selected large to give the frame a capability of testing larger members and to minimize their size effect on the test results.

3.3 INSTRUMENTATION

The MTS system was used with stroke control to apply the load. The load value was read directly from the MTS control panel. The deflection of the sidesway of the portal was measured using a Linear Variable Differential Transducer (LVDT) with read out directed to the MTS control panel.

3.4 TEST PROCEDURE

The chosen test procedure was selected to ensure that the compression diagonal was well seated and compressed before the tension diagonal sustained any load. This was an attempt to minimize the bolt shippage in the compression test member connection.

The test procedure was as follows

- 1) mount the compression diagonal in the test frame
- 2) Apply a load at the joint B (Fig. 43) using the actuator of the MTS system until the compression member is well seated. Five hundred pounds is the normal load value used.
- 3) mount the tension diagonal

4) load until failure of the tension diagonal.

The members tested and final results are given in Table IV. The theoretical load capacity of the truss was determined by statics assuming zero load resistance in the compression diagonal and a yield force in the tension diagonal. A plot of the load deflection curves obtained from these truss tests are presented in Figures 44 to 52. The load is the load applied by the actuator and the deflection is the sideways of the portal.

3.5 STEEL PROPERTIES AND COUPON TESTS

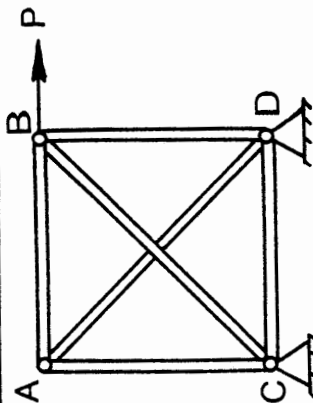
To obtain data on the material properties of the steel angles tested, coupon tests were performed using the MTS Testing Machine. Details of these tests are documented in Chapter II, section 2.6. A typical stress-strain curve is illustrated in Fig. 14. Table V summarizes the steel properties of steel members used in the indeterminate truss tests.

3.6 DISCUSSION OF RESULTS

Table IVA summarizes the properties and configuration of diagonal members used in preliminary truss tests. The areas listed for tension members are for net sections calculated in accordance with the provisions of section 1.14.2 of Ref. 8. The tension member used in test Fx3 was a C 5 x 9 and was coped at its ends to facilitate mounting. Comparison of experimental and analytical results of the preliminary truss tests are given in Table IVB. The theoretical frame load capacity of the frame is that load sustained by the frame when the tension diagonal is

TABLE IVA
 DIAGONAL MEMBER CONFIGURATION IN
 PRELIMINARY TRUSS TESTS

TEST	LENGTH OF DIAGONAL MEMBER (in.)	MEMBER SIZE		L/r		A (in.)		F _y (ksi)	
		MEMB. AD	MEMB. BC	MEMB. AD	MEMB. BC	MEMB. AD	MEMB. BC*	MEMB. AD	MEMB. BC
Fx1	67.88	1½x1½x3/16	1½x1½x3/16	231.7	231.7	0.53	0.39	50.5	50.5
Fx2	67.88	1½x1½x3/16	1½x1½x3/16	231.7	231.7	0.53	0.39	50.5	50.5
Fx3	67.88	3x3x¼	C5x9	114.7	138.8	1.44	1.45**	54.8	41.6
Fx4	67.88	3x3x¼	3x3x¼	114.7	114.7	1.44	1.12	51.0	51.0
Fx4A	67.88		3x3x¼	114.7	114.7	1.44	1.12	51.0	51.0
Fx5	67.88	3x3x¼	3x3x¼	114.7	114.7	1.44	1.12	51.0	51.0
Fx5A	67.88		3x3x¼	114.7	114.7	1.44	1.12	51.0	51.0
Fx5B	67.88	3x3x¼	3x3x¼	114.7	114.7	1.44	1.12	48.2	48.2
Fx6	67.88	3x3x¼	3x3x¼	114.7	114.7	1.44	1.12	48.2	48.2
Fx7	67.88	3x3x¼	3x3x¼	114.7	114.7	1.44	1.12	48.2	48.2
Fx7A	67.88		3x3x¼	114.7	114.7	1.44	1.12	48.2	48.2
Fx7B	67.88	3x3x¼	2x2x¼	173.6	173.6	0.94	0.75	52.5	52.5
Fx8	67.88	2x2x¼	2x2x¼	173.6	173.6	0.94	0.75	52.5	52.5
Fx8A	67.88	1½x1½x3/16	1½x1½x3/16	231.7	231.7	0.53	0.39	50.0	50.0
Fx9	67.88								



* NET AREA

** NET AREA ON COPED SECTION

TABLE IVB

COMPARISON OF RESULTS IN PRELIMINARY TRUSS TESTS

TEST	THEORETICAL FRAME LOAD CAPACITY (KIPS)*** P (THEO.)	THEORETICAL FRAME LOAD WHEN COMPRESSION DIAGONAL BUCKLES (KIPS)	EXPERIMENTAL ULTIMATE LOAD (KIPS) P	% **** DIFFERENCE
Fx1	13.9	4.0	20.0	30.5
Fx2	13.9	4.0	20.0	30.5
Fx3	42.7	44.3	78.2	45.4
Fx4	40.4	44.3	49.3	18.1
Fx4A	40.4		37.6	7.4
Fx5	40.4	44.3	64.3	37.2
Fx5A	40.4		42.5	5.0
Fx5B	22.2	22.2	21.1	5.2
Fx6	38.2	44.3	46.5	17.8
Fx7	38.2	44.3	47.7	19.9
Fx7A	38.2		40.5	5.7
Fx7B	22.2	22.2	29.2	24.0
Fx8	27.8	12.6	36.2	23.2
Fx8A	27.8		32.0	13.1
Fx9	13.8	4.0	18.7	26.2

*** (AREA) (Fy) Sin 45° **** = (EXP. ULT. LOAD - THEO. FRAME LOAD CAP) x 100

For tests with tension and comp. diagonals $2\lambda^2 \frac{EI}{L^2} \sin 45^\circ$
(EXP. ULT. LOAD)

For tests with compression diagonal only $\lambda^2 \frac{EI}{L^2} \sin 45^\circ$
(I is for compression member)

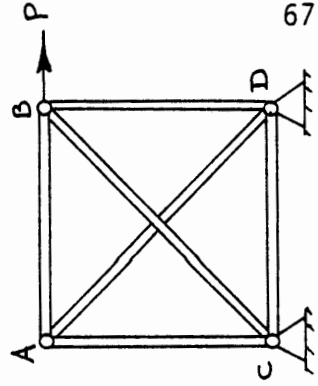


TABLE V
STEEL PROPERTIES OF INDETERMINATE TRUSS TESTS

TEST	YIELD STRESS (KSI)	ULTIMATE STRESS (KSI)	MODULUS OF ELASTICITY	PERCENTAGE ELONGATION (%)
Fx1	50.5	72.3	29100	31.0
Fx2	50.5	72.3	29100	31.0
Fx3 (TM) *	41.6	59.0	29700	38.0
Fx3 (CM) **	54.8	71.2	29100	38.0
Fx4	51.0	67.8	29200	34.0
Fx5	51.0	67.8	29200	34.0
Fx6	48.2	65.6	29100	35.0
Fx7	48.2	65.6	29100	35.0
Fx8	52.5	72.7	29100	34.0
Fx9	50.0	67.5	29300	39.0

* TM = TENSION MEMBER IN TEST Fx3

**CM = COMPRESSION MEMBER IN TEST Fx3

TEST CONFIGURATION

— Tension and Compression Diagonals (Fx1)

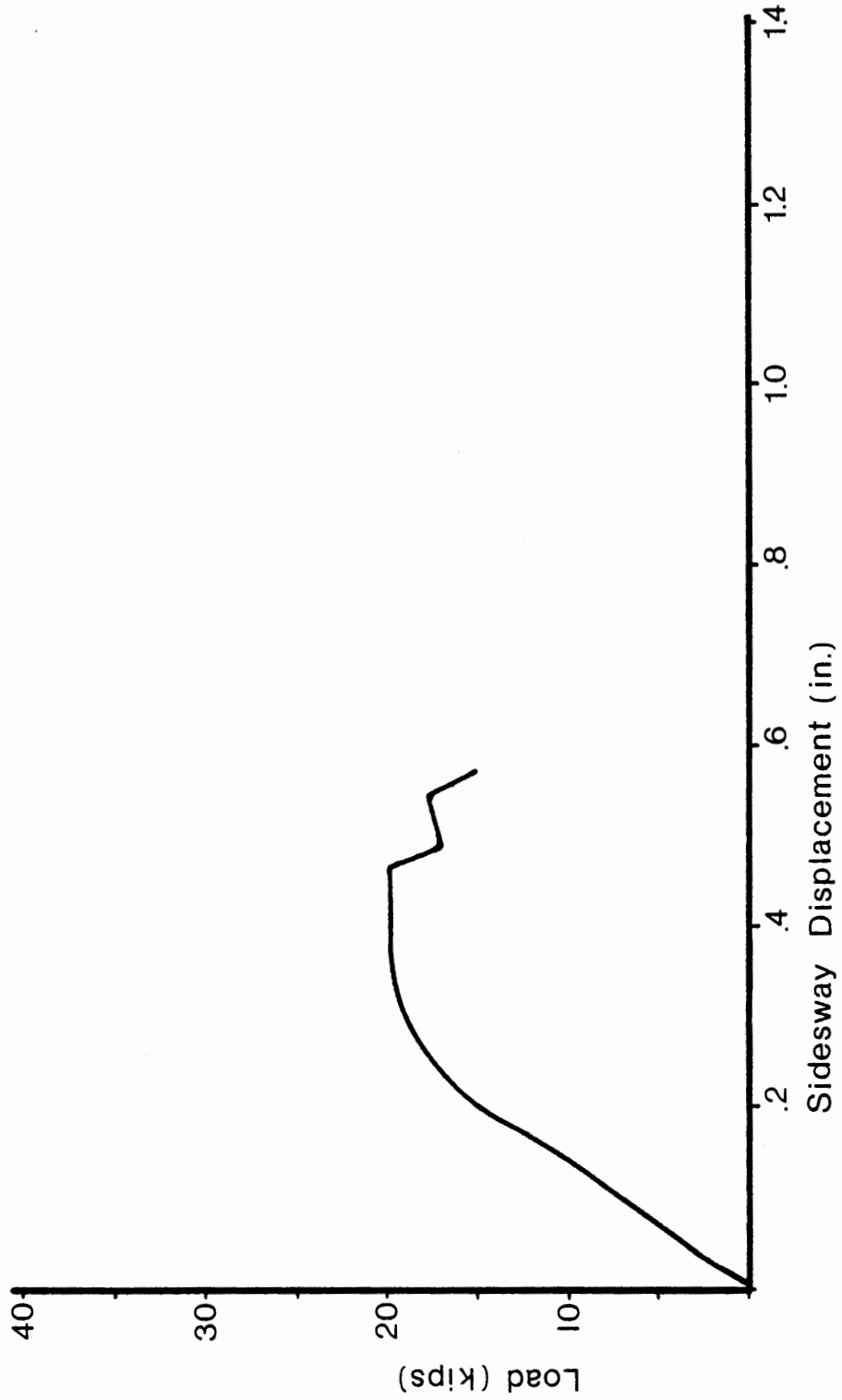


Figure 44 Test Fx1

TEST CONFIGURATION

— Tension and Compression Diagonals (Fx2)

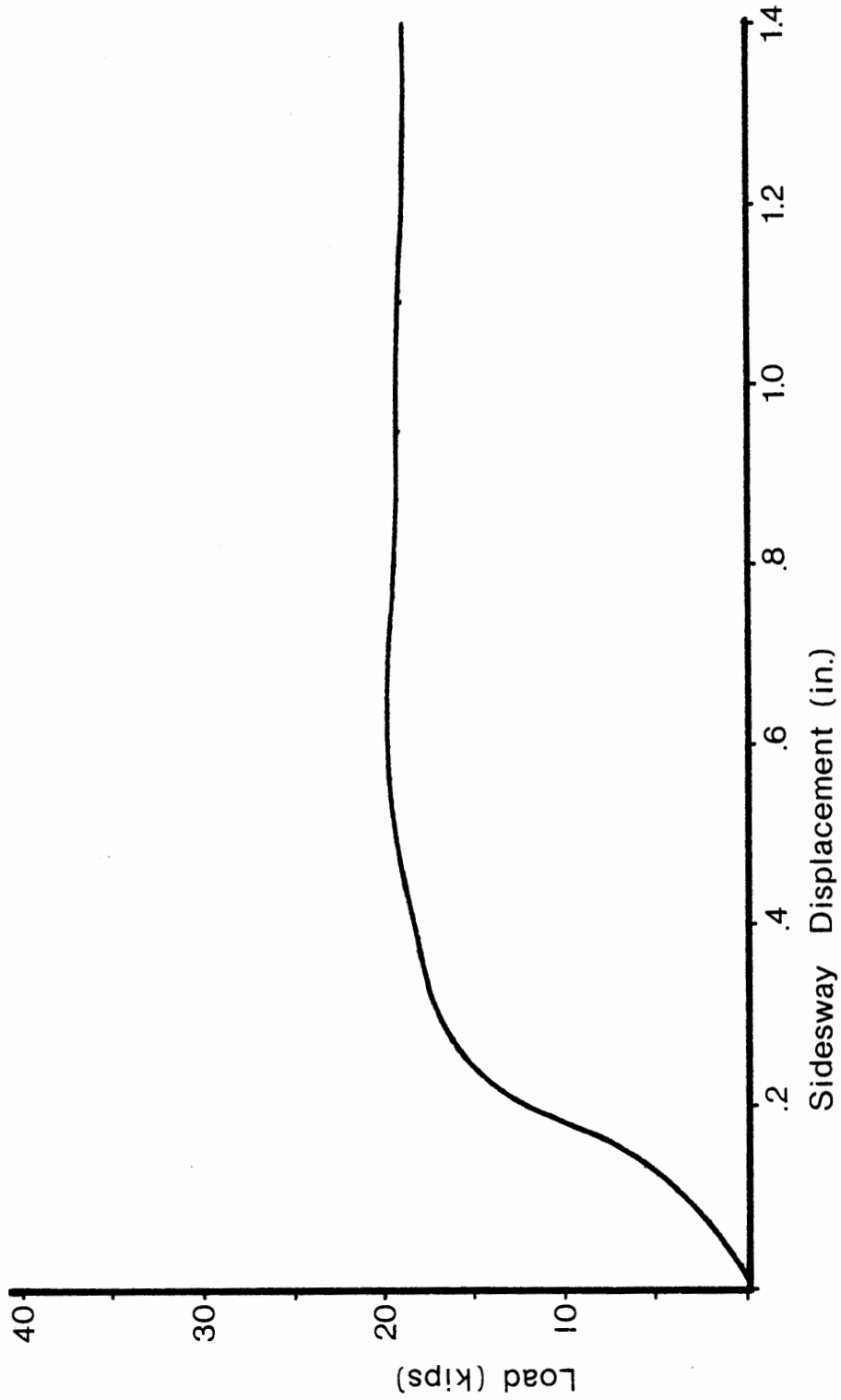


Figure 45 Test Fx2

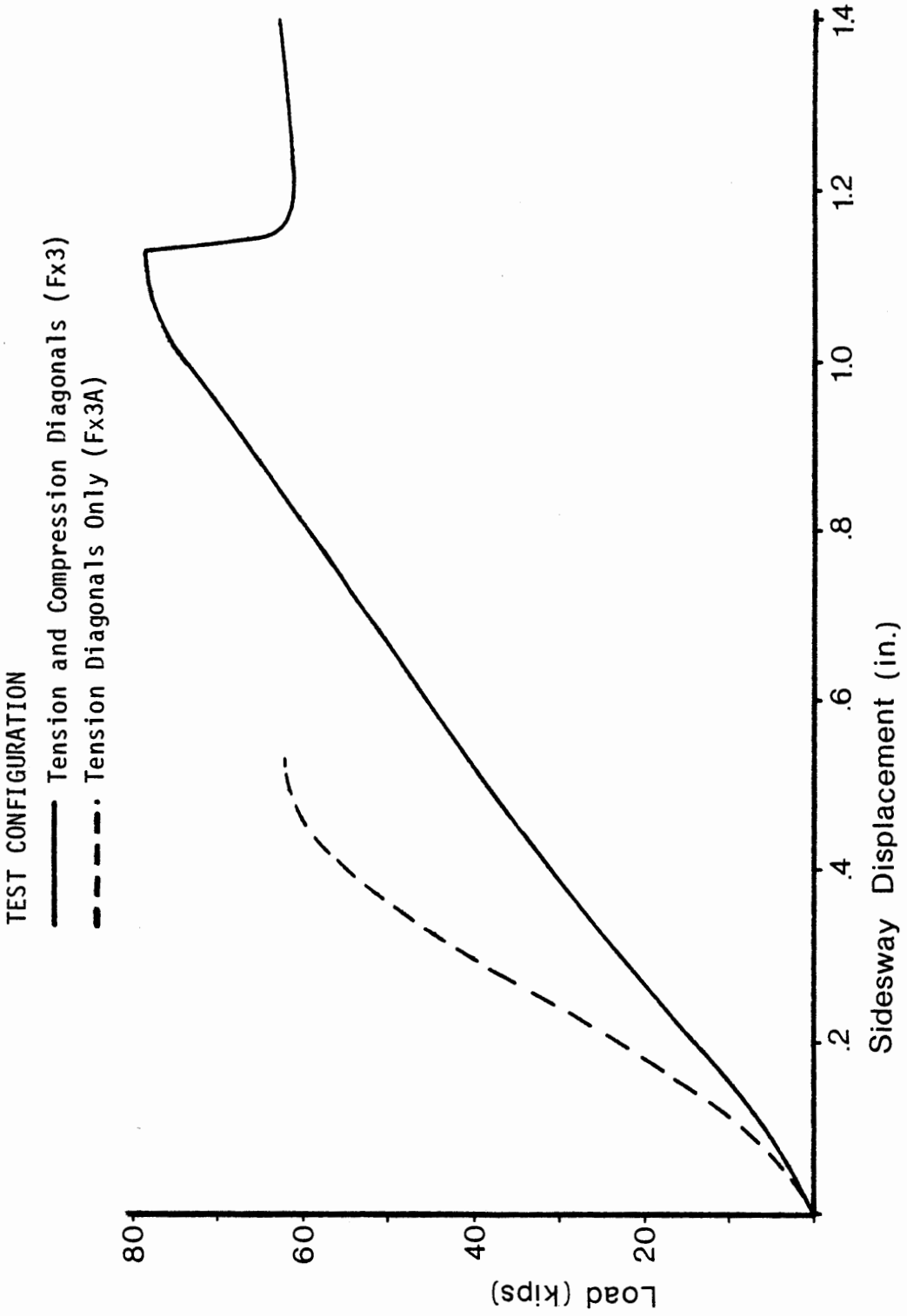


Figure 46 Test Fx3 and Fx3A

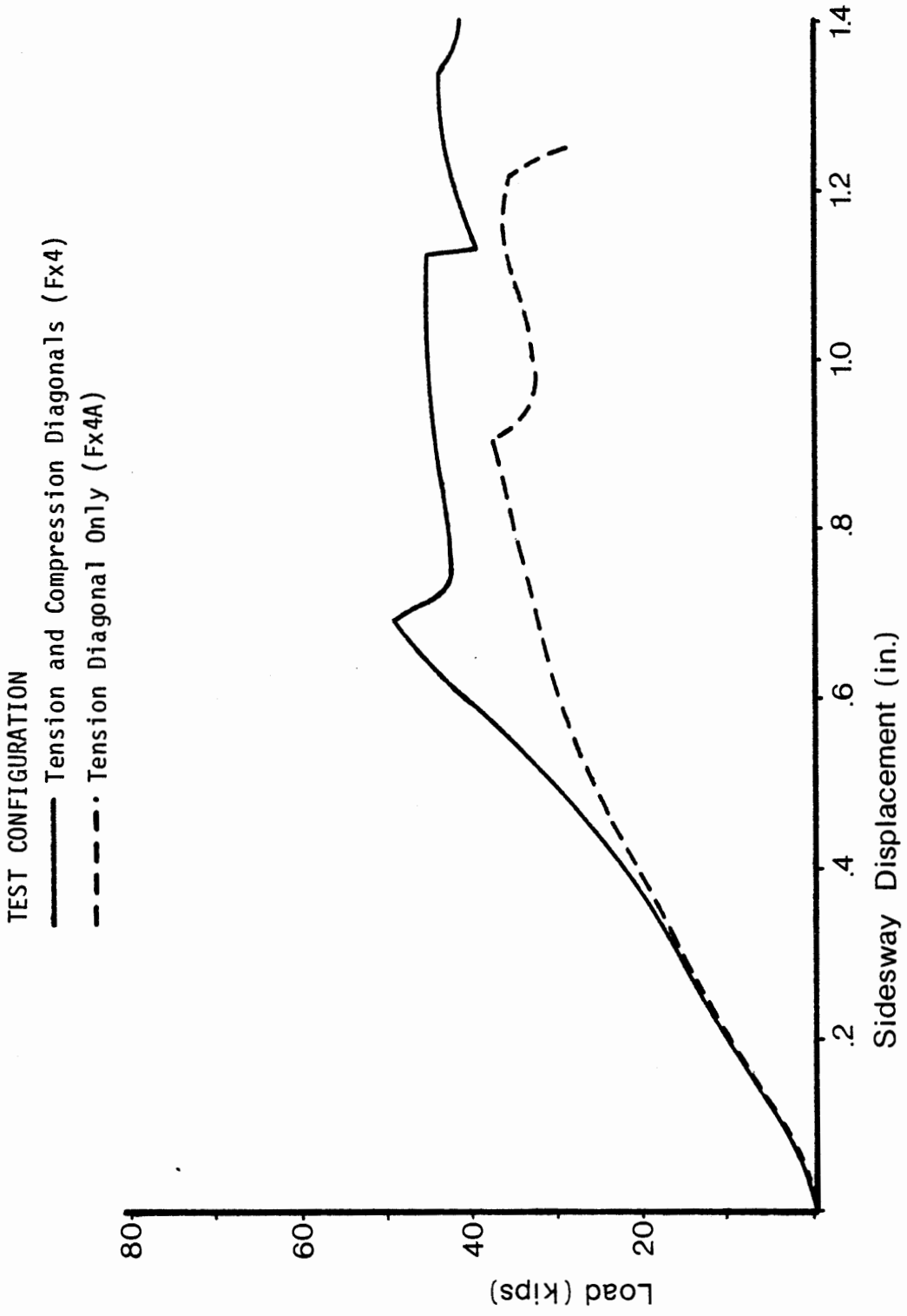


Figure 47 Test Fx4 and Fx4A

TEST CONFIGURATION

- Tension and Compression Diagonals (Fx5)
- - - Tension Diagonal Only (Fx5A)
- - - Compression Diagonal Only (Fx5B)

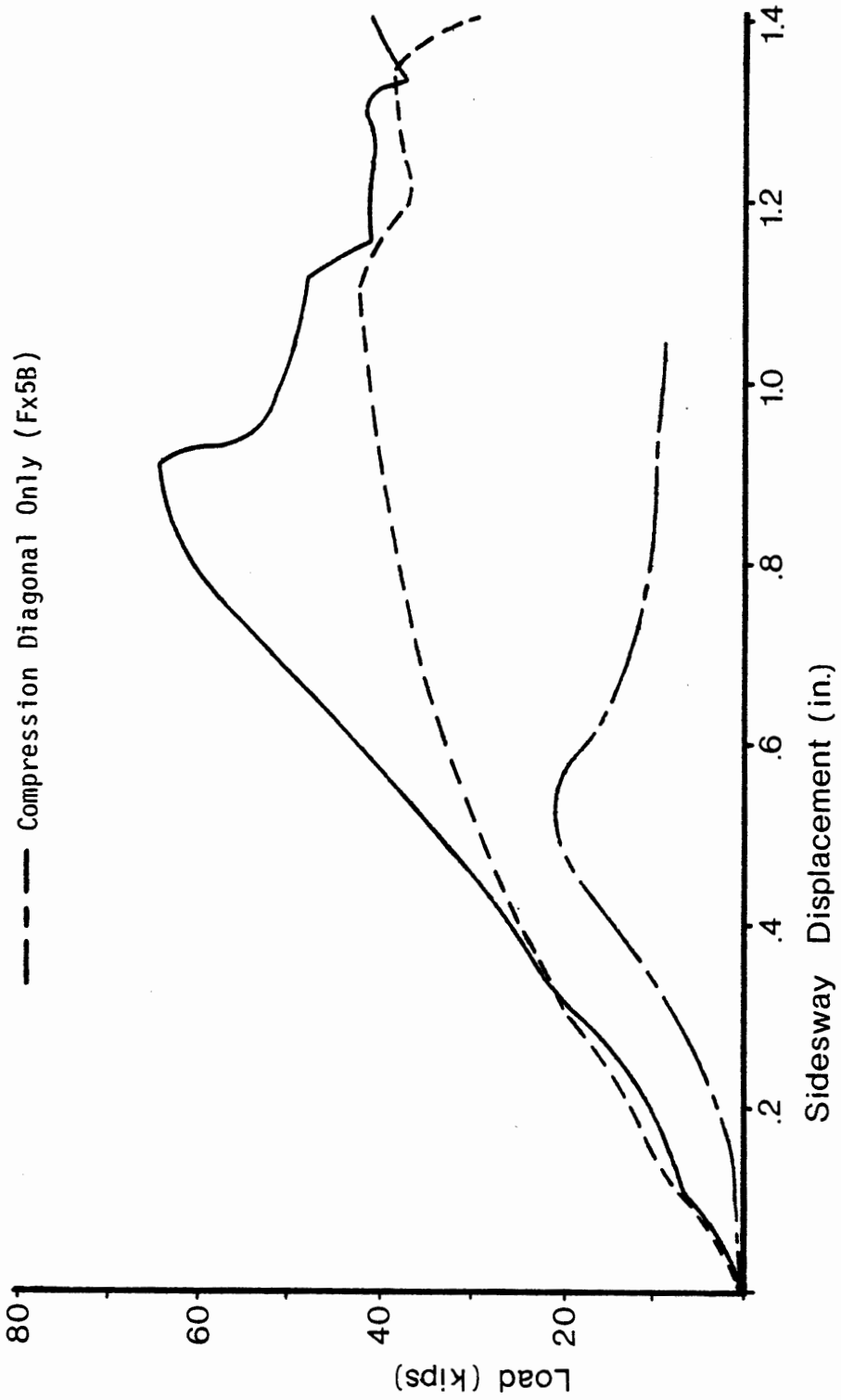


Figure 48 Test Fx5, Fx5A and Fx5B

TEST CONFIGURATION
— Tension and Compression Diagonals (Fx6)

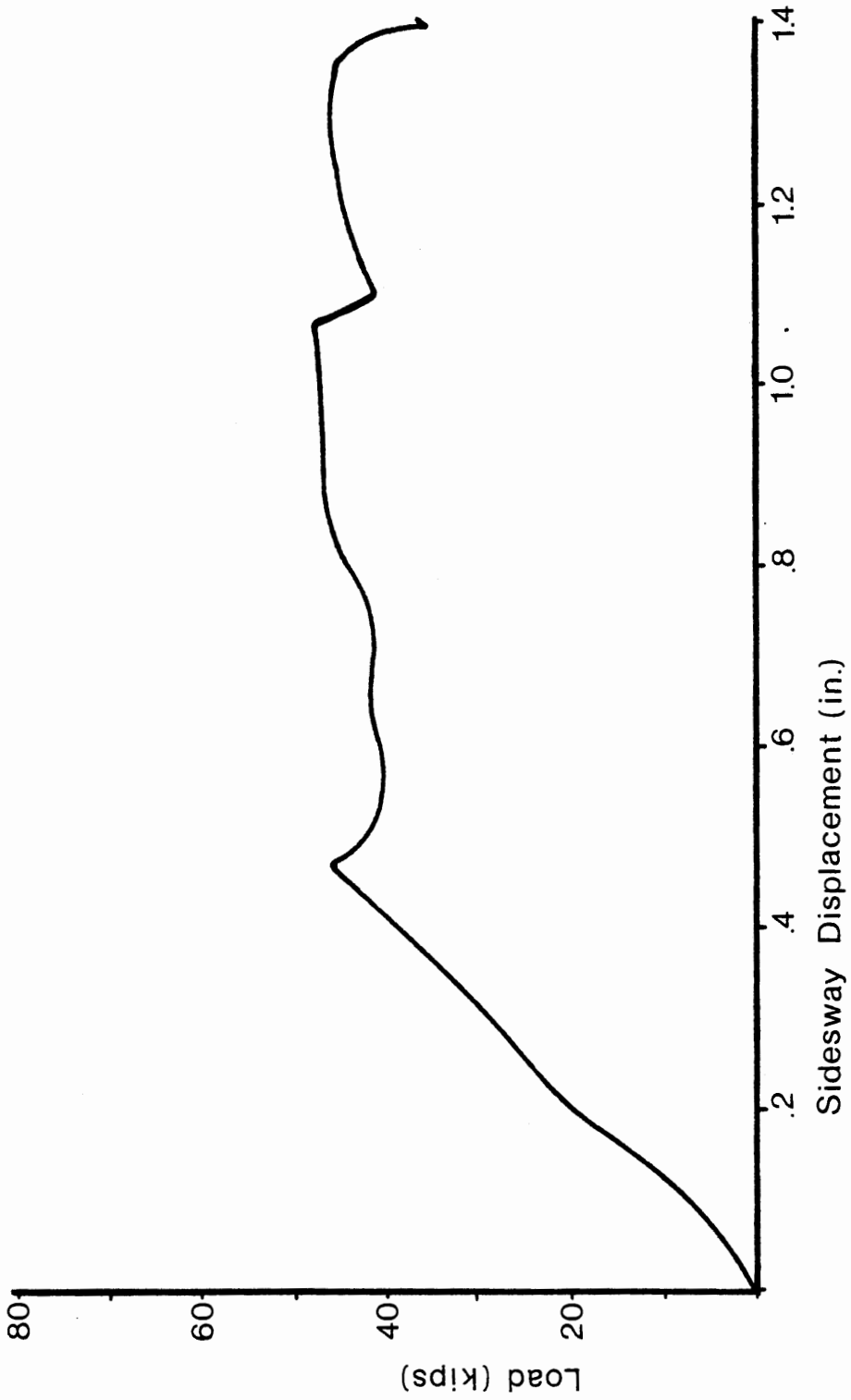


Figure 49 Test Fx6

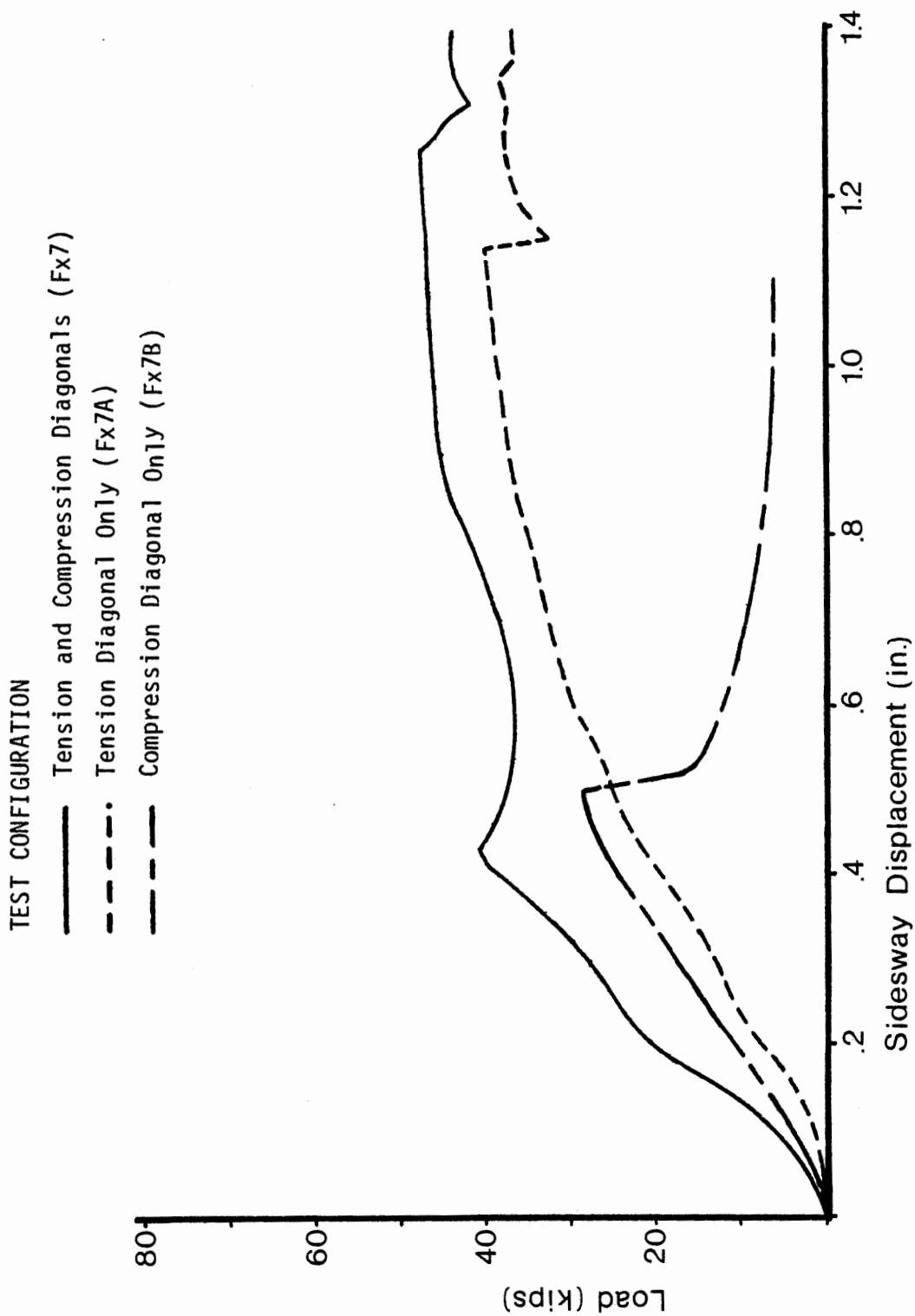


Figure 50 Test Fx7, Fx7A and Fx7B

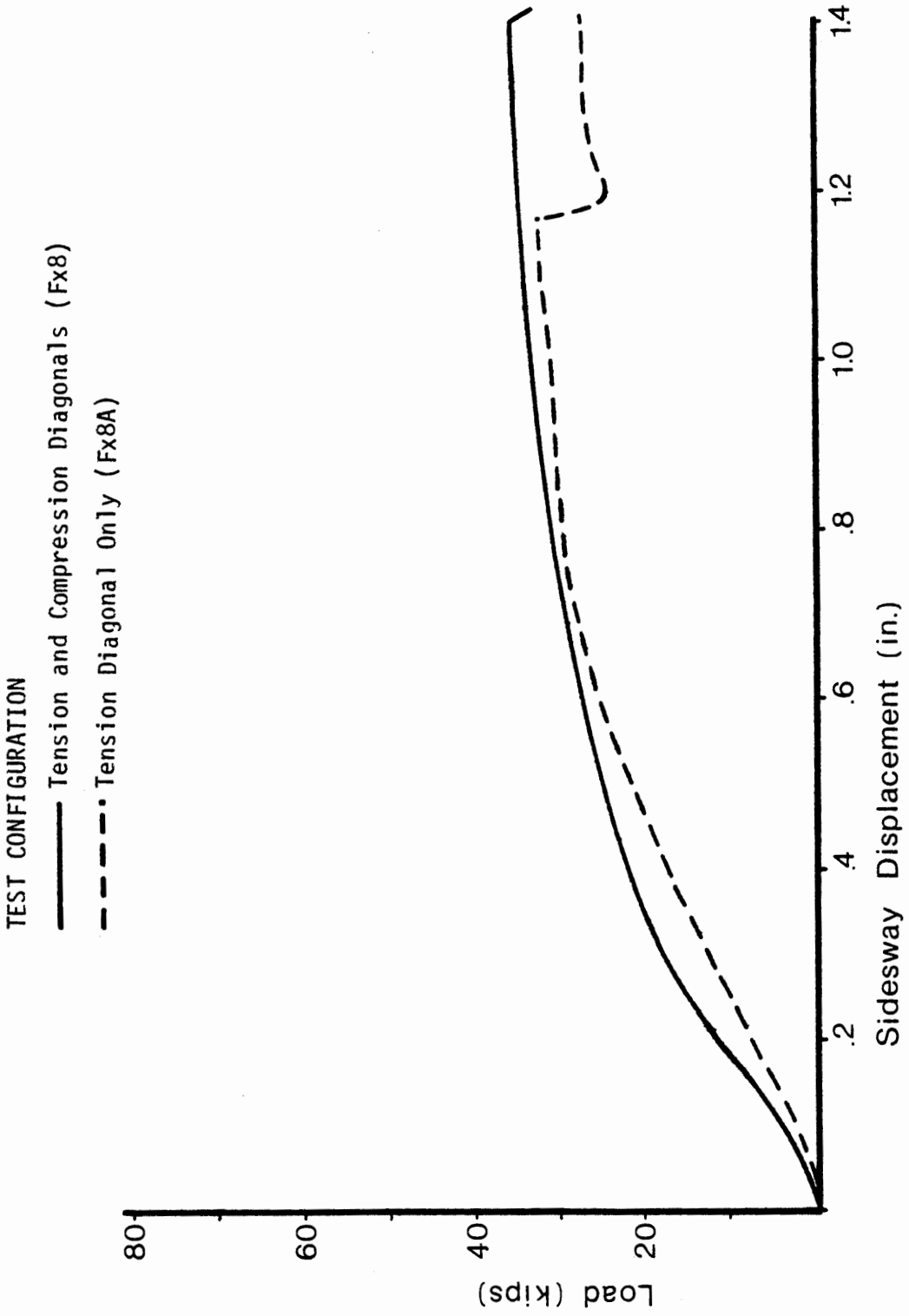


Figure 51 Test Fx8 and Fx8A

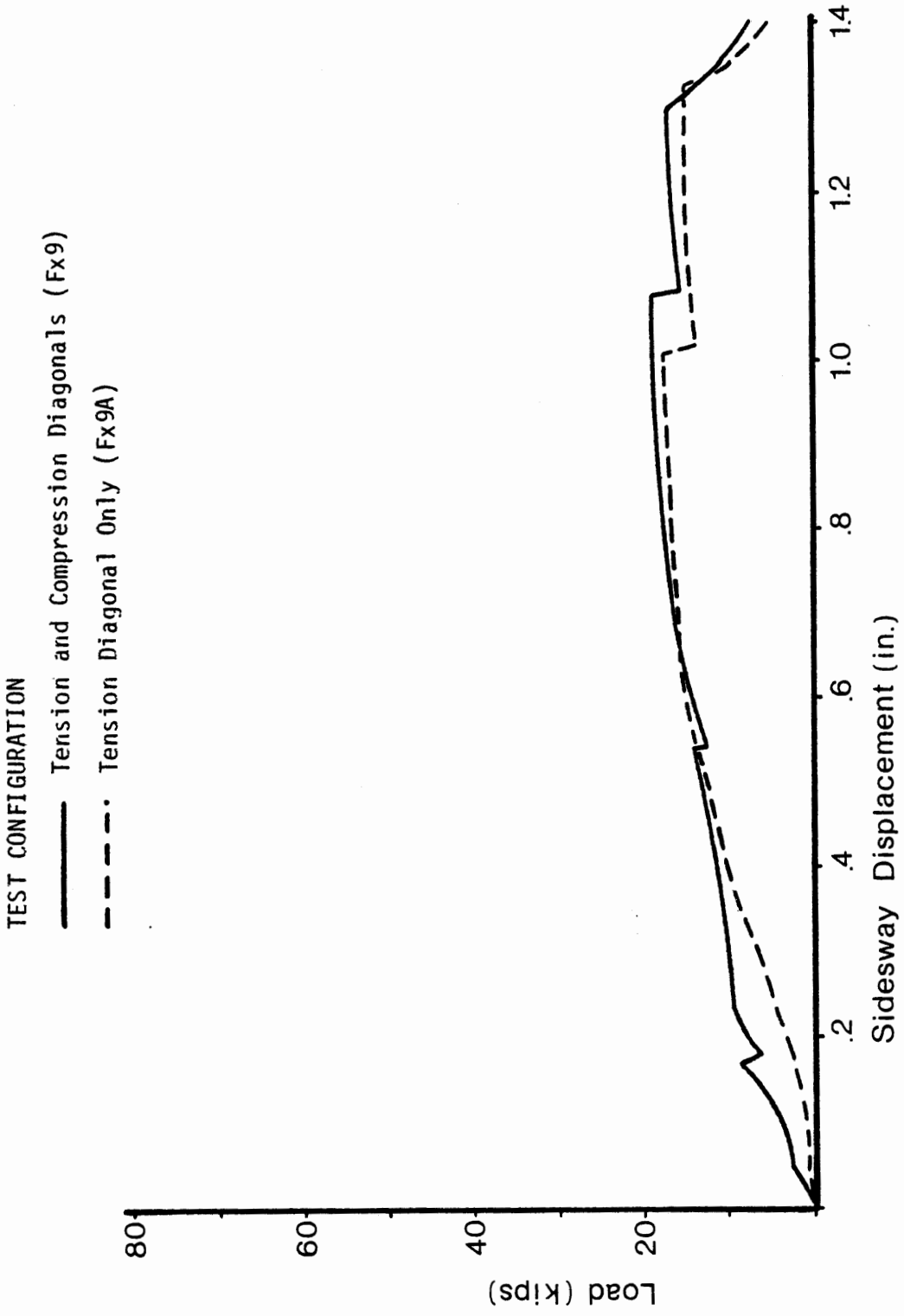


Figure 52 Test Fx9 and Fx9A

stressed to yield and the compression diagonal carries a zero load. The theoretical buckling load of a compression diagonal is the Euler Buckling load of the member assuming a pinned-pinned connection. It is assumed that the shear is equally distributed between the diagonal members before the failure of the compression member and hence the tension member carries the same load as the compression member. Hence the theoretical frame load when compression diagonal buckles listed in Table IVB is twice the component of the buckling load for the compression member in the case of the tests with two diagonals.

The experimental results are presented in Figures 44 to 52.

The tests performed can be categorized into three as follows

- (1) Tests with compression and tension diagonals
- (2) Tests with tension diagonal only
- (3) Tests with compression diagonal only

These three categories enable the study of the contribution of each diagonal member and both members together in sustaining the applied frame load.

Tests with compression diagonal only (Tests Fx5B and Fx7B) showed a gradual increase of load capacity and a steep drop of load after the member buckles. However these tests showed that the frame had some resistance to the applied load after the compression diagonal buckles. The shape of these curves are similar to that obtained in single member tests (Figs. 48 and 50).

Tests with both tension and compression diagonals showed a gradual increase of load until the compression diagonal buckles and then showed a little drop in load. The structural system has the ability to sustain

load until yielding of the tension member. This occurred at the bolt holes. It is shown in tests Fx4 and Fx5 that the load sustained in the case of tension and compression members is higher than that of tension member only tests in the post buckling region. The experimental ultimate load was shown to be 17.8 and 45.4 percent more than the theoretical frame load capacity calculated using statics. It was shown in single member tests that the compression members do sustain axial load in the post buckling region. This post buckling strength was instrumental in increasing the frame load capacity above the expected in the idealized situation. When the compression member loses load, it transfers to the tension member thus enabling the system to sustain an increase in load.

CHAPTER IV

CONCLUSIONS AND RECOMMENDATIONS

Basically the experimental results obtained in the single member tests verified the analytical computer program of Ref. 7. The load spike for members with no eccentricity was an important observation made in this study. These members pretend to show a higher ultimate load but a little disturbance causes sudden drop in load carrying capacity.

Experimental results of this investigation as well as the analytical computer model of Ref. 7 verifies that members with large length to radius of gyration ratio possess a wider plateau in the post buckling region. Hence these long members would be able to sustain their maximum load capacity for additional deformation. The implications of this on a Limit State Analysis of a three dimensional truss is that long members would allow the redistribution of loads to other parts of the structural system. Long member performance may conceivably be modeled as a bi-linear load-deflection curve. Members with a small length to radius of gyration ratio showed an unloading immediately after the ultimate load was reached. These short members could not sustain their maximum load for additional deformations. This suggests that a Limit State Analysis technique may be required to be able to account for member performance depicted by load-deflection curves other than bi-linear. This refinement should account for any unloading which exists after the ultimate load is passed. The secant stiffness approach could be used in this case. It assumes a lower stiffness of the member in the post ultimate region. This secant stiffness approach is independent

of the shape of the load deflection curve of the member and hence ideally suitable.

Eccentricity of the member tends to provide a greater plastic plateau but a lower ultimate load of the member. This makes a shorter member with large eccentricity of loading perform like a longer member with no eccentricity.

The non compact long members tested showed that they were not susceptible to local buckling even though their width to thickness ratio was much greater than that of compact sections. This is because these members being long are not subjected to a high enough stresses to cause local buckling. This shows that the load carrying capacity of long members with larger width to thickness ratios is not affected by the fact that they are not compact.

This study of single member tests provides a foundation to formulate axial load vs axial displacement curves for various parameters of members. These curves are needed to obtain the modified stiffness of members (secant stiffness) to use in Limit Analysis of Trusses such as transmission towers.

The preliminary truss tests conducted supports the fact that the buckled compression member aids in the load carrying capacity of the indeterminate truss by transferring loads to other members in the structural system. When the compression members reach their ultimate load and it through large deflections, the structure is able to redistribute it and resist higher structural loads by utilizing the reserve strength inherent in the indeterminate truss.

The bolt slippage of members was a cause for considerable axial displacement. It is recommended that further study of this bolt slippage

be undertaken to ascertain its effect on member performance. This investigation was not concerned with the effect of intermediate supports of compression members. It is also recommended that testing of single angle members with intermediate supports and diagonal members connected at their common point in the case of indeterminate trusses be undertaken. This will yield further data as to how various members behave in this type of situation.

REFERENCES

1. Beedle, L. S., "Plastic Design of Steel Frames," John Wiley and Sons, Inc., 1958.
2. Wang, C., "Matrix Methods of Structural Analysis," American Publishing Co., 2nd edition, 1970.
3. Lee, J. W. and Jensen, H. G., "Limit Truss Analysis by Linear Programming Technique," Preprint No. 80-006, 1980 ASCE National Convention, Portland, Oregon, April 1980.
4. Smith, E. A. and Epstein, H. I., "Progressive Collapse in the Hartford Space Truss," Preprint No. 80-062, 1980 ASCE National Convention, Portland, Oregon, April 1980.
5. Schmidt, L. C. and Hanaor, A., "Force Limiting Devices in Space Trusses," ASCE Journal of the Structural Division, May 1979.
6. Khan, L. F. and Hanson, R. D., "Inelastic Cycles of Axially Loaded Steel Members," ASCE Journal of the Structural Division, May 1976.
7. "Study of Limit State on Ultimate Load Behavior of Steel Columns," Portland State University - Bonneville Power Administration Contract 79-80BP24005, October 1981.
8. "Manual of Steel Construction," American Institute of Steel Construction, Inc., 8th Edition, 1980.
9. "1975 Annual book of ASTM Standards, Part 10," American Society for Testing and Materials.

APPENDIX A

COMPUTATION OF AXIAL DISPLACEMENT USING THE DATA OBTAINED IN SINGLE MEMBER TESTS FOR THE HINGED-HINGED CONFIGURATION

Derivation of Equations

Definition of symbols used in this Appendix are as follows

<u>Symbol</u>	<u>Description</u>
$X_0(N)$ $N = 1 \text{ to } 8$	Gage reading at location N (Fig. 55) at pre-load
$X(N)$ $N = 1 \text{ to } 8$	Gage reading at location N after member is loaded
B_n $n = 1 \text{ to } 2$	Distance between concentric gages at member end n
α_n $n = 1 \text{ to } 2$	Rotation about y axis (Fig. 54)
R_H	Distance from the hinge to the end plate

In this Hinged-Hinged configuration the end plates are free to rotate about the y axis and free to translate in the Z direction (Fig. 53). $X_0(1)$, $X_0(2)$, $X_0(3)$ and $X_0(4)$ are the initial gage readings at locations 1, 2, 3 and 4 which forms a square of size B_1 . $X(1)$, $X(2)$, $X(3)$ and $X(4)$ are the gage readings after displacements.

When a load is applied through the actuator the end plate translates a distance $O_1 O_2$ in the Z direction (Fig. 54) and rotate an angle α_1 about the y axis. The length of the member is measured from the hinge of one end to the hinge of the other end. Hence the displacement

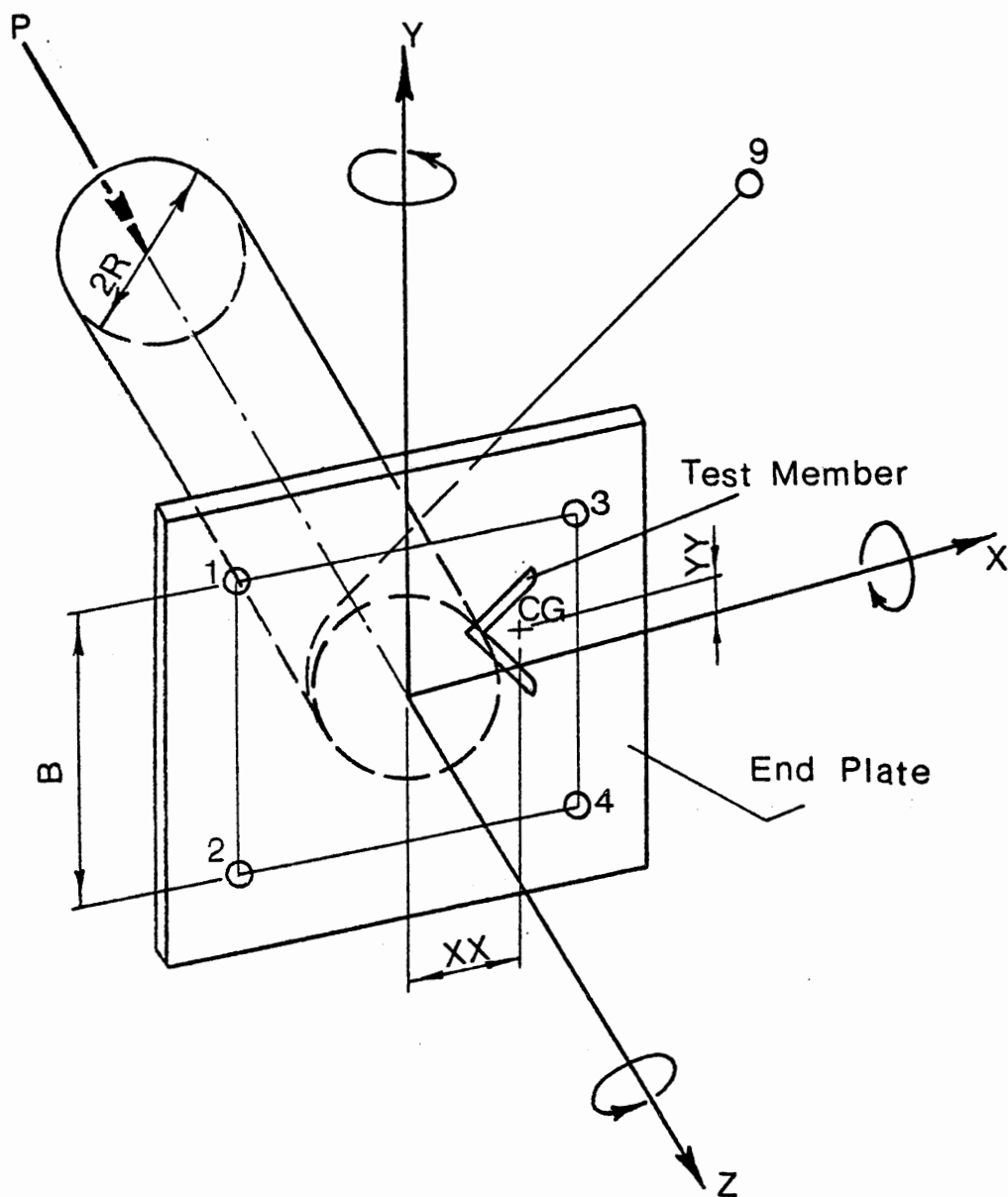


Figure 53 The end plate and gage layout at one end of the test member

of the member at one end is given by $O_1 O_2$ in Fig. 54.

The sum of displacements at both ends gives the total axial displacement for the member.

It follows that in Fig. 54.

$$O_1 A_1 = O_2 A_2 = R_H$$

$$C_1 C_3 = G_2 = \frac{X(1) + X(2) - X\phi(1) - X\phi(2)}{2}$$

$$B_1 B_3 = G_1 = \frac{X(3) + X(4) - X\phi(3) - X\phi(4)}{2}$$

$$DC_1 = B_3 B_1 = G_1$$

$$\tan \alpha_1 = \frac{G_1 + G_2}{B_1}$$

In triangle $EC_1 C_3$

$$EC_1 = C_1 C_3 \cot \alpha_1$$

$$EC_1 = G_2 \cot \alpha_1$$

$$EA_1 = EC_1 - B_1/2$$

$$EA_1 = G_2 \cot \alpha_1 - B_1/2$$

$$A_1 A_3 = EA_1 \tan \alpha_1$$

$$A_1 A_3 = (G_2 \cot \alpha_1 - B_1/2) \tan \alpha_1$$

$$O_2 A_3 = R_H \sec \alpha_1$$

$$\begin{aligned} A_2 A_3 &= O_2 A_3 - R_H \\ &= R_H (\sec \alpha_1 - 1) \end{aligned}$$

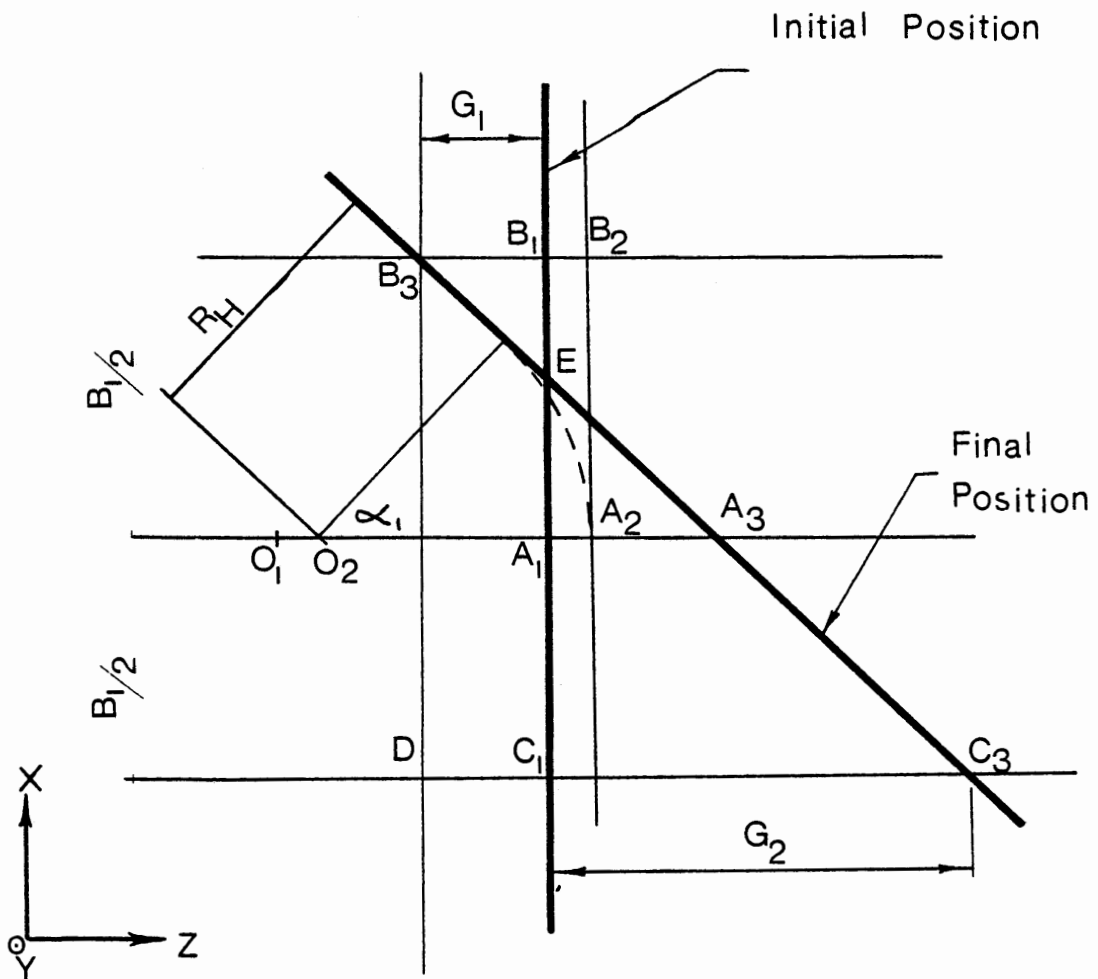


Figure 54 Translation of the end plate and rotation about the y axis for the hinged-hinged configuration

$$\begin{aligned}
 A_1 A_2 &= A_1 A_3 - A_2 A_3 \\
 &= G_2 - (B/2) \tan \alpha_1 - R_H \sec \alpha_1 - R_H \\
 &= G_2 - (1/2)(G_1 + G_2) - R_H (\sec \alpha_1 - 1)
 \end{aligned}$$

$$A_1 A_2 = (G_2 - G_1)/2 - R_H (\sec \alpha_1 - 1)$$

$$O_1 O_2 = A_1 A_2$$

The displacement at the first end = $O_1 O_2$

$$O_1 O_2 = \frac{1}{2} (G_2 - G_1) - R_H (\sec \alpha_1 - 1)$$

Applying proper signs to G_1 and G_2 ; the displacement at the first end is = $\frac{1}{2} (G_2 + G_1) - R_H (\sec \alpha_1 - 1)$

$$\text{where } \tan \alpha_1 = (G_2 - G_1)/B_1$$

Similarly at the other end let the initial gage readings be $X\emptyset(5)$, $X\emptyset(6)$, $X\emptyset(7)$ and $X\emptyset(8)$ at locations 5, 6, 7 and 8 (Fig. 55) and $X(5)$, $X(6)$, $X(7)$ and $X(8)$ be the gage readings after displacements.

Then we can find G_3 , G_4 , and $\tan \alpha_2$ such that

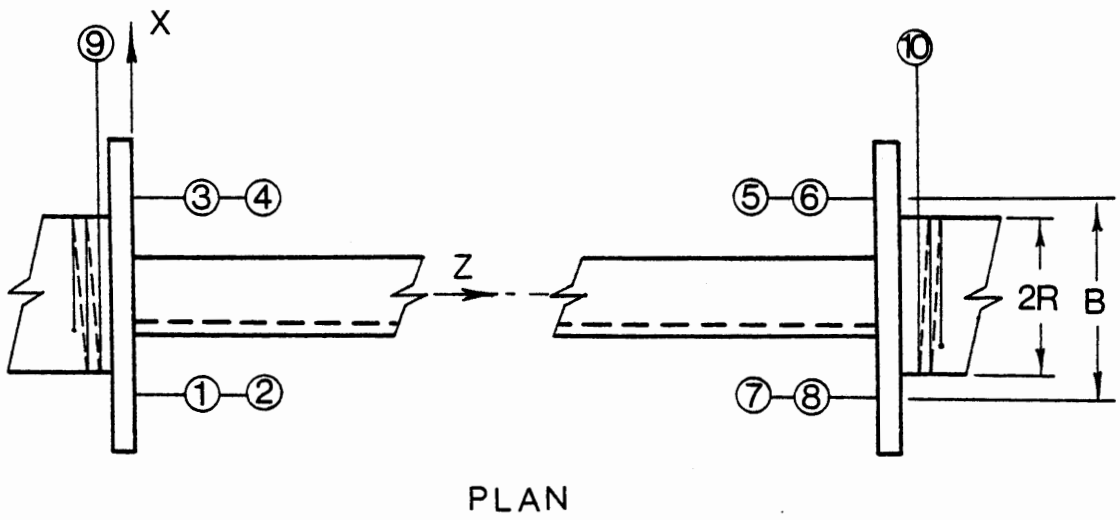
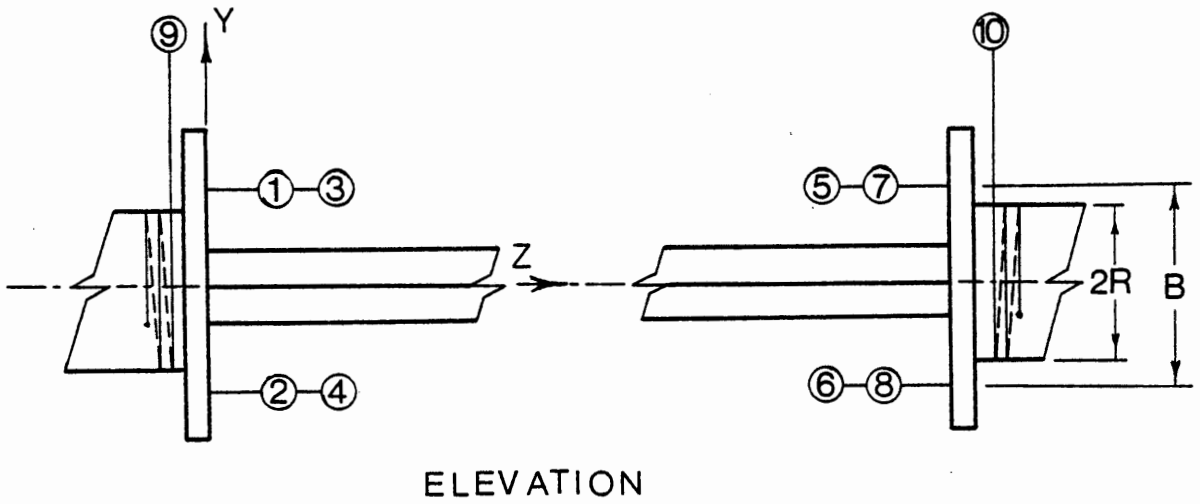
$$G_3 = (X(5) + X(6) - X\emptyset(5) - X\emptyset(6))/2$$

$$G_4 = (X(7) + X(8) - X\emptyset(7) - X\emptyset(8))/2$$

$$\tan \alpha_2 = (G_4 - G_3)/B_2$$

Hence the displacement at the other end is = $\frac{1}{2} (G_4 + G_3) - R_H (\sec \alpha_2 - 1)$

The computer program used to perform the above calculations are shown on the following pages.



End 1

End 2

Figure 55 Gage layout for single member tests including the rotational gages

Input data for the computer program:

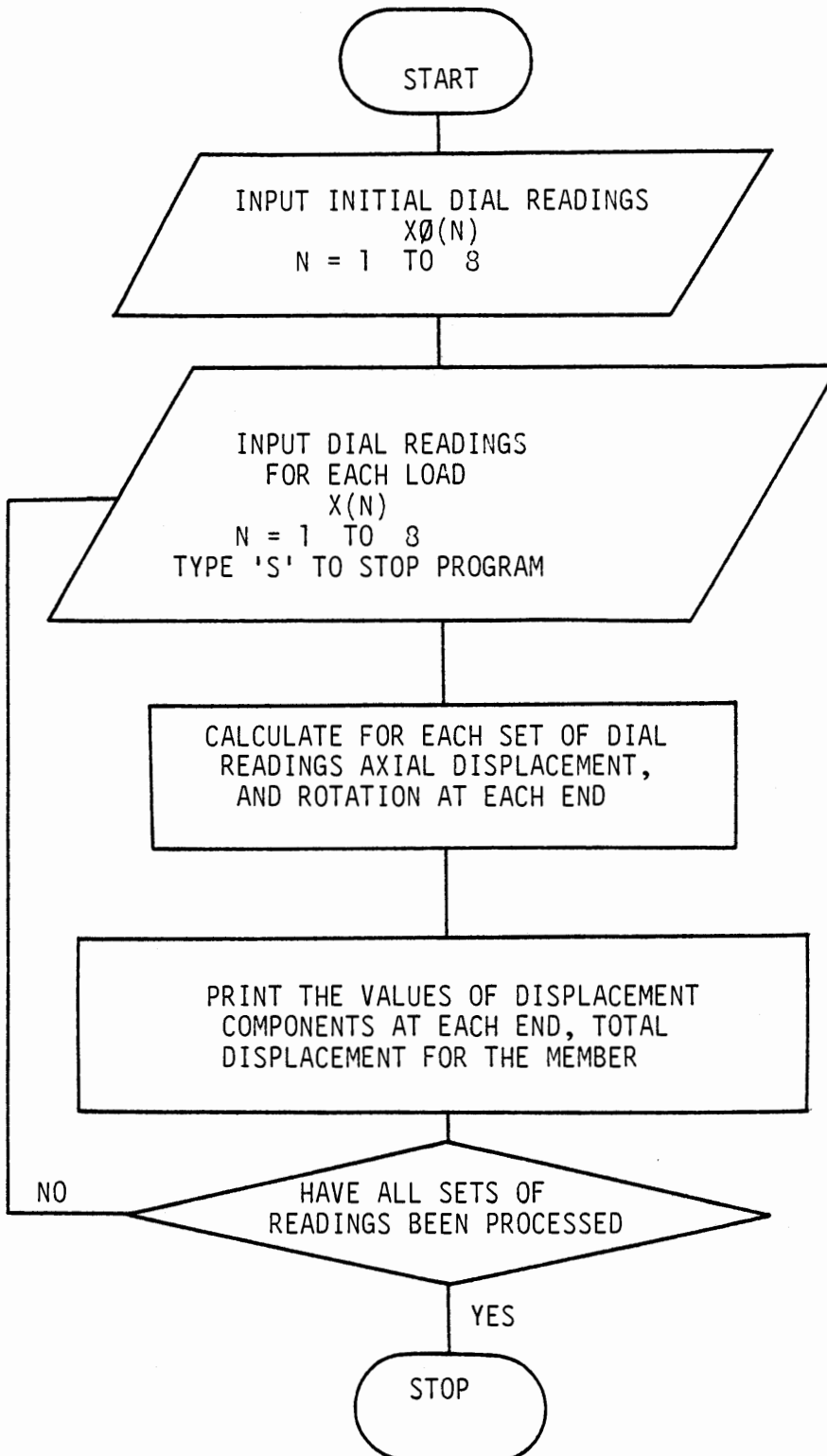
$X_0(N)$ = Gage reading at location N (Fig. 55) at preload
N = 1 to 8

$X(N)$ = Gage reading at location N after member is loaded
N = 1 to 8

Resetting of gages need to be done just before any of the dial gages reach their maximum range. The reading of such a gage in its current position is noted and then moved to a new position either towards or away from the end plate to facilitate further readings with the same gage. Readings of gages after resetting were taken into account for the difference.

Reset readings are input to the computer with a number 999.

The output printed is the displacement of the member at the actuator end, the displacement of the member at the reaction block end and the total axial displacement of the member.

FLOW DIAGRAM TO CALCULATE AXIAL DISPLACEMENT
FOR HINGE HINGE CONFIGURATION

COMPUTER PROGRAM

```

10 REM THIS PROGRAM WILL CALCULATE DELTA AND END ROTATION
20 REM AT BOTH ENDS OF THE ANGLE GIVEN 8 GAGE READINGS.
30 REM ** TO RESET ZERO ENTER 999 FOR EACH GAGE VALUE**
32 DIM X(8),X0(8),X1(8)
35 D3=0
36 D4=0
37 A3=0
38 A4=0
40 PRINT
50 PRINT
60 PRINT "GAGE LAYOUT"
65 PRINT "      ACT      REACT"
70 PRINT "      X      X      X      X"
80 PRINT "      1      3      5      7"
90 PRINT
91 PRINT
92 PRINT
93 PRINT
94 PRINT "      X      X      X      X"
95 PRINT "      2      4      6      8"
97 PRINT
98 PRINT
100 PRINT "INPUT 8 ZERO READINGS"
110 MAT INPUT X0
120 PRINT "INPUT 8 GAGE READINGS"
130 MAT INPUT X
135 IF X(1)>5 THEN 500
140 MAT X1=X-X0
150 FOR I=1 TO 8 STEP 2
155 I1=I/2+1
160 X(I1)=(X1(I)+X1(I+1))/2
170 NEXT I
175 A=5.7
176 R=1.75
180 A1=ATN((X(1)-X(2))/A)+A3
190 A2=ATN((X(3)-X(4))/A)+A4
200 D1=.5*(X(1)+X(2))-R*(1/COS(A1)-1.0)+D3
210 D2=.5*(X(3)+X(4))-R*(1/COS(A2)-1.0)+D4
220 PRINT "      DELTA(ACT)      DELTA(React)      DELTA "
230 PRINT D1,D2,D1+D2
240 PRINT "      ALPHA(1)      ALPHA(2) "
250 PRINT A1,A2
260 GOTO 120
500 D3=D1
510 D4=D2
520 A3=A1
530 A4=A2
540 GO TO 100
999 END

```

*BASIC
*RUN

GAGE LAYOUT

ACT		REACT	
X	X	X	X
1	3	5	7
X	X	X	X
2	4	6	8

INPUT 8 ZERO READINGS

?.452, .573, .494, .507, .491, .485, .495, .510

INPUT 8 GAGE READINGS

?.473, .599, .500, .518, .477, .468, .495, .507

DELTA(ACT)	DELTA(REACT)	DELTA
.0159939	-.0085053	.0074887

ALPHA(1) ALPHA(2)

.0026316 -.0024561

INPUT 8 GAGE READINGS

?.490, .619, .501, .522, .466, .455, .499, .511

DELTA(ACT)	DELTA(REACT)	DELTA
.0264741	-.0125242	.0139499

ALPHA(1) ALPHA(2)

.0054385 -.0052631

INPUT 8 GAGE READINGS

?.538, .675, .487, .515, .429, .419, .525, .539

DELTA(ACT)	DELTA(REACT)	DELTA
.0470146	-.0174854	.0295291

ALPHA(1) ALPHA(2)

.016402 -.016402

INPUT 8 GAGE READINGS

?.735, .884, .470, .515, .319, .318, .621, .644

DELTA(ACT)	DELTA(REACT)	DELTA
.1419965	-.0221641	.1198324

ALPHA(1) ALPHA(2)

.0534578 -.0524956

INPUT 8 GAGE READINGS

?999, 999, 999, 999, 999, 999, 999, 999

INPUT 8 ZERO READINGS

?.100, .000, .470, .515, .319, .318, .621, .644

INPUT 8 GAGE READINGS

? .198, .091, .489, .538, .277, .281, .680, .688

DELTA(ACT)	DELTA(React)	DELTA
.1958872	-.020273	.1756142

ALPHA(1)	ALPHA(2)
.0663518	-.0684591

INPUT 8 GAGE READINGS

?S

APPENDIX B

COMPUTATION OF AXIAL DISPLACEMENT USING THE DATA OBTAINED IN SINGLE MEMBER TESTS FOR BALL-BALL CONFIGURATION

Derivation of Equations

Definition of symbols used in this Appendix are as follows

<u>Symbol</u>	<u>Description</u>
$X\emptyset(N)$ $N = 1 \text{ to } 10$	Gage reading at location N (Fig. 55) at pre-load
$X(N)$ $N = 1 \text{ to } 10$	Gage reading at location N after member is loaded
E_n $n = 1 \text{ to } 2$	Displacement of the center of end plate in Z direction at member end n
B_n $n = 1 \text{ to } 2$	Distance between concentric gages (Fig. 53) at member end n
θ $n = 1 \text{ to } 2$	Rotation about X axis (Fig. 58) at member end n
β_n $n = 1 \text{ to } 2$	Rotation about Y axis (Fig. 59)
γ_n $n = 1 \text{ to } 2$	Rotation about Z axis (Fig. 57)
d_N $N = 1 \text{ to } 10$	Gage reading at location N (Fig. 55) corrected for the initial value
R_0	Distance from the center of end plate to center of gravity of test member (Fig. 57)
R	Radius of the ball (Fig. 53)

In this ball-ball configuration the end plates are free to rotate about x, y and z axes and free to translate in the z direction. Figure 53 details these directions. $X\emptyset(1)$, $X\emptyset(2)$, $X\emptyset(3)$, $X\emptyset(4)$ and $X\emptyset(9)$ are the initial gage readings at locations 1, 2, 3, 4 and 9 (Fig. 55). Locations 1, 2, 3 and 4 forms a square of side B_1 . Gage 9 is located perpendicular to the test member to measure rotations about z axis as in Fig. 55. $X(1)$, $X(2)$, $X(3)$, $X(4)$ and $X(9)$ are the gage readings after displacements. E_1 is the translation of the center of the end plate in the z direction. Layout details are given in Fig. 56.

The following define the relationship between displacements and geometry.

$$X\emptyset(1) + E_1 + (1/2)B_1 \tan \theta_1 + (1/2)B_1 \tan \beta_1 = X(1) \quad 1$$

$$X\emptyset(2) + E_1 - (1/2)B_1 \tan \theta_1 + (1/2)B_1 \tan \beta_1 = X(2) \quad 2$$

$$X\emptyset(3) + E_1 + (1/2)B_1 \tan \theta_1 - (1/2)B_1 \tan \beta_1 = X(3) \quad 3$$

$$X\emptyset(4) + E_1 - (1/2)B_1 \tan \theta_1 - (1/2)B_1 \tan \beta_1 = X(4) \quad 4$$

Adding equations 1, 2, 3 and 4

$$X\emptyset(1) + X\emptyset(2) + X\emptyset(3) + X\emptyset(4) + 4E_1 = X(1) + X(2) + X(3) + X(4)$$

$$E_1 = \frac{1}{4} (X(1) - X\emptyset(1) + X(2) - X\emptyset(2) + X(3) - X\emptyset(3) + X(4) - X\emptyset(4))$$

$$\text{Let } X(1) - X\emptyset(1) = d_1$$

$$X(2) - X\emptyset(2) = d_2, \text{ etc.}$$

Equations 1-2

$$B_1 \tan \theta_1 = d_1 - d_2$$

$$\theta_1 = \text{Arc Tan } ((d_1 - d_2)/B_1)$$

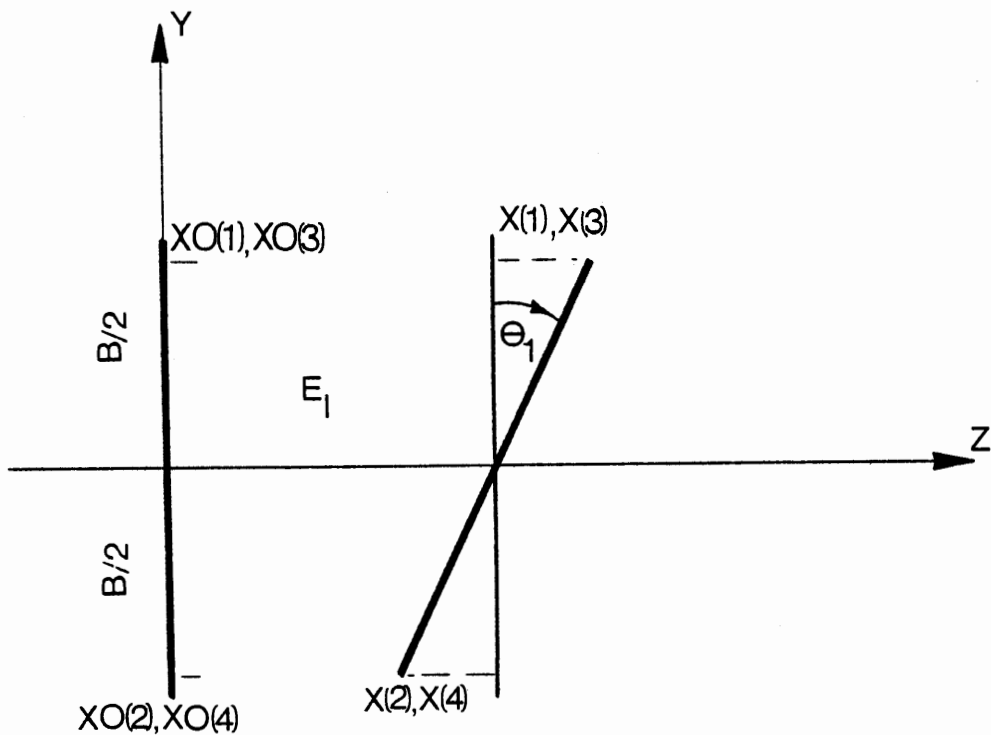


Figure 56 Translation of the end plate with rotation about the x axis

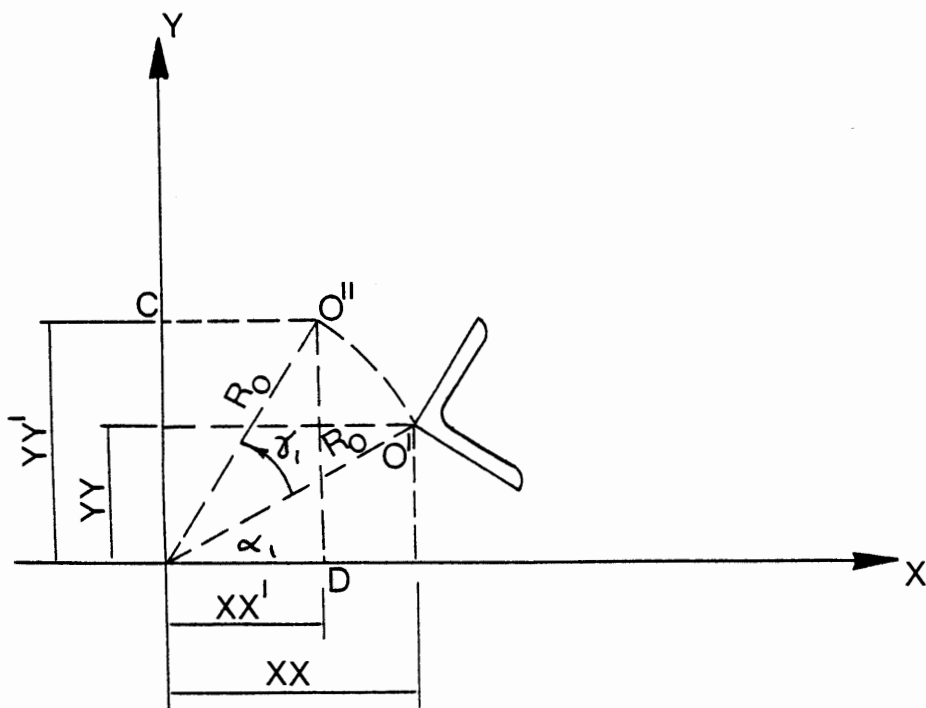


Figure 57 Rotation of the end plate about the z axis

Hence rotation about X axis

$$\theta_1 = \text{Arc Tan } ((d_1 - d_2)/B_1)$$

Equations 1-3

$$B_1 \text{ Tan } \beta_1 = d_1 - d_3$$

$$\text{Tan } \beta_1 = (d_1 - d_3)/B_1$$

$$\beta_1 = \text{Arc Tan } ((d_1 - d_3)/B_1)$$

Rotation about y axis

$$\beta_1 = \text{Arc Tan } ((d_1 - d_3)/B_1)$$

Equations 1 + 2 + 3 + 4

$$4E_1 = X(1) - X\emptyset(1) + X(2) - X\emptyset(2) + X(3) - X\emptyset(3) + X(4) - X\emptyset(4)$$

$$E_1 = \frac{1}{4} (d_1 + d_2 + d_3 + d_4)$$

Rotation about Z axis γ_1 is given by

$$\gamma_1 = (X(9) - X\emptyset(9))/R$$

Consider the γ_1 rotation about Z axis (Fig. 57).

The location of the center of gravity of the angle is given by

$$R_0 = (XX^2 + YY^2)^{\frac{1}{2}}$$

In Fig. 57

$$O''C = R_0 \text{ Cos } (\alpha_1 + \gamma_1)$$

$$O''C = R_0 \text{ Cos } \alpha_1 \text{ Cos } \gamma_1 - R_0 \text{ Sin } \alpha_1 \text{ Sin } \gamma_1$$

$$O''C = (XX^2 + YY^2)^{\frac{1}{2}} XX \text{ Cos } \gamma_1 / (XX^2 + YY^2)^{\frac{1}{2}} - (XX^2 + YY^2)^{\frac{1}{2}} \times \\ YY \text{ Sin } \gamma_1 / (XX^2 + YY^2)^{\frac{1}{2}}$$

$$XX^1 = O^1C = XX \cos \gamma_1 - YY \sin \gamma_1$$

Similarly

$$O^1D = R_0 \sin (\alpha_1 + \gamma_1)$$

$$O^1D = R_0 \sin \alpha_1 \cos \gamma_1 + R_0 \cos \alpha_1 \sin \gamma_1$$

$$YY^1 = O^1D = YY \cos \gamma_1 + XX \sin \gamma_1$$

Now consider the rotation θ_1 about X axis (Fig. 58)

$$ZZ_1'' = YY^1 \sin \theta_1$$

$$YY^1 = O^1D = YY \cos \gamma_1 + XX \sin \gamma_1$$

$$ZZ'' = (YY \cos \gamma_1 + XX \sin \gamma_1) \sin \theta_1$$

$$YY'' = YY^1 \cos \theta_1$$

$$YY'' = (YY \cos \gamma_1 + XX \sin \gamma_1) \cos \theta_1$$

$$Y^1 = YY^1 - YY''$$

$$Y^1 = (YY \cos \gamma_1 + XX \sin \gamma_1)(1 - \cos \theta_1)$$

For rotation β_1 about Y axis (Fig 59)

$$XX'' = XX^1 \cos \beta_1$$

$$XX'' = (XX \cos \gamma_1 - YY \sin \gamma_1) \cos \beta_1$$

$$X^1 = (XX \cos \gamma_1 - YY \sin \gamma_1)(1 - \cos \beta_1)$$

$$ZZ_1'' = XX^1 (\sin \beta_1)$$

$$ZZ_1'' = - (XX \cos \gamma_1 - YY \sin \gamma_1) \sin \beta_1$$

The new location of center of gravity of the angle at the first end is given by

$$M = XX'' = (XX \cos \gamma_1 - YY \sin \gamma_1) \cos \beta_1$$

$$N = YY'' = (YY \cos \gamma_1 + XX \sin \gamma_1) \cos \theta_1$$

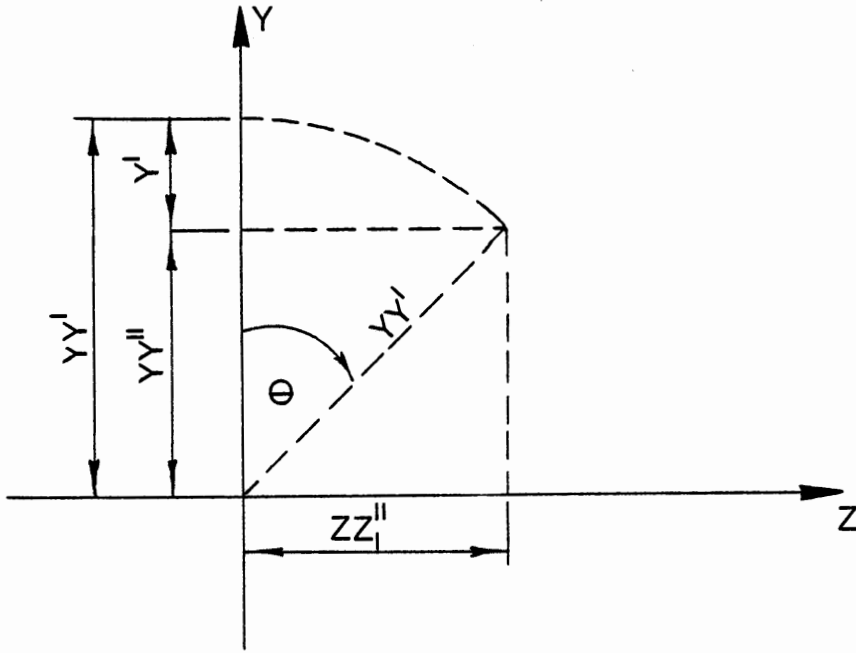


Figure 58 Rotation of the end plate about the x axis

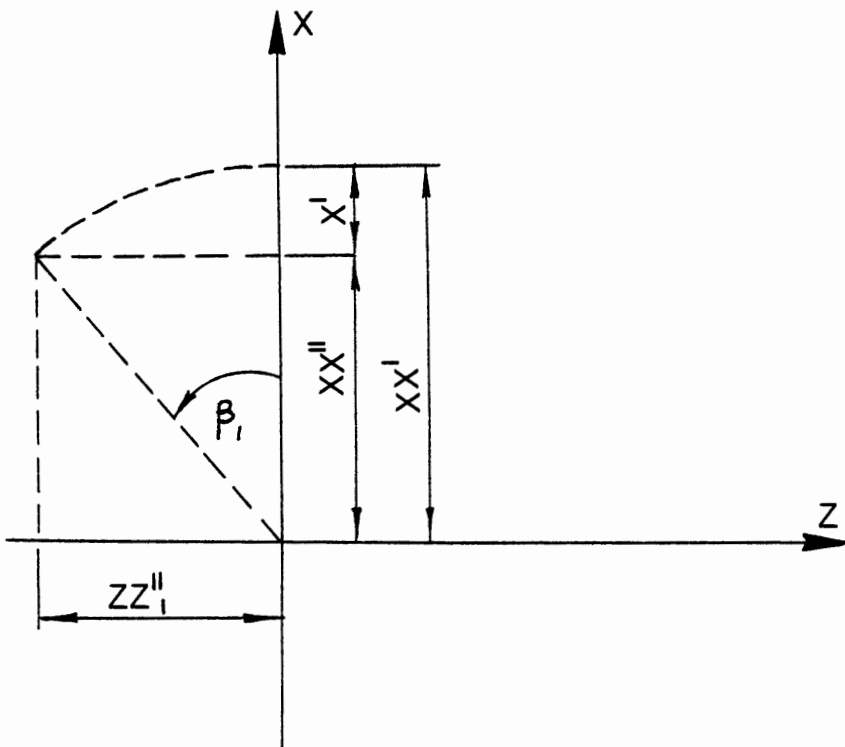


Figure 59 Rotation of the end plate about the y axis

$$\begin{aligned}
P = E_1 + ZZ'' &= (YY \cos \gamma_1 + XX \sin \gamma_1) \sin \theta_1 \\
&\quad - (XX \cos \gamma_1 - YY \sin \gamma_1) \sin \beta_1 + E_1 \\
&= YY (\cos \gamma_1 \sin \theta_1 + \sin \gamma_1 \sin \beta_1) \\
&\quad + XX (\sin \gamma_1 \sin \theta_1 - \cos \gamma_1 \sin \beta_1) \\
&\quad + E_1
\end{aligned}$$

Hence the position vector of the center of gravity of angle V_1 at the first end is given by

$$\underline{V}_1 = \underline{M}_i + \underline{N}_j + \underline{P}_k$$

\underline{i} , \underline{j} and \underline{k} are unit position vectors in x , y and z directions respectively.

Similarly let $X\emptyset(5)$, $X\emptyset(6)$, $X\emptyset(7)$, $X(8)$ and $X\emptyset(10)$ be the initial gage readings at locations 5, 6, 7, 8 and 10 (Fig. 55). Let $X(5)$, $X(6)$, $X(7)$, $X(8)$ and $X(10)$ be the gage readings after displacements. Let E_2 be the translation of the center of the end plate in the z direction.

Writing similar equations for the second end

$$X\emptyset(5) + E_2 + (1/2)B_2 \tan \theta_2 + (1/2)B_2 \tan \beta_2 = X(5) \quad 5$$

$$X\emptyset(6) + E_2 - (1/2)B_2 \tan \theta_2 + (1/2)B_2 \tan \beta_2 = X(6) \quad 6$$

$$X\emptyset(7) + A_2 + (1/2)B_2 \tan \theta_2 - (1/2)B_2 \tan \beta_2 = X(7) \quad 7$$

$$X\emptyset(8) + A_2 - (1/2)B_2 \tan \theta_2 - (1/2)B_2 \tan \beta_2 = X(8) \quad 8$$

$$\begin{aligned}
\text{Adding equations 5, 6, 7 and 8 we get } E_2 &= \frac{1}{4} (X(5) - X\emptyset(5) + \\
X(6) - X\emptyset(6) &+ X(7) - X\emptyset(7) + X(8) - X\emptyset(8))
\end{aligned}$$

Similarly we obtain location of center of gravity of the angle at the second end as follows

$$R = XX_2'' = (XX \cos \gamma_2 - YY \sin \gamma_2) \cos \beta_2$$

$$S = YY_2'' = (YY \cos \gamma_2 + XX \sin \gamma_2) \cos \theta_2$$

$$T = ZZ_2'' = -YY (\cos \gamma_2 \sin \theta_2 + \sin \gamma_2 \sin \beta_2) + \text{continued}$$

$$- XX (\sin \gamma_2 \sin \theta_2 - \cos \gamma_2 \sin \beta_2) - E_2 + L$$

Position vector of the center of gravity of the angle at the second end V_2 is given by

$$\underline{V}_2 = R\underline{i} + S\underline{j} + T\underline{k}$$

$$L^1 = ((M - R)^2 + (N - S)^2 + (P - T)^2)^{\frac{1}{2}}$$

L^1 is the distance between the center of gravity of the test member from one end to the other.

Hence the axial displacement of the test member is given by

$$\delta L = L - L^1$$

The computer program used to perform the above calculations is as follows.

INPUT DATA FOR THE COMPUTER PROGRAM

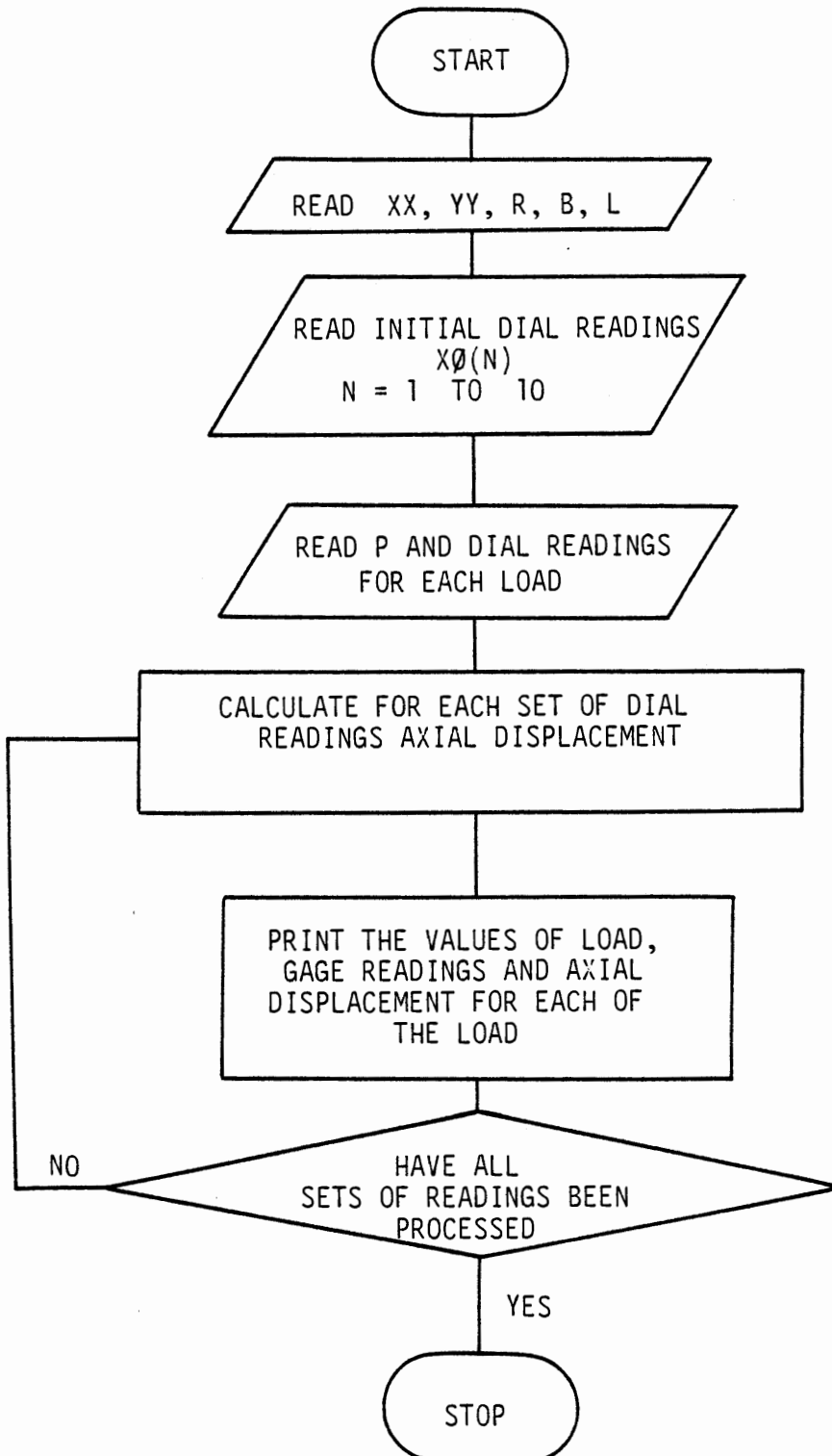
XX	= Eccentricity of the test member in the X direction (Fig. 53)
YY	= Eccentricity of the test member in the Y direction (Fig 53)
B	= Distance between concentric gages (Fig 53)
L	= Length of the test member
P	= Load value at each increment step
P_M	= Ultimate load of the test member
R	= Radius of the ball
X(N)	= Gage reading at location N (Fig 55)
N = 1 to 10	

Resetting of gages need to be done just before any of the dial gages reach their maximum range. The reading of such a gage in its current position is noted and then moved to a newer position either

towards or away from the end plate to facilitate further readings with the same gage. Readings of gages after resetting were taken into account for the difference.

Reset readings are indicated to the computer by a character "Z" for the load.

The output printed is axial load, gage readings and axial displacement for each load step.

FLOW DIAGRAM TO CALCULATE AXIAL
DISPLACEMENT FOR BALL-BALL CONFIGURATION

COMPUTER PROGRAM

*LIST

```

10 REM THIS PROGRAM CALCULATES THE AXIAL DISPLACEMENT FOR
20 REM A MEMBER WITH BALL BALL CONFIGURATION
25 DIM XO(10),X(10),X1(10),L$(30)
26 READ Y1,Y2,R,B,L,P
30 PRINT "XX =";Y1;"YY=";Y2;"R=";R;"B=";B;"L=";L
35 PRINT "LOAD      GAGE READINGS"
36 A3=0
37 A4=0
38 T3=0
39 T4=0
40 B3=0
41 B4=0
42 G3=0
43 G4=0
50 FOR N=1 TO 10
51 READ XO(N)
53 NEXT N
55 READ L$
60 IF L$="Z" GOTO 500
70 IF L$="STP" GOTO 4002
190 FOR N=1 TO 10
191 READ X(N)
192 X1(N)=X(N)-XO(N)
193 IF N>4 THEN 195
194 GOTO 200
195 IF N<9 THEN 198
196 GOTO 200
198 X1(N)=-X1(N)
200 NEXT N
210 A1=(X1(1)+X1(2)+X1(3)+X1(4))/4+A3
220 A2=(X1(5)+X1(6)+X1(7)+X1(8))/4+A4
230 T1=ATN((X1(1)-X1(2))/B)+T3
240 T2=ATN((X1(5)-X1(6))/B)+T4
250 B1=ATN((X1(1)-X1(3))/B)+B3
260 B2=ATN((X1(7)-X1(5))/B)+B4
270 G1=X1(9)/R+G3
275 G2=X1(10)/R+G4
280 I1=(Y1*COS(G1)-Y2*SIN(G1))*COS(B1)
290 J1=(Y2*COS(G1)+Y1*SIN(G1))*COS(T1)
300 K1=Y2*(COS(G1)*SIN(T1)+SIN(G1)*SIN(B1))
305 K1=K1+Y1*(SIN(G1)*SIN(T1)-COS(G1)*SIN(B1))+A1
310 I2=(Y1*COS(G2)-Y2*SIN(G2))*COS(B2)

```

```

320 J2=Y2*COS(G2)+Y1*SIN(G2))*COS(T2)
330 K2=Y2*(COS(G2)*SIN(T2)+SIN(G2)*SIN(B2))
335 K2=K2+Y1*(SIN(G2)*SIN(T2)-COS(G2)*SIN(B2))+A2+L
340 D=L-SQR((I1-I2)^2+(J1-J2)^2+(K1-K2)^2)
400 PRINT L#;X(1);X(2);X(3);X(4);X(5)
402 PRINT X(6);X(7);X(8)
405 PRINT X(9);X(10)
410 PRINT"          DELTA=";D
420 GOTO 55
500 A3=A1
510 A4=A2
520 B3=B1
530 B4=B2
540 T3=T1
550 T4=T2
560 G3=G1
570 G4=G2
600 GOTO 50
3000 DATA -.842,-.721,2,5.7,66,25.0
3002 DATA .542,.529,.539,.517,.483,.388,.468,.326,.548
3003 DATA .561
3004 DATA "3.00",.542,.529,.539,.517,.483,.388,.468,.326
3005 DATA .548,.561
3006 DATA "5.85",.563,.541,.564,.532,.485,.372,.469,.316
3007 DATA .548,.558
3008 DATA "9.05",.581,.550,.586,.545,.489,.366,.470,.308
3009 DATA .546,.555
3010 DATA "12.2",.596,.558,.607,.558,.494,.362,.472,.298
3011 DATA .544,.553
3012 DATA "15.2",.617,.568,.633,.573,.500,.356,.476,.290
3013 DATA .542,.551
3014 DATA "17.7",.649,.583,.670,.593,.508,.350,.481,.281
3015 DATA .541,.550
3016 DATA "20.95",.735,.620,.744,.618,.521,.320,.508,.263
3017 DATA .550,.548
3018 DATA "21.3",.808,.631,.880,.591,.531,.276,.549,.250
3019 DATA .544,.555
3020 DATA "19.8",.970,.667,.860,.544,.553,.175,.648,.227
3021 DATA .593,.576
3022 DATA "Z",.031,.667,.860,.544,.553,.175,.648,.223
3023 DATA .593,.576
3024 DATA "16.25",.210,.722,.480,.540,.085,.588,.233,.690
3025 DATA .606,.588
3026 DATA "9.5",.746,.968,.890,.658,.167,.402,.422,.604
3027 DATA .607,.595
3030 DATA "STP"
4002 END

```

OUTPUT OF RESULTS

XX=-.842 YY=-.721 R= 2 B= 5.7 L= 66

LOAD GAGE READINGS

3.00	.542	.529	.539	.517	.483
	.388	.468	.326		
	.548	.561			
	DELTA= 0				
5.85	.563	.541	.564	.532	.485
	.372	.469	.316		
	.548	.558			
	DELTA= .0083513				
9.05	.581	.550	.586	.545	.489
	.366	.470	.308		
	.546	.555			
	DELTA= .0181723				
12.2	.596	.558	.607	.558	.494
	.362	.472	.298		
	.544	.553			
	DELTA= .0273285				
15.2	.617	.568	.633	.573	.500
	.356	.476	.290		
	.542	.551			
	DELTA= .0404015				
17.7	.649	.583	.670	.593	.508
	.350	.481	.281		
	.541	.550			
	DELTA= .0608206				
20.95	.735	.620	.744	.618	.521
	.320	.508	.263		
	.550	.548			
	DELTA= .1065569				
21.3	.808	.631	.880	.591	.531
	.276	.549	.250		
	.544	.555			
	DELTA= .1339445				
19.8	.970	.667	.860	.544	.553
	.175	.648	.227		
	.593	.576			
	DELTA= .1709814				
16.25	.210	.722	.480	.540	.085
	.588	.233	.690		
	.606	.588			
	DELTA= .3157578				
9.5	.746	.968	.890	.658	.167

.402	.422	.604
.607	.595	
DELTA=		.6049776

READY

*